MOLECULAR BIOLOGY STUDY OF SATELLITE PANICUM MOSAIC VIRUS CAPSID PROTEIN

A Dissertation

by

DONG QI

Submitted to the Office of Graduate Studies of
Texas A&M University
in partial fulfillment of the requirements for the degree of

DOCTOR OF PHILOSOPHY

December 2007

Major Subject: Plant Pathology

MOLECULAR BIOLOGY STUDY OF SATELLITE PANICUM MOSAIC VIRUS CAPSID PROTEIN

A Dissertation

by

DONG QI

Submitted to the Office of Graduate Studies of
Texas A&M University
in partial fulfillment of the requirements for the degree of

DOCTOR OF PHILOSOPHY

Approved by:

Chair of Committee,	Karen-Beth G. Scholthof
Committee Members,	Ellen W. Collisson
	T. Erik Mirkov
	Herman B. Scholthof
Head of Department,	Dennis C. Gross

December 2007

Major Subject: Plant Pathology

ABSTRACT

Molecular Biology Study of Satellite Panicum Mosaic Virus Capsid Protein.

(December 2007)

Dong Qi, B.A, Shandong Agricultural University

Chair of Advisory Committee: Dr. Karen-Beth G. Scholthof

Satellite panicum mosaic virus (SPMV) depends on its helper *Panicum mosaic virus* (PMV) for replication and movement in host plants. The positive-sense single-stranded genomic RNA of SPMV encodes a 17-kDa capsid protein (CP) to form 16-nm virions. Previous studies showed that SPMV CP has multiple functions during infection including encapsidation, symptom exacerbation, inhibiting the accumulation of SPMV DIs, and facilitating systemic movement.

This dissertation confirms and extends the results of our previous reports with new biological and biochemical evidence. For example, the dosage effect of SPMV CP on symptom severity supports its function as a pathogenicity factor. Biological assays also demonstrate compensatory effects of SPMV CP on virus mutants defective in systemic movement. In addition, it is shown for the first time that SPMV CP is involved in cell-to-cell movement of SPMV RNA and associated with the cell wall and membranes, a signature property of plant virus movement proteins. However, SPMV CP in the cytosol exists exclusively as virions and is dispensable for symptom exacerbation.

SPMV CP contains a distinctive N-terminal arginine-rich motif (N-ARM), which is required for the in vitro binding of SPMV and PMV genomic RNAs by SPMV CP. Mutations of this region impair all known functions of SPMV CP. Interestingly, manipulation of the C-terminus of SPMV CP resulted in the same phenotypes as alterations in the N-ARM except that this does not affect the RNA binding activity of SPMV CP. Biological experiments demonstrate that virions are not required for the properties of SPMV CP to facilitate local and systemic movement and inhibit the accumulation of SPMV DIs, suggesting that SPMV CP and RNA form alternative complexes for these purposes. This dissertation study reveals the nucleolar localization of SPMV CP and its interaction with PMV CP in the form of virions.

The identification of distinct functional domains of SPMV CP and its complex subcellular localization profile resulted in the proposal of a tentative model on how the functions of SPMV CP are coordinated for a robust infection. This dissertation provides a foundation for further understanding of the complex interactions among host plants, helper viruses, and satellites.

DEDICATION

I dedicate this dissertation to my wife, Mrs. Sha Li, for her company and support in this challenging graduate study at Texas A&M.

ACKNOWLEDGMENTS

I would like to thank my committee chair, Dr. Karen-Beth Scholthof, for her great mentoring and advising during my graduate study in the plant pathology program at Texas A&M. I also want to thank Dr. Herman Scholthof, my committee member, for his advice in experimental design and critical reviewing of the manuscripts. I would like to thank my other committee members, Dr. Erik Mirkov and Dr. Ellen Collisson, for their support.

I would like to give special thanks to our research associate scientist, Dr. Rustem Omarov, for his training in techniques and collaboration in Chapter III and IV. I want to thank Ms. Jessica Ciomperlik for proofreading my manuscripts and helping with the chromatography experiments. I also appreciate the technical help from the other PhD candidate, Mr. Yicheng Hsieh, in our laboratory. I would like to thank our student worker, Ms. Kristina Twigg, for maintaining our common laboratory supplies and helping with the greenhouse work. I appreciate the helpful conversations and assistance from other laboratory members, Mr. Anthany Everett and Ms. Bonnie Seaberg.

Last but not least, I would like to thank my wife, parents, and sisters for their encouragement during my graduate study.

TABLE OF CONTENTS

CHAPTER Page

LIST OF FIGURES

FIGURE Page

LIST OF TABLES

CHAPTER I

INTRODUCTION

Viruses can be considered as the ultimate obligate parasites. Outside their host cells, viruses are merely macromolecules primarily composed of proteins and nucleic acid. Lacking their own protein synthesis and energy generation machinery, viruses depend on the host cells to synthesize a pool of their particle components, which are assembled into progeny. Interestingly, even viruses have their "molecular parasites" called virus satellites, which depend on their helper viruses for amplification (158). This group of subviral agents is widespread in plants and further divided into satellite viruses and satellite nucleic acids (satellite RNAs and satellite DNAs). Table I-1 lists some representatives of reported satellite viruses and satellite nucleic acids. Both satellite viruses and satellite nucleic acids lack significant sequence similarity with their helper viruses. By definition, satellite viruses differ from satellite nucleic acids in their capacity to encode capsid proteins (CP) to encapsidate the cognate RNAs into their own virions. To date, only four satellite viruses have been identified and they are all exclusively associated with plant RNA viruses in a pair-specific manner (210). These are satellite tobacco necrosis virus (STNV), satellite tobacco mosaic virus (STMV), satellite panicum mosaic virus (SPMV), and satellite maize white line mosaic virus (SMWLMV). In contrast, more than twenty-five plant satellite RNAs (satRNAs) have been described.

This dissertation follows the style of Journal of Virology.

Table I-1. Representative plant satellite viruses and satellite nucleic acids

Satellite Name	Taxonomy of helper virus	[a]Genome property and coding capacity	Reference
Satellite maize white line mosaic virus	Unassigned Unassigned	+ssRNA[a], linear, CP	(260)
Satellite panicum mosaic virus	Panicovirus Tombusviridae	+ssRNA, linear, CP	(142, 174)
Satellite tobacco mosaic virus	Tobamovirus Unassigned	+ssRNA, linear, CP[b]	(152, 190)
Satellite tobacco necrosis virus	Necrovirus Unassigned	+ssRNA, linear, CP	(127, 255)
Tomato leaf curl virus satellite DNA	Begomovirus Geminiviridae	ssDNA[c], circular, none	(65)
Bamboo mosaic virus satellite RNA	Potexvirus Flexiviridae	+ssRNA, linear, 20 kDa nonstructural protein	(132)
Grapevine fan-leaf virus satellite RNA	Nepovirus Comoviridae	+ssRNA, linear, 39 kDa nonstructural protein	(71, 154)
Tomato black ring virus satellite RNA	Nepovirus Comoviridae	+ssRNA, inear, 48 kDa nonstructural protein	(64, 87)
Cucumber mosaic virus satellite RNA	Cucumovirus Bromoviridae	ssRNA[d], linear, none	(46, 187, 220)
Cymbidium ringspot virus satellite RNA	Tombusvirus Tombusviridae	ssRNA, linear, none	(191)
Pea enation mosaic virus satellite RNA	Enamovirus Unassigned	ssRNA, linear, none	(55, 56)
Groundnut rosette virus satellite RNA	Umbravirus Unassigned	ssRNA, linear, none	(15, 156)
Panicum mosaic virus satellite RNA	Panicovirus Tombusviridae	ssRNA, linear, none	(27, 153)
Turnip crinkle virus satellite RNA	Carmovirus Tombusviridae	ssRNA, linear, none	(215-217)
Tomato bushy stunt virus satellite RNA	Tombusvirus Tombusviridae	ssRNA, linear, none	(35, 36)
Arabis mosaic virus small satellite RNA	Nepovirus Comoviridae	ssRNA, circular, none	(106)
Chicory yellow mottle virus satellite RNA	Nepovirus Comoviridae	ssRNA, circular, none	(193)
Tobacco ringspot virus satellite RNA	Nepovirus Comoviridae	ssRNA, circular, none	(25, 170, 203)
Velvet tobacco mottle virus satellite RNA	Sobemovirus Unassigned	ssRNA circular, none	(83)

[a] Positive-sense single stranded RNA genome.
[b] STMV also enodes a putative 6.8 kilodalton protein. But its biological functions have not been shown yet.
[c] Single-stranded DNA genome.
[d] Single-stranded RNA genome.

SatRNAs can be roughly grouped into two classes: large satRNAs that may encode nonstructural proteins and small satRNAs without encoding capacity (189, 218). A few satellite DNAs have been identified in association with some viruses in the genus *Begomovirus* (65, 199).

The complex interactions among helper viruses, satellites, and host plants make the ultimate outcome of pathogenesis variable from case-to-case. Generally, the co-infection of satellites attenuates symptoms induced by the helper viruses (158, 218). However, some variants of the satRNAs associated with *Cucumber mosaic viruses* (CMV) induce aggravated symptoms such as systemic necrosis on infected tomato plants (105, 148). In addition, satC, a satellite RNA associated with *Turnip crinkle virus* (TCV), always exacerbates the symptoms of crinkle and stunting induced by TCV on host plants, despite the reduced accumulation of the helper viruses (78, 79, 130, 257). In our lab, the co-infection of PMV+SPMV always induces aggravated symptoms including severe leaf mosaic, stunting of infected plants, and failure to set seeds (173). Little is known about the molecular mechanisms behind this property of symptom modulation except that symptom attenuation is usually associated with the reduced accumulation of helper viruses (189, 218). There are also reports that the presence of some satellites affects the movement of helper viruses (116) or or triggers the defense responses of host plants (251). A more complete understanding of these mechanisms will provide valuable insight for the control of plant virus diseases.

Although virus satellites are infectious agents, they have the potetntial to be developed into tools for biotechnology. One possible use is their possible application as vectors for the production of foreign proteins. Some plant viruses have been successfully

developed into such vectors for expressing economically important products or as tools for basic research in plant biology (207). However, one concern with designing plant virus based vectors is to avoid inserting target genes into positions where it may harm the viability of the parental virus. Since virus satellites are not required for accumulation of their respective helper viruses, they offer a more flexible platform for expressing foreign genes and the use of plant virus satellites as vectors has been reported (126, 128, 133).

SPMV provides a model system for studying satellite-helper-host interactions. SPMV depends on its helper virus *Panicum mosaic virus* (PMV) for replication and movement. The co-infection of PMV and SPMV causes St. Augustine Decline (SAD), a widespread disease of lawn grasses in the southern United States (26, 27, 95). PMV and SPMV infections have been reported on forage grasses, such as switchgrass, pearl millet, proso millet and foxtail millet. In proso millet, SPMV enhances PMV accumulation and movement and induces a severe chlorotic mottle and stunting in infected plants (208).

Chapter I is intended to provide a general review of several systems of plant virus satellites for which there has been a substantial body of published knowledge. It also includes the non-structural functions of viral CPs and an introduction of SPMV and PMV as a model system to study satellite-helper-host interactions.

Satellite panicum mosaic virus and its helper virus

Satellite panicum mosaic virus (SPMV) has a positive-sense, single-stranded genomic RNA of 824 nt and encodes a 17 kDa CP (142). SPMV is completely dependent on its helper *Panicum mosaic virus* (PMV) (genus *Panicovirus*; family *Tombusviridae*) for replication as well as local and systemic spread in plants (27, 142, 208). There is no

significant sequence similarity between SPMV and PMV (142). PMV was first identified as the causal agent of St. Augustine decline disease and it was later discovered that diseased plants were often associated with a mixed-infection of PMV, SPMV, and sometimes satellite RNAs (27). Therefore, PMV has an unusual property of supporting both a satellite virus and satRNAs.

The genomic RNA (gRNA) of PMV is 4,326 nt and encodes six open reading frames (ORFs) (232, 233). The two 5'-proximal proteins, p48 and p112, are the replicase components and expressed directly from PMV gRNA. Their functions have been preliminarily characterized (11). Three smaller proteins (p6.6, p8, and p15) and the 26 kDa CP are all translated from a polycistronic subgenomic RNA (sgRNA). These proteins are functionally implicated in local and systemic translocation of PMV (232). The p8 and CP of PMV are localized to the cell wall enriched fractions, a signature property of cell-to-cell movement proteins (18, 72, 232). Like other members of the *Tombusviridae*, PMV gRNA and sgRNA are not capped or polyadenylated. Uncapped in vitro transcripts are routinely used as inoculum, which indicates that PMV must employ other strategies for the translation of its encoded protein. One possibility is the use of translational enhancers (TEs) for the cap-independent translation of PMV gRNA. In fact, a *cis*-acting sequence for this function has been mapped to the 3'-untranslated region (UTR) of PMV gRNA (10). This TE functions only in the positive-sense orientation but its position is irrelevant to its activity. In addition, the PMV TE displayed a conserved Y shaped secondary structure, which is essential for the appropriate function of TE. Since uncapped SPMV transcript is also infectious, it is likely that similar elements exist on SPMV gRNA.

One interesting property of the PMV and SPMV system is that synergistic effects are consistently observed in the mixed infections (208). The co-infection of PMV+SPMV induces more severe symptoms on millet plants, including chlorotic mottle with bleaching effects, severe growth stunting, and failure to set seed. This property of symptom modulation is attributed to SPMV CP (172, 173), which is supported by several lines of evidence in this dissertation (Chapters III-V). SPMV CP also elicits aggravated symptoms on a non-host plant, *Nicotiana benthamiana,* when expressed from a *Potato virus X* (PVX) based vector (175). However, the mechanism behind this property of symptom exacerbation remains elusive, although cytopathology studies suggest that it is correlated to the disruption of organelles and internal membranes in infected host cells (247). The synergistic interactions between PMV and SPMV are not limited to symptom modulation. RNA blots show an increased titer of PMV RNA in plants co-infected with SPMV. Furthermore, SPMV enhances the expression of two movement related proteins of the helper viruses, P8 and CP of PMV, in the mixed infections (208), which is likely to be responsible for the accelerated systemic movement of PMV and provides PMV with an advantage in its plant-to-plant transmission in nature.

A comprehensive reverse-genetic study of SPMV deletion mutants has identified several *cis*-acting elements on SPMV gRNA (174). Based on their functions, these *cis*-acting elements were grouped into three categories: (i) nt 1 to 16 and nt 490 to 824 (covering 73 nt upstream of the CP stop codon and the entire 3'-UTR) are absolutely required for SPMV replication in protoplasts, (ii) nt 17 to 67, though not required, up-regulate SPMV replication, (iii) nt 68 to 104 are involved in SPMV movement in a host-specific manner. The continuous passage of PMV+SPMV results in the generation of

SPMV specific defective interfering RNAs (DIs), which has never been observed for other systems of plant virus satellites (172). Sequence analyses of different cloned SPMV DIs confirmed the results of the reverse-genetic study about the minimal *cis*-acting elements required for replication. However, there is little information about the possible secondary structures of these *cis*-acting elements except that nt 68 to 104 forms a putative hairpin structure.

The SPMV CP ORF contains four in-frame start codons (AUG) and translation has been shown to be initiated from the third AUG start codon to express a 10 kDa SPMV CP related protein, possibly by a ribosome leaky scanning mechanism (119, 173). This truncated (C-terminal) version of SPMV CP still maintains the symptom modulation activity but only the full-length 17 kDa SPMV CP is incorporated into the 16 nm spherical SPMV virions. As expected, SPMV CP binds its cognate RNA cooperatively with a high affinity, as shown by gel-mobility shift assays (57). Interestingly, the cooperative interaction between SPMV CP and RNA seems to include two phases: a basal phase that is not sensitive to the addition of competitor RNA and a cooperative phase that is. SPMV CP contains a distinct N-terminal arginine-rich motif (N-ARM), which is predicted to be buried inside the virion and interact with the encapsidated SPMV RNA (8). However, there is still no biological evidence about its functions during infection. In addition to SPMV RNA, SPMV CP also encapsidates the satRNA associated with PMV (27, 57). SPMV CP is not absolutely required for replication and systemic movement of SPMV RNA in millet plants. But the absence of full-length SPMV CP expression accelerates the generation of SPMV DIs, suggesting an additional role of the CP in maintaining SPMV RNA integrity (173). A recent study indicates that SPMV CP

affects the suppressor activity of the PVX p25 protein in virus induced gene silencing but the mechanism behind this phenomenon remains unknown (175).

Satellite RNAs associated with *Bamboo mosaic virus*

Bamboo mosaic virus (BaMV) is a member of the *Potexvirus* genus in the *Flexiviridae* family. BaMV features a positive-sense, single-stranded RNA genome, which contains a 5'-cap and a 3'-poly(A) tail and encodes five conserved ORFs (134, 253). BaMV is naturally associated with a small positive-sense single-stranded satellite RNA of 836 nt, excluding the poly(A) tail (132). BaMV satRNA encodes a 20 kDa nonstructural protein (P20). Interestingly, this protein shares a 46% sequence identity to SPMV CP (132, 142) and can be functionally substituted by it (N.-S. Lin, Academia Sinica, Taiwan, ROC, personal communication). The BaMV satRNA was first isolated from *Bambusa vulgaris* McClure (132). A subsequent survey of naturally infected plants showed that 26 of 61 BaMV isolates collected worldwide are associated with this satRNA (254). The BaMV satRNA is encapsidated by BaMV CP to form rod-shaped particles approximately 60 nm long (132).

Sequence analyses indicates that all the reported BaMV satRNA isolates can be divided into two phylogenetical groups with a genetic diversity of ~7% (254). However, the 5'-UTR contains a hypervariable region with a diversity of up to 21%. Both RNA secondary structure modeling and enzymatic probing indicate an apical hairpin stem-loop (AHSL) structure for this hypervariable region, which is in a large stem-loop (LSL) (4, 254). Any deletions in the LSL region abolishes the replication of BaMV satRNA, but the interchange of this region among different satBaMV isolates does not have any

detectable negative effects, suggesting the importance of this evolutionarily conserved secondary structure (254). Detailed studies demonstrate that subtle structural variation and certain specific nucleotides on the AHSL are involved in the activity of some BaMV satRNAs to down-regulate the accumulation of the helper virus and the consequent attenuation of symptoms (38, 99). The presence of a similar secondary structure in the 5'-UTR of BaMV gRNA suggests that BaMV satRNA interferes with the replication of BaMV by competitively binding to some viral or host factors that are required for BaMV replication (38).

The P20 protein encoded by BaMV satRNA is dispensable for replication in protoplasts and the p20 ORF can be substituted with the coding sequence for chloramphenicol acetyltransferase (133) as a demonstration for the potential application of BaMV satRNA as an expression vector. In addition, BaMV satRNA constructs expressing the triple gene block (TGB) proteins of different potexviruses were used in *trans*-complementation assays to study the species-specific interactions among movement proteins (131). It was also used as a reporter system for the identification of promoter sequences required for the synthesis of BaMV sgRNAs (126). Although the P20 protein was not required for the replication of BaMV satRNA in protoplasts, it was of vital importance for the systemic accumulation of BaMV satRNA in *N. benthamiana* plants, which is used for the laboratory studies of BaMV (240). However, it is not known if P20 is of the same importance for the infections in bamboo plants, which are the natural hosts of BaMV and its satRNA.

In vitro experiments confirmed that the P20 protein is an RNA binding protein and it preferentially binds satBaMV RNA and helper virus RNA in a highly cooperative manner

when compared to unrelated RNAs (231). Gel mobility shift assays using satBaMV RNAs truncated at different sites map the P20 binding regions to the 5'- and 3'-UTRs of satBaMV. The P20 protein contains a distinct N-terminal arginine-rich motif (N-ARM), which is identified as an RNA binding domain (231). Accordingly, alterations the P20 N-ARM impaired systemic movement of BaMV satRNA (231, 240). Detailed studies indicate that the P20 protein also promotes cell-to-cell movement and its N-ARM overlaps with some other functional domains such as the self-interaction domain essential for oligomerization of P20 and the subcellular localization signal sequence targeting P20 to the cell wall (240).

Other plant virus satellite systems

There are only a few in-depth studies of the molecular biology of other plant virus satellites so far. Therefore, I will elaborate on some selected examples of others virus satellites and results that are pertinent to the research for my dissertation.

Satellite tobacco mosaic virus (STMV) has a positive-sense, single-stranded RNA genome of 1,059 nt. In nature, it is only associated with *Tobacco mild green mosaic virus* (TMGMV) (234, 235). However, it can adapt to be replicated by other *Tobamovirus* species in a broad range of host plants (162). This adaption in helper virus-host relationship usually necessitates specific sequence changes in the 5'-UTR of STMV gRNA. In most tested plants, STMV does not usually affect the symptoms induced by the helper viruses. The only known exception is in pepper plants, where the presence of STMV greatly reduces the accumulation of helper viruses and attenuates the leaf blistering symptom induced by TMGMV (188). STMV gRNA comprises two

overlapping ORFs (152). The 5'-ORF encodes a putative 6.8 kDa protein. But mutagenesis studies indicate that this putative protein does not have any biological functions (190). Any mutations in the CP ORF resulted in decreased accumulation of STMV RNA in tobacco plants and also impaired the activity of STMV as a symptom attenuator (190).

Satellite tobacco necrosis virus (STNV) was the first discovered satellite virus (109). It also has a positive-sense, single-stranded RNA genome of 1239 nt and from its gRNA, a 21 kDa CP is expressed (51, 238). A unique feature of STNV among all plant satellite viruses and their helper viruses is its efficient soil-borne transmission by the zoospores of the chytrid fungus *Olphidium brasssicae* (29, 108). Three strains of STNV have been proposed according to serological analyses, fungal vector specificity, and dependence on specific isolates of helper virus for replication. In host plants, the co-infection of STNV greatly reduces the accumulation of its helper viruses (110) and attenuates the symptoms caused by its helper viruses. Recent studies have mainly focused on the cap-independent translation mechanism of STNV. The gRNA of STNV lacks a 5'-cap and a 3'-poly(A) tail, two signature properties of eukaryotic mRNA. However, it directs the synthesis of STNV CP very efficiently. Deletion analyses indicate that the 3'-UTR of STNV genomic RNA contains translation enhancer (TE) elements, which can stimulate the expression of foreign genes. The 3’-TE functions best in combination with the 5'-UTR of STNV gRNA (50, 149, 236), suggesting the interactions between different elements in 5'- and 3'-UTRs are required for the cap-independent translation of STNV CP (150). The functional mechanism the STNV translation enhancer has been shown to be via recruiting translation machinery to the RNAs (75).

A satellite virus of maize white line mosaic virus, SMWLMV, has a positive-sense, single-stranded gRNA of 1168 nt and encodes a 24 kDa CP (260). But no biological or molecular studies have been reported about SMWLMV or its helper virus for more than a decade. Recently, a new satellite virus-like agent has been characterized in association with the *Macrobrachium rosenbergii* nodavirus, a pathogen of white-tail disease on fresh water prawns (246). Sequence analysis shows that this small satellite virus-like particle encapsidates its positive-sense single-stranded gRNA that encodes a 17 kDa CP. It is not related to any known virus families. Therefore, the status of a satellite virus has been proposed for it.

Cucumber mosaic virus (CMV) is the type member of the genus *Cucumovirus*. CMV is a tripartite RNA virus of positive-sense polarity (5, 85, 94, 164, 190) and associated with more than 20 strains of satRNAs. Most CMV satRNAs attenuate the symptoms (189) and this is usually associated with a reduced accumulation of the helper virus (249). In addition, the co-infection of of CMV and its satRNAs can induce plant-defense responses including callose deposition, hydrogen peroxide accumulation, and up-regulation of several tomato defense genes such as PR-1a1, PR-1b1, PR-2, and PR-10 (251). However, D-satRNA of CMV induces lethal programmed cell death-like necrosis on tomato plants (105, 148, 251, 252). Genetic studies have mapped the necrogenic property of D-satRNA to a specific region close to the 3'-end (58, 141, 221) and show that the presence of minus-strand D-satRNA itself is sufficient to induce systemic necrosis (221, 229). A couple of reports demonstrated the existence of *cis*-acting elements involved in systemic accumulation in some satRNAs (13, 259).

Turnip crinkle virus (TCV) is a member from the genus of *Carmovirus* (Family: *Tombusviridae*). It also has a positive-sense single-stranded RNA genome of ~4 kilo base pair (kbp) and encodes five ORFs (81, 245). Three satRNAs have been reported in association with TCV (1, 214). They are named satD (194 nt), satF (231 nt), and satC (356 nt). One interesting property of the TCV satellite system is the frequent recombination events observed between different TCV satRNAs (34) or between satRNAs and its helper virus (34, 256). One suggested function of this homology independent RNA recombination is to maintain a functional 3'-end for replication of sat RNAs (31, 32). Interestingly, the presence of satC in TCV infections always intensifies the symptoms on all tested host plants (130, 257) despite its substantial interference with the accumulation of helper virus in both infected plants and protoplasts (130, 217, 224, 258). This symptom exacerbation activity is attributed to the property of satC to decrease the accumulation of TCV virions (257) while increasing the relative titer of free TCV CP, which is recently discovered to be involved in facilitating movement and suppressing the plant defense response of post transcriptional gene silencing (PTGS) (116, 176, 218). Therefore, it may be evolutionarily beneficial for the helper virus to "support" satRNA infections. In addition, the 3'-proximal region of satC is required for the reduced accumulation of TCV virions in plants (224, 257). Collectively, the presence of satC facilitated the TCV infection on the whole plant level despite its interference with TCV replication on the cellular level. Therefore, the relationship between TCV and satC becomes more of mutualism and less of parasitism (218).

Groundnut rosette virus (GRV) is a member of the genus *Umbravirus*. GRV does not encode a typical CP. Instead, it depends on an assistor virus, usually a luteovirus, to

provide CPs for *trans*-encapsidation of GRV gRNAs. GRV is associated with a single-stranded satRNA ranging from 895-903 nt (157, 159). This satRNA contains five small putative ORFs (15) but none of them has been shown to be biologically functional. Although the GRV-associated satRNA is not required for the replication and movement of GRV in infected plants, it is essential for the *trans*-encapsidation of GRV by the GRV assistor *Luteovirus* CP. Because virion formation is required for GRV to be vectored by aphids, the satRNA of GRV is also indirectly involved in the aphid transmission of GRV (156), an inherent stage of the GRV infection cycle in nature. This presents an exception to the classical definition of virus satellites because the presence of satRNA is essential for GRV to complete its natural infection cycle. Interestingly, it is actually the satRNA that is responsible for the symptoms of groundnut (peanut) rosette disease on infected plants and the infection by GRV alone induces either no symptoms or a transient mild mottle (228).

SatRNAs are also reported to be associated with some *Tombusvirus* members (35, 192). A satRNA associated with *Tomato black ring virus*, a member of *Nepovirus*, encodes a 48 kDa protein that is essential for its replication in protoplasts (87). SatRNAs are also reported for a fungal viruses (90) and a virus infecting the human parasistic protozoan, *Trichomonas vaginalis* (225).

Nonstructural functions of virus capsid protein

The capsid proteins of plant viruses are defined based on their function to encapsidate their cognate viral nucleic acids into the well-organized structures of viral particles. However, these proteins usually have other functions beyond encapsidation in

viral infections. In fact, viral CPs are involved in almost every aspect of the virus life cycles. This section provides a general review of some of the interesting functions and features of plant virus CPs.

For a successful infection in host plants, viruses have to move from initially infected cells to neighboring cells (cell-to-cell movement). For this purpose, the viruses have to traverse the tiny passages called the plasmodesmata, which connect the adjacent cells. However, the diameter of the plasmodesmata is smaller than the size of the smallest viruses. To bypass this physical constraint, plant viruses encode specialized movement proteins (MPs) for their translocation in the host plants (33, 145, 205). Interestingly, viral CPs usually participate in this process of cell-to-cell movement. Based on the functional form of CPs in planta, plant viruses can be divided into three groups. The first group is represented by members from the genera of *Tobamovirus* and *Dianthovirus*. These viruses require CP for long-distance movement but not for cell-to-cell movement (52, 53, 60). Virion assembly is not required by tobamoviruses in its long-distance movement (195). Studies using chimeras with replicase, MP, and CP from different tobamoviruses indicate that the CP functions in a host-specific manner to facilitate long distance movement (52, 89). In contrast, systemic movement of dianthoviruses requires the formation of virions, which was confirmed by an observation that some CP mutants cannot move systemically but still assemble virions in protoplasts or inoculated leaves (219). Cucumoviruses typify the second kind of virus movement strategy. These viruses require CP for cell-to-cell movement but virion formation is not required (107, 202). It is likely that the specific interactions among MPs, CPs and viral RNAs lead to the formation of ribonucleoprotein (RNP) complexes that are essential for virus cell-to-cell

movement (160, 169). Furthermore, the CP is also involved in long-distance movement of cucumoviruses in a host specific manner (227). The third group comprises *Brome mosaic virus* (genus *Bromovirus*) and *Closterovirus* members. The movement of these viruses absolutely requires the formation of virions (2, 3, 196, 198, 201). *Beet yellow virus* (BYV) is a typical member of *Closterovirus* and its virions consist of a filamentous body and a tail structure. The formation this tail structure on the 5' end of the gRNA, which is composed of a minor CP, has been shown to be required but not sufficient for cell-to-cell movement of BYV (3).

Even when viruses are successful at systemically infecting the whole plants, their fitness in nature is still limited unless they can be successfully transmitted to new uninfected host plants. An important approach of virus spread in the field is by vectors including insects, fungi, nematodes and parasitic plants. Since viral genetic material is well-protected by the capsids, it is not surprising that virions serve as inoculum during the vectored transmission. From this, CP can be the major determinant of vector-virus interaction and specificity. One well-studied example of CP involvement in vectored transmission is *Beet western yellows virus* (BWYV), a member of the *Polerovirus* genus of the *Luteoviridae* family (49, 69, 239). An important feature of luteoviruses is that they are transmitted by aphids in a persistent circulative manner (147). After being taken up during feeding, the luteovirus virions cross the epithelial cells between the alimentary canal and the hemocoel by receptor-mediated endocytosis and exocytosis (73, 74). By a similar process of endocytosis and exocytosis, virions diffuse through the hemolymph and penetrate the accessory salivary gland basal lamina to gain entry to the salivary duct (76, 77). The viruses are then transmitted from the salivary gland to new host plants with

the saliva secreted during feeding. BWYV virions comprise a 22 kDa major CP and a 74 kDa minor CP. The 74 kDa minor CP is expressed as a read-through translation product of the 22 kDa ORF and contains a long C-terminal extension called the read-through domain (RTD). The RTD is involved in the aphid transmission (20) and is further divided into functional domains. The conserved N-terminal region is responsible for virus accumulation and aphid transmission and the variable C-terminal region is involved in symptom expression (24). A study using chimeras with the RTD exchanged between different luteoviruses showed that this region was the determinant for vector specificity and intestinal tropism in aphids (19), suggesting that the 74 kDa minor CP is the ligand for the unidentified vector receptor in endocytosis and exocytosis. However, there is also evidence suggesting that the RTD is involved in stabilizing luteovirus virions in the hemolymph by mediating interactions with symbionin, a chaperonin produced by a endosymbiotic bacteria in aphids (184). Regions on the virions required for vector transmission have also been determined for other viruses such CMV (136) and *Beet mild curly top virus* (genus *Curtovirus*, family *Geminiviridae*) (165, 223).

Additionally, viral CP has a role in replication. *Alfalfa mosaic virus* (AlMV) is the type member of *Alfamovirus* (family *Bromoviridae*). The genomic RNAs of AlMV or other alfamoviruses are not infectious unless CP or CP sgRNAs are present in the inoculum (17, 102). Therefore, the CP is required as a co-factor to activate the AlMV gRNA for replication. This genome activation property requires that gRNA is bound by the CPs. The CP binding site on the RNA and the RNA binding domain of the CP have been determined (6, 16, 185, 186, 237). However, the exact functional mechanism of genome activation by CP remains elusive and controversial. Several different models

have been proposed including: (i) genome stabilization (97, 137, 161), (ii) participation in the replicase complex (178), and (iii) as a switch from minus-strand synthesis to plus-strand synthesis (54, 98, 177). A recent study shows that the presence of AlMV CP enhances the template binding affinity of the replicase (183) and suggests a fourth model where the RNA-CP co-folding organizes the 3'-terminus of the template into a transfer RNA (tRNA) like structure (80), which is commonly found on other members in *Bromoviridae* and is essential for replication. Other studies suggest that CP can participate in replication by interacting with host factors and targeting virions to the active replication sites (250, 262). Collectively, it might be a common property of viral CP to participate in virus replication either directly by participating in the formation of the replication complex or indirectly by trafficking the virions to the proximity of replication sites.

In some cases, viral capsid proteins act as virulence factors to suppress the defense responses of host plants such as PTGS. PTGS is a process of sequence specific degradation of target RNAs and is suggested to be a natural defense mechanism against invading viruses (12, 23, 66). Therefore, it is reasonable that viruses have evolved silencing suppressors to counter this potent host-defense system. So far, several viral suppressors have been identified and they target different stages of PTGS (48, 129, 213). These suppressors include the p25 proteins of potexviruses, the helper component protease (HC-Pro) of potyviruses, the 2b protein of cucumoviruses, and the p19 protein of tombusviruses. Recently, the CP of *Turnip crinkle virus* (TCV) was added to the list of viral PTGS suppressors. TCV CP is a strong suppressor that targets the early initiation

step of PTGS and inhibits the generation of siRNAs probably by interfering with the function of the Dicer-like RNase in plants (176).

This brief review suggests that virus capsid proteins have multiple functions and be implicated in almost every stage of viral infection. Therefore, caution has to be taken during the interpretation of the results of virus CP studies since manipulation of CP may affect the infection cycle of viruses at multiple steps. Our preliminary study has shown a multi-functional role of SPMV CP in its co-infection with PMV and it does not negatively affect the viability of its helper virus in plants or protoplasts. The availability of SPMV CP structure information (resolved to 1.9 Å) and the small SPMV genome amenable to reverse genetic studies makes SPMV an elegant system to understand the multifunctional properties of virus CP.

CHAPTER II

A ONE-STEP PCR-BASED METHOD FOR RAPID AND EFFICIENT SITE-DIRECTED FRAGMENT DELETION, INSERTION AND SUBSTITUTION MUTAGENESIS

Introduction

One important goal of molecular biological studies is to understand the structure-function relationship of proteins. The most commonly used strategy for this purpose is to introduce mutations at different sites of the open reading frame of target genes and evaluate the effects on protein function. Site-directed mutagenesis (SDM) has become an invaluable and indispensable tool for such molecular biological and genetic research. The application of the polymerase chain reaction (PCR) technique has revolutionized the way we isolate and manipulate DNA (155), making it both fast and inexpensive to clone and sequence a gene. PCR-based mutagenesis has supplanted the traditional single primer method developed by Kunkel using M13 bacteriophage (121), a time-consuming and inefficient process. Several PCR-based SDM methods, including overlap extension PCR (93), megaprimer PCR (122), and inverted PCR (88), are routinely used for rapid mutagenesis. However, these PCR-based methods require multiple primers and/or multiple steps of enzymatic treatment and template or primer purification. The introduction of recombination PCR minimized the number of primers and steps required for PCR-based SDM methods (103, 104). The technique uses a single round of inverse PCR amplification with a pair of complementary primers bearing the desired mutations in the middle of the sequences. The PCR products are later transfected into *Escherichia coli*

(*E. coli*) and subsequently circularized by an in vivo recombination event between the overlapping 5'- and 3'-ends (103, 104). From this, a commercial kit, QuikChange Site-Directed Mutagenesis Kit (QCM), was developed by Stratagene (La Jolla, CA). Other commercial kits are also developed for these purposes such as the Mutan^{TM} Km system from TakaraBio (Madison, WI) and the Pushion^{TM} system from Finnzyme (Espoo, Finland). But these kits require either cloning the target genes into proprietary plasmid vectors or the use of phosphorylated primers and an extra step of ligation. However, the utility of the QCM kit is limited to only point mutations up to several nucleotides. In this study, we demonstrate a novel primer design strategy that enables efficient and accurate site-directed fragment insertion, substitution, and deletion via a standard QCM protocol with only one pair of partially complementary primers. To our knowledge, this is the simplest method reported for introducing fragment mutations at target sites.

Materials and methods

Plasmid pUC119-SPMV 4 kbp (173) represents a full-length cDNA (824-nt) of satellite panicum mosaic virus (SPMV) cloned immediately downstream of a T7 RNA polymerase promoter. This plasmid was used for insertion mutagenesis. Plasmid pDEST17-SPCP (5 kbp) contains the cDNA sequence of the SPMV CP open reading frame inserted into plasmid pDEST17 (Invitrogen, Carlsbad, CA). This construct was originally designed to over-express SPMV CP in *E. coli*. In this study, pDEST17-SPCP was used as a template for insertion, substitution and deletion mutagenesis. All plasmid templates were prepared with the QIAprep Spin Miniprep Kit (Qiagen, Hilden,

Germany). All primers were synthesized by Invitrogen as de-salted grade, which is the least purified and least expensive grade commercially available.

Plasmid PCR amplification was performed with the proofreading Pfu Turbo system from Stratagene. A 50 μl PCR reaction was composed of 1 μl template (~200 ng), 1 μl of each primer (~20 pM each), 1 μl dNTP mixture (12.5 mM each), 5 μl 10X buffer, 1 μl Pfu Turbo DNA polymerase (2.5 U) and 40 μl dH_2O. The extension reaction started with 2 min at 95°C to pre-denature the template. This was followed by 18 cycles of 1 min at 95°C, 1 min at 55°C, and 1 min/kbp at 68°C. Following the PCR reaction, 1 μl *Dpn*I (20 U) (NEB, Ipswich, MA) was added and the mixture was incubated at 37°C for 1 hr to degrade the original unmodified plasmid templates. After *Dpn*I digestion, 5 μl of the mixture was used to transfect XL1-Blue competent cells by heat-shock (197). After a 1 hr recovery in 300 μl LB broth without antibiotics, the transformed XL-Blue *E. coli* was spread on LB plates containing 50 μg/ml ampicillin and incubated at 37°C overnight. Colonies were selected and grown overnight in 3 ml LB with 50 μg/ml ampicillin. Plasmid DNA was isolated using a QIAprep Spin Miniprep Kit and sequenced. The pUC119-SPMV derivative constructs were confirmed by sequence analysis and then further tested using a T7 polymerase-based in vitro transcription-translation kit (TNT, Promega, Madison, WI). The SPMV CP was detected by [^{35}S]-methionine labeling and immunoprecipitation (168) with mouse monoclonal anti-HA antibody (Sigma, St Louis, MO). The intended pDEST17-SPCP mutations were confirmed by sequence analysis and subsequently transformed into BL21 (DE3)-RIL competent cells (Stratagene, La Jolla, CA). The expression of these SPMV CP derivatives was confirmed by standard western

blot analysis (168) with anti-SPMV, anti-HA, and/or anti-FLAG antibodies (Sigma, St Louis, MO).

Results

The primer design strategy for double-stranded DNA is illustrated in Figure II-1A. Primers comprise two major parts: a 5'-complementary region of 18 nt and a 25 nt 3'-region. The primers are designed to anneal to the template sequences flanking the target site where mutations are introduced. The 18 nt 5'-complementary sequence varied from case to case. For insertion (Fig. II-1B) or substitution (Fig. II-1C), the 5'-complementary sequence included the foreign sequences to be introduced. If the foreign sequences were longer than 18 nt, extra nucleotides could be incorporated between the 5'-complementary region and the 3'-template-annealing region. In the case of deletion, the 18 nt 5'-complementary sequence was composed of 9 nt immediately upstream of the 5'- end of the fragment to be deleted and 9 nt immediately downstream of the 3'-end (Fig. II-1D). Thereby, the linear PCR products contained an overlapping sequence of 18 nt at the 5'- and 3'- ends, which enabled circularization into a viable plasmid by in vivo recombination *E. coli*.

If the 5'-complementary regions of the primers were foreign sequences and the full-length plasmid sequence was amplified, the foreign sequence would be incorporated as an insert (Fig. II-1B). In contrast, with foreign sequences as the complementary region and a target sequence not amplified during PCR, a sequence substitution was accomplished (Fig. II-1C). If the target sequence was not amplified and the complementary regions were the flanking sequences of target, the target sequence would

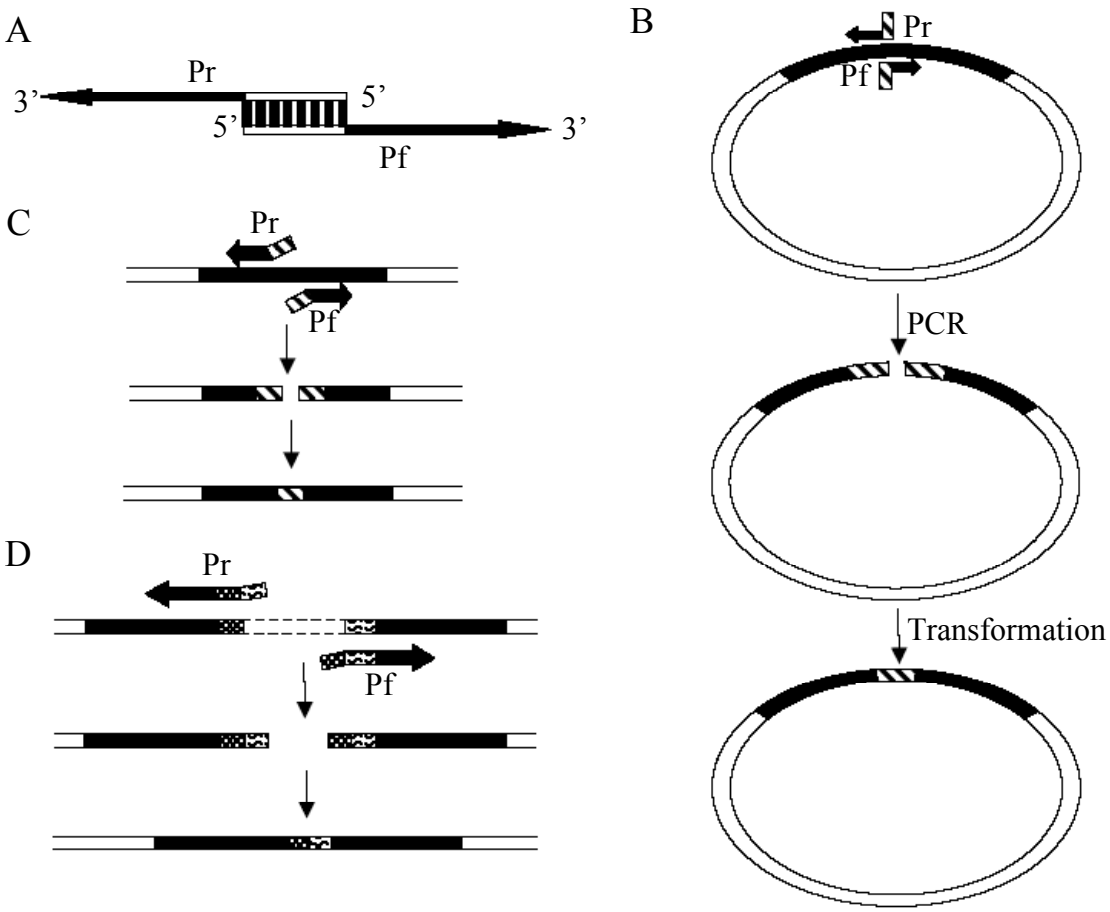

FIG. II-1. Schemes for the primer design strategy and their use for insertion, substitution, and deletion mutagenesis. (A) Primer design. Two partially overlapping primers are designed. Pf is the forward primer and Pr is the reverse one. The black arrows are sequences annealing to regions flanking the target site. The open boxes represent the 18 nt complementary sequence, which varies for each mutagenesis experiment. For insertion or substitution (B, C) mutagenesis, the complementary region represents the foreign sequences to be introduced (striped box). For deletion (D) mutagenesis, the 5'-complementary region is composed of 9 nt flanking the fragment intended to be deleted on the 5'-end (checkered box) and the 3'-end (rippled box). (B) Insertion mutagenesis. In addition to the full-length template sequence, the linear PCR product contains the insert sequence at its 5'- and 3'-end with 18 overlapping nucleotides. In *E. coli* these overlapping regions are resolved by in vivo recombination giving rise to a circular plasmid with an insert at the desired site. For convenience, only the local regions of initial primer binding and final mutated regions are shown for substitution (C) and deletion (D) scenarios. (C) Substitution mutagenesis. Similar as insertion mutagenesis except that the fragment to be exchanged is not amplified in the PCR product so that after recombination, the foreign sequence substitutes for the target fragment. (D) Deletion mutagenesis. The deleted region is shown as a dashed box. Reminiscent of substitution mutagenesis, the fragment to be deleted is not amplified. The primers contain a 9 nt tailing sequence (checkered box or rippled box), which is the 9 nt flanking the fragment to be deleted on the other side so that the linear PCR product has an 18 nt overlapping region of endogenous plasmid sequence at both ends. Accordingly, the dashed box is removed after recombination.

be deleted after recombination in *E. coli* (Fig. II-1D). Following these basic principles, a series of primers were designed for different types of sequence manipulation. Table II-1 provides detailed information about the primers we used in this study. The mutagenesis PCR, transfection and miniprep were performed as described in the Material and Methods.

In-frame codon deletions representing about 35 amino acids (AA) were introduced at four different sites of SPMV CP ORF in the plasmid pDEST17-SPCP. The mutants were named based on the amino acid deletions: SPCP-B, representing a deletion of amino acids 13 to 45 (Δ13-45); SPCP-C (Δ46-80); SPCP-D (Δ81-116); and, SPCP-E (Δ117-151). Five colonies of each mutagenesis reaction were selected for further analysis. Altogether, 20 candidate colonies were selected and first screened by double digestion with restriction enzymes *Nde*I and *Eco*RI (NEB, Ipswich, MA). The double digestion of pDEST17-SPCP released a 495 bp fragment containing the full-length SPMV CP ORF. From this, a deletion of about 35 codons (105 bp) on the plasmid would release a fragment approximately 390 bp following *Nde*I-*Eco*RI digestion. Of the 20 selected colonies, 15 showed this size increase and they were all confirmed to contain the correct in-frame deletions by sequence analyses (data not shown). A correct construct of each mutation was transformed into BL21 (DE3)-RIL (Stratagene) competent cells for over-expression of the SPMV CP mutants. Following the manufacturer's instructions, 1.5 ml culture of each mutant was collected and analyzed by western blot with anti-SPMV antiserum. As predicted, the four deletion mutants expressed a truncated protein of ca. 12 kD compared to the 17 kD wild-type SPMV CP (Fig. II-2A). Interestingly, it was

Table II-1. Primers used for mutagenesis PCR

Primer	Mutation	Sequence (5' to 3') [a]
$32HA_f$	Insertion	**TATGATGTGCCAGATTATGCC**acggagcgagatactgatactacct
$32HA_r$		**ATAATCTGGCACATCATAAGGGTA**caaggtgacgtagcacgta
$43HA_f$	Insertion	**TATGATGTGCCAGATTATGCC**agtttcccgactctcaaggggatgg
$43HA_r$		**ATAATCTGGCACATCATAAGGGTA**ctgcctctgaaaagaggta
$82HA_f$	Insertion	**TATGATGTGCCAGATTATGCC**acagactctgtccatgccaccggg
$82HA_r$		**ATAATCTGGCACATCATAAGGGTA**gtcgcccgggttatacagg
$116HA_f$	Insertion	**TATGATGTGCCAGATTATGCC**actgaagaagccgagaccattttgg
$116HA_r$		**ATAATCTGGCACATCATAAGGGTA**gttaccaaagaaccagttgt
SPCP-$82F_f$	Insertion	**GACTACAAGGACGATGAC**acagactctgtccatgccaccggggta
SPCP-$82F_r$		**GTCATCGTCCTTGTAGTC**gtcgcccgggttatacaggcgcgcg
SPCP-NHA_f	Substitution	**TATGATGTGCCAGATTATGCC**gcgggctcccgggctactgccaca
SPCP-NHA_r		**ATAATCTGGCACATCATAAGGGTA**aggagccatatgtatatctc
SPCP-B_f	Deletion	*AATCGTCGG*actctcaaggggatggggga
SPCP-B_r		*CTTGAGAGT*ccgacgattagatcgcctgg
SPCP-C_f	Deletion	*AGTTTCCCG*gacacagactctgtccatgc
SPCP-C_r		*GTCTGTGTC*cgggaaactctgcctctgaa
SPCP-D_f	Deletion	*AACCCGGGC*gaagaagccgagaccatttt
SPCP-D_r		*GGCTTCTTC*gcccgggttatacaggcgcg
SPCP-E_f	Deletion	*GGTAACACT*gggggttctcatcatcatca
SPCP-E_r		*AGAACCCCC*agtgttaccaaagaaccagt

[a] Sequences annealing to templates are in lowercase, foreign sequences for insertion or substitution are in bold upper case, and the complementary regions are underlined. For deletion, primer sequences in italic uppercase are the 9 nt flanking the fragment to be deleted as shown in Fig. II-1D.

observed that SPCP-D (Δ81-116) protein signal intensity was much reduced when compared to the other deletion mutants. This suggests that the region of the SPMV CP, from AA 81 to 116, may have a stronger immunoreactivity and immunogenicity than other regions on the CP. From this, it is reasonable to speculate that this deletion mutagenesis strategy may be useful for epitope typing and mapping. This strategy was also tested on a larger plasmid (ca. 8 kbp) derived from an infectious cDNA of *Tomato bushy stunt virus* (86) with positive results (data not shown).

Insertions were introduced into both pUC119-SPMV and pDEST17-SPCP. The nine-amino-acid HA epitope (YPYDVPDYA) coding sequence from the hemagglutinin gene of *Influenza A virus* was inserted at different sites (AA32, AA43, AA82 and AA116) on the SPMV CP ORF in pUC119-SPMV. A six amino acid FLAG epitope (DKYDDD) coding sequence was introduced at AA82 on the SPMV CP ORF in pDEST17-SPCP. Again, five candidate colonies of each mutation were selected for sequencing and 23 out of 25 had the predicted in-frame insertion. Correct constructs of four pUC119-SPMV HA insertion mutants were further analyzed by in vitro translation using [^{35}S]-methionine labeling, followed by immunoprecipitation with anti-HA antibodies (168). As predicted, gel electrophoresis followed by autoradiography revealed that all of the HA insertion mutants directed the synthesis of a protein of a slightly higher molecular weight than wild-type CP. And these SPMV CP-derivatives were specifically pulled down in immunoprecipitation with the anti-HA antibodies (Fig. II-2B). As expected, the wild-type SPMV CP could not be immunoprecipitated with the anti-HA antibodies (Fig. II-2B). Similarly, when the FLAG epitope-coding sequence was introduced at AA82 of the SPMV CP ORF, to create pDEST17-SPCP (SPCP-82F), the recombinant protein was

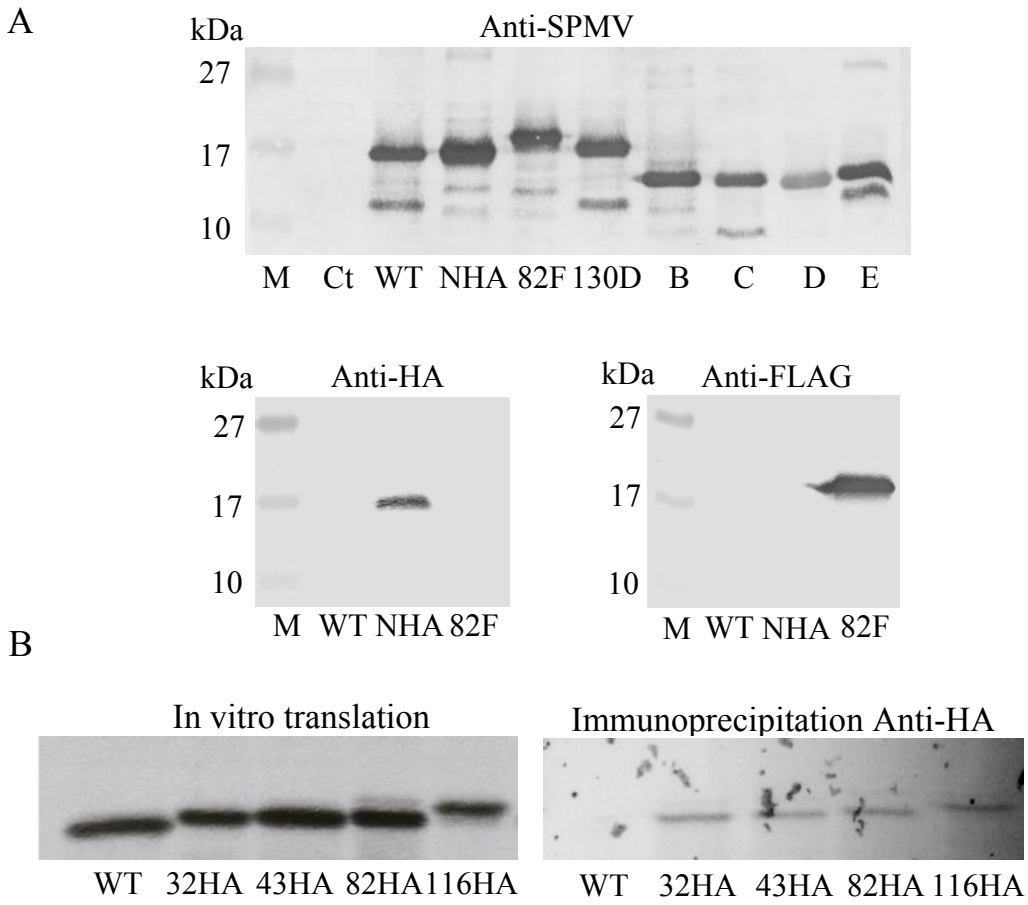

FIG. II-2. Immuno-assays of mutated satellite panicum mosaic virus (SPMV) capsid protein (CP). (A) Immunoblot of SPMV CP and its derivatives following over-expression in *E. coli*. WT represents the full-length SPMV CP. NHA is SPCP-NHA containing the sequence exchange of SPMV CP AA 4 to 12 for the HA epitope. Lane 82F represents SPCP-82F with the insertion of a FLAG epitope at the site AA82. In 130D, AA130 is changed from serine to aspartic acid and was employed as a control. B/C/D/E refers to the SPCP-B/C/D/E deletion mutants described in the text. Ct is an untransformed BL21 (DE3)-RIL cell culture and M is the protein marker (PAGE-ruler, Fermentas). Each sample was blotted with rabbit polyclonal antibodies specific to SPMV CP (upper panel). In addition, WT, NHA and 82F derivatives of SPMV CP were probed with anti-HA and anti-FLAG antibodies (lower panel). (B) In vitro translation and immunoprecipitation of SPMV CP and the HA insertion mutants. The HA epitope was inserted at four different sites on the SPMV CP gene, represented as 32HA, 43HA, 82HA, and 116HA. As predicted, each HA mutant protein had a slightly higher molecular weight than WT SPMV CP (left panel) and was specifically pulled down by immunoprecipitation with mouse anti-HA antibodies (right panel).

recognized by anti-SPMV antibodies and specifically by anti-FLAG antibodies in western blot (Fig. II-2A). The 9 AA HA epitope coding sequence was also used to replace the AA codons 4 to 12 on the SPMV CP ORF in pDEST17-SPCP (SPCP-NHA). The recombinant protein was recognized by both the HA- and the SPMV CP-specific antibodies by western blot analysis (Fig. II-2A). In summary, the overall mutagenesis efficiency for insertion was 92%, for substitution was 100%, and for deletion was 75% as indicated in Table II-2.

Discussion

PCR-based methods have become commonplace for site-directed mutagenesis of double-stranded DNA. These methods include, but are not limited to, overlap extension PCR (93), megaprimer PCR (122), inverted PCR (88) and recombination PCR (104). Recently, there have been reports about methods for fragment insertion, substitution, and deletion using the QCM based protocol (39, 243). However, all of the alternative methods to date require multiple primers (93, 122, 243) and/or additional steps of extra PCR amplification and purification (93, 122), ligation (88), primer extension(243), and hybridization (39).

To address this problem, we have developed a unique, straightforward primer design strategy, which allows insertion or substitution of up to 27 nucleotides as well as deletion of 105 nucleotides using the QCM protocol. As reported here, this strategy centers on the use of a pair of 5'-partially complementary primers. By manipulating the combination of 5'-complementary sequences (foreign sequences vs. target flanking sequences) and 3'-annealing sequences (consequent full-length amplification vs. partial amplification), all

Table II-2. Efficiency of mutagenesis PCR

Mutation	Colonies screened by restriction digestion	Colonies sequenced	Colonies of correctly mutated sequence	Efficiency
Insertion	0[a]	25	23	92%
Substitution	0[a]	5	5	100%
Deletions	20[b]	15[c]	15	75%

[a] Insertion/substitution mutants could not be screened by restriction enzyme digestion.
[b] Five colonies of each deletion mutagenesis reaction were selected for screening by restriction enzyme digestion.
[c] Only colonies tested positive in restriction digestion assay were sequenced.

three types of mutagenesis (insertion, substitution and deletion) can be acquired using the standard QCM protocol.

The advantages of this method are summarized as follows: (i) a minimal requirement for a single pair of primers and a standard QCM-based protocol, (ii) the use of inexpensive and minimally processed primers, (iii) the flexibility of performing simultaneously multiple and different mutagenesis reactions using a single PCR parameter, (iv) precise in-frame introduction and/or deletion of codons via in vivo recombination, and (v) manipulation of large fragments of DNA. In fact, the size limit of insertion and/or substitution is dependent on the maximal length of commercially available primers; therefore, the size of deletion is theoretically unlimited. The efficiency of mutagenesis was 92% for insertions and 100% for substitutions. The efficiency of deletion mutagenesis was 75% and can easily be improved by increasing the comparatively short template annealing sequence (20 nt vs. 18 nt of the complementary region) to prioritize primer-template annealing over primer-primer annealing, resulting in more efficient PCR amplification (261).

A particular advantage of our primer design method for deletion mutagenesis is that it makes in-frame codon truncation independent of the occurrence of DNA restriction enzyme sites. As a result, there is more flexibility in choosing candidate sites for deletion mutagenesis. One use of this in-frame deletion technique is epitope mapping, which is usually performed by introducing small in-frame deletions at different sites of a protein and studying the effect on immunoreactivity to different monoclonal antibodies (200), as suggested in Figure II-2A (lane D). In-frame insertion mutagenesis allows epitope-tagging of a protein and subsequent immunodetection without having to prepare protein-

specific antibodies, which can be expensive and time-consuming. In addition, in-frame insertion/substitution is useful for epitope display studies, which requires the insertion of target epitopes at different sites of carrier proteins. Studies related to protein topology and functions can also be facilitated by inserting an epitope into different sites of a protein followed by *in situ* immuno-detection (30).

Compared with other PCR-based mutagenesis methods, the protocol presented in this study makes it possible to perform all three types of site-directed mutagenesis (deletion, insertion and substitution) on a plasmid using the same PCR parameters with the minimal requirement of primers and steps of manipulation. These features will facilitate high-throughput gene engineering and library construction and will consequently accelerate our understanding of the structure-function relationship of proteins.

CHAPTER III

THE CAPSID PROTEIN OF SATELLITE PANICUM MOSAIC VIRUS CONTRIBUTES TO SYSTEMIC INVASION AND INTERACTS WITH ITS HELPER VIRUS*

Introduction

Satellite viruses and satellite nucleic acids [satellite RNAs (satRNAs) and satellite DNAs (satDNAs)] represent a group of subviral nucleic acid molecules that require a helper virus for replication and movement (210, 218). Satellite viruses differ from satRNAs and satDNAs in their capacity to direct translation of a cognate coat protein (CP), a structural component required for RNA packaging via virion assembly. Satellite viruses do not share significant sequence similarity with their helper virus. However, specific recognition by the helper virus-encoded proteins, such as the replicase and movement proteins, necessarily dictates the involvement of *cis*-acting elements on satellite virus RNA; secondary structures are possibly responsible for such interactions. To date, four satellite viruses have been characterized in plants in pair-specific relationships with a helper virus (62, 210). A satellite virus in an invertebrate host has recently been reported as a co-infection with *Macrobrachium rosenbergii* virus, a nodavirus (246).

---

*Reprinted with permission from "The capsid protein of satellite panicum mosaic virus contributes to systemic invasion and interacts with its helper virus" by Omarov, R. T., D. Qi, and K.-B. G. Scholthof, 2005. Journal of Virology, **79**:9756-9764, Copyright 2005 by American Society for Microbiology.

Satellite panicum mosaic virus (SPMV) is completely dependent on its helper *Panicum mosaic virus* (PMV) (genus *Panicovirus*; family *Tombusviridae*) for replication as well as local and systemic spread in plants (208, 232, 233). There is no significant sequence similarity between SPMV and PMV (142, 233). PMV virions encapsidate the positive-sense, single-stranded genomic RNA (gRNA). The 4,326 nucleotide (nt) gRNA encodes six open reading frames (ORFs) and is the template for expression of the p48 and p112 proteins, both of which are necessary for PMV and SPMV replication (233). The 26 kDa capsid protein (CP), and three smaller proteins (p6.6, p8, and p15) are translated from a polycistronic subgenomic RNA (sgRNA). These proteins have been functionally implicated in local and systemic translocation of PMV (232). Mixed infections of PMV and SPMV are synergistic, inducing severe symptoms on millet plants, including stunting and failure to set seed (208).

A 17-kDa capsid protein (CP) is expressed from the 824-nucleotide (nt) plus-sense, single-stranded SPMV RNA (142). The CP is used to assemble 16 nm spherical satellite virus particles (8). As expected, SPMV CP has a high affinity for binding SPMV RNA, as shown by gel-mobility shift assays (57). In addition to RNA encapsidation, the SPMV CP is implicated in exacerbation of symptoms in millet plants (173). The capsid protein also elicits symptoms on a non-host plant, *N. benthamiana*, a feature that maybe related to the unconventional role of SPMV CP in regulating a suppressor of gene silencing (175). SPMV CP is not essential for replication and systemic movement of the satellite virus RNA in millet plants (172, 174). However, the absence of CP expression stimulated the accumulation of SPMV defective interfering RNAs, suggesting an additional role of the CP in maintaining SPMV RNA integrity (173).

Cis-active elements on the SPMV RNA are required for SPMV replication and capsid protein translation (172, 174). In particular, nt 63-104 on the 5'-untranslated region (UTR) were associated with host-specific spread of the SPMV. However, deletion of this segment also abolished wild type CP expression (172, 174). The aim of this study was to investigate translation of the SPMV CP gene and to dissect the contribution of the CP and the 5'-UTR in SPMV infection.

We determined that 5'-UTR deletions had host-specific effects on movement, but these effects could be neutralized by the presence of the full-length 17-kDa SPMV CP. The results also show that the SPMV RNA can direct the translation of a 9.4 kDa protein that initiates translation downstream and in-frame with the authentic SPMV CP start codon. Subcellular fractionation of infected plant tissues showed that the 17 kDa CP accumulated in the cytosol, presumably the site of virion assembly, as well as with the cell wall- and membrane-enriched fractions. In contrast, the 9.4-kDa protein was exclusively found in cell wall- and membrane-enriched fractions. The CP was also shown to have the novel capacity for specific interaction with the helper virus capsid protein. The collective results indicate that the unique properties of SPMV CP facilitate and enhance satellite virus viability, including its spread and accumulation.

Materials and methods

Plants. Proso millet (*Panicum miliaceum* cv. 'Sunup') and foxtail millet (*Setaria italica* cv. 'German R') were grown in the greenhouse (30^{o}C) or growth chamber (28^{o}C, 14 h of light; 24^{o}C, 10 h of dark). Typically, four millet plants at the three-leaf stage were

mechanically rub-inoculated by mixing equal volumes of uncapped RNA transcripts (~5µg) and RNA inoculation buffer (232).

In vitro transcription and in vitro translation. To obtain linearized DNA templates for in vitro transcription reactions, purified plasmids containing full-length PMV cDNA were digested with *Eco*ICR1, and plasmids carrying SPMV or mutagenized SPMV cDNAs were digested with *Bgl*II. In vitro transcription reactions were conducted as previously described (172). In vitro protein translation was carried out using the TnT-Coupled System (Promega, Madison, WI) using wheat germ extract or rabbit reticulocyte lysate according to the manufacturer's instructions.

In planta ^{35}S-methionine protein labeling. Two weeks after germination, proso millet seedlings were rub-inoculated with a mixture of PMV and SPMV transcripts. At 5 days post inoculation (dpi) the plants were transferred to distilled water containing ~0.5 mCi of ^{35}S-methionine (Amersham, Piscataway, NJ). After 6 days of incubation in the presence of ^{35}S-methionine total proteins were isolated from the millet leaves and the extracts were subjected to immunoprecipitation as described below.

Immunoprecipitation. Immediately after harvesting, 1 g of leaf tissue was quick frozen in liquid nitrogen and pulverized with a pestle in an ice-cold mortar with 1.5 ml of ice-cold extraction medium [150 mM HEPES (pH 7.5), 0.5% Triton X-100, 0.2% CHAPS, 150 mM NaCl, 1 mM EDTA, 2 mM DTT] and a protease inhibitor cocktail (Roche Diagnostics Indianapolis, IN). The homogenized plant material was centrifuged at 10,000 g at 4^{o}C for 15 min. The resulting supernatant was used for immunoprecipitation.

A volume of 800 µl of the extract was mixed with 2 µl of PMV CP- or SPMV CP-specific rabbit polyclonal antibodies and rotated for 2 hours at 4^{o}C, followed by the

addition of 30 μL ImmunoPure immobilized protein G agarose beads (Pierce, Rockford, IL). The samples were then incubated at room temperature for 2 hours. The beads were washed six times with ice-cold extraction buffer and the immunoprecipitated material was separated on sodium dodecyl sulfate-12% polyacrylamide gels by electrophoresis (SDS-PAGE) followed by autoradiography or/and western blotting.

The specificity of anti-SPMV antiserum was verified by immunoprecipitation of ^{35}S-methionine-labeled capsid protein that was synthesized by in vitro translation of full-length SPMV transcripts. As a negative control for immunoprecipitation pre-immune antiserum was used for the pull-down assay. To suppress irrelevant background signals caused mainly by cross reaction between primary and secondary antibodies after the pull-down assay, pre-conjugated primary and secondary antibodies were used to probe immunoblots after immunoprecipitation.

Western blot assays. Protein samples were separated by SDS-PAGE in 15% polyacrylamide gels and transferred to nitrocellulose membranes (Osmonics, Westborough, MA). After transfer, the membranes were stained with Ponceau S (Sigma, St. Louis, MO) to verify protein transfer efficiency. The SPMV CP antibodies and PMV CP antibodies were diluted 1:2000 and 1:5000, respectively. Alkaline phosphatase conjugated to goat anti-rabbit antiserum (Sigma) was used as a secondary antibody at a dilution of 1:1000. The immune complexes were visualized by hydrolysis of tetrazolium-5-bromo-4-chloro-3-indolyl phosphate as the substrate.

Site-directed mutagenesis. A QuikChange Site-Directed Mutagenesis Kit was used to generate site-directed mutants (Stratagene, La Jolla, CA). SPMV/U-91 was generated by single-base insertion of uracil (U) [thymidine (T) in cDNA clone] immediately

downstream of the first SPMV CP start codon at position nt 88 on the SPMV cDNA. SPMV/U-301 was derived from the SPMV/U-91 mutant with an additional insertion of uracil (U) [thymidine (T) in cDNA clone] immediately after the AUG codon at position 297. The SPMV-AUC mutant with substitution of the authentic AUG start codon at nucleotide 88 to an AUC codon was previously described (173). The SPMV/UAA-234 mutant was constructed by replacing six nucleotides immediately up-stream of the second AUG (underlined; nt 235), changing the SPMV sequence from 5'-AAGGGGAUG-3' to 5'-UGAUAAAUG-3'. All mutations were confirmed by sequencing the entire SPMV cDNA.

Construction of SPMV deletion mutants. Internal sequences from full-length SPMV cDNA clones were excised with selected restriction enzymes in various combinations, followed by Klenow treatment, and ligation. Mutants SPMV/Δ*Spe*I-*Bam*HI and SPMV/AUC/Δ*Spe*I-*Bam*HI were generated by digestion of the full-length SPMV or SPMV/AUC cDNAs with *Spe*I and *Bam*HI, respectively (Fig. III-1A). Construct SPMV/Δ*Bsm*I-*Msc*I was obtained by digestion of the full-length SPMV cDNA with *Bsm*I and *Msc*I (Fig. III-1A). The insertion of a *Cla*I restriction site was performed by digestion with *Bam*HI followed by a fill-in reaction with Klenow fragment. All constructs were verified by sequencing the entire SPMV cDNA.

RNA analyses. Total RNAs from 100 mg inoculated- or systemically-infected leaves of millet plants were extracted at 14 dpi. The samples were pulverized in 1 ml of ice-cold extraction buffer [100 mM Tris-HCl (pH 8.0), 1 mM ETDA, 0.1 M NaCl and 1% SDS] and extracted twice with phenol/chloroform (1:1, vol/vol) at room temperature. Total RNA was precipitated with 8 M lithium chloride (1:1, vol/vol) at 4^{o}C for 1 hour. The

resulting pellets were washed with 70% ethanol, resuspended in RNase-free distilled water, and used for northern blot hybridization. Approximately 10 μg of total plant RNA was electrophoretically separated in 1% agarose gels and transferred to nylon membranes (Osmonics, Westborough, MA). PMV and SPMV RNAs were detected by hybridization with [^{32}P]-dCTP-labeled PMV- and SPMV-specific probes, respectively (232).

Results

SPMV RNA directs synthesis of an alternative downstream-in frame translated version of CP. Immunoblot assays of PMV+SPMV infected proso and foxtail millet plants and in vitro translation assays of SPMV RNA typically include several SPMV CP-specific bands smaller than the full-length product (Fig. III-1). This observation was particularly evident when leaf extracts of infected foxtail millet plants were subjected to SDS-PAGE followed by immunoblot assays. The addition of protease inhibitor cocktail to the extraction solution did not prevent the detection of smaller protein bands extracted from PMV+SPMV infected leaf tissue (data not shown). The presence of four in-frame start codons on the SPMV CP sequence, at nt 88 (denoted as AUG1), nt 235 (AUG2), nt 297 (AUG3) and nt 364 (AUG4) (Fig. III-1A), raised the possibility that the lower molecular mass proteins might be authentic SPMV CP translation products.

To examine if the shortened N-terminal truncated versions of CP were expressed by the mechanism of ribosome leaky scanning (117), full-length wild type SPMV transcripts were translated in vitro and labeled with ^{35}S-methionine (Fig. III-1B). Three proteins were detected (Fig. III-1B) and immunoprecipitation with antiserum specific to SPMV CP verified that they represented CP products (data not shown). The amount of the

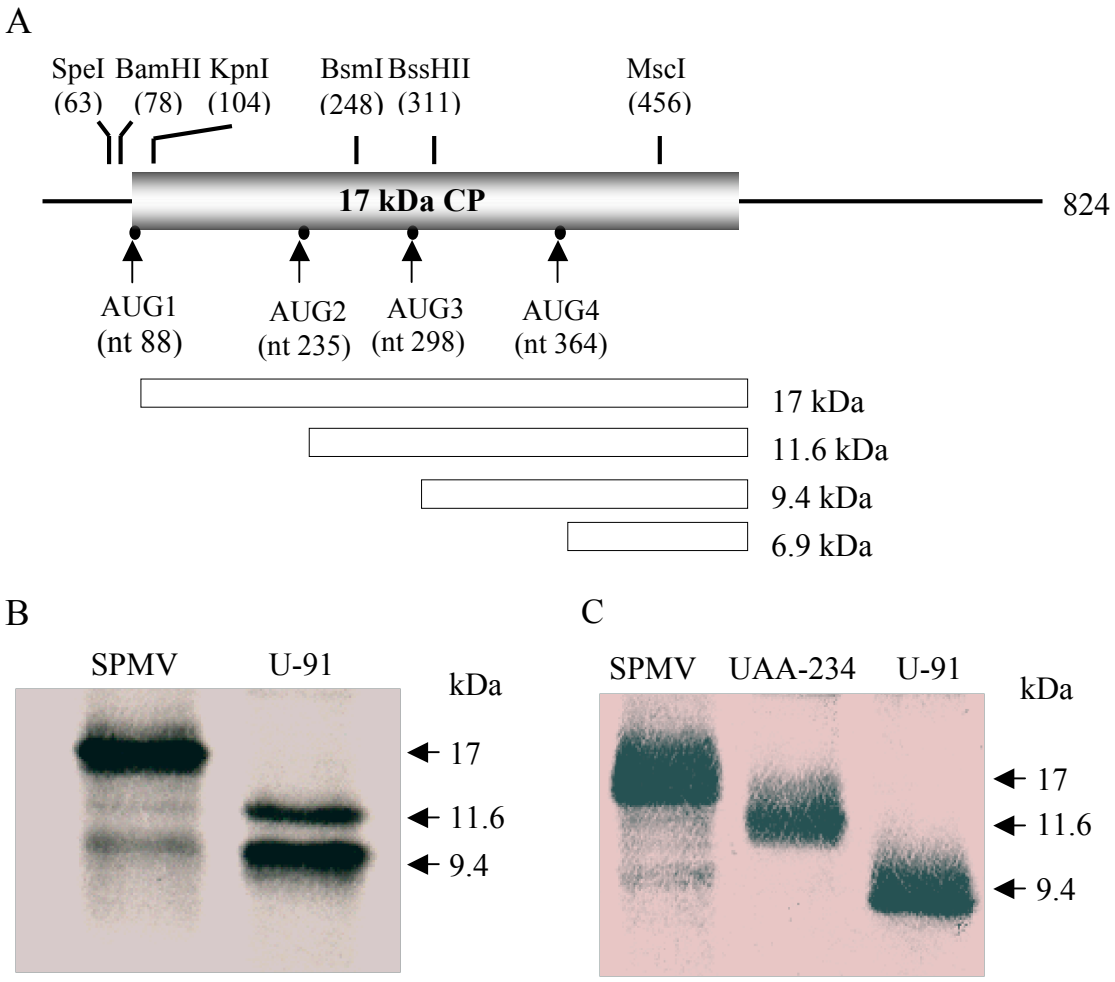

FIG. III-1. SPMV genome and expression of CP. (A) Schematic representation of the 824-nt SPMV RNA (solid line) and the full-length 17 kDa CP. The restriction enzyme sites used to assemble the cDNA constructs and the positions of the predicted in-frame start codons (arrows) are indicated. The 17 kDa CP (AUG1) and N-terminal truncated proteins (AUG2 to AUG4) are indicated by white rectangles. (B) In vitro translation products labeled with ^{35}S-methionine were generated from infectious transcripts of SPMV wild type and SPMV/U-91. (C) Western blot analyses of SPMV CP products in millet plants co-infected with the helper virus and wild type (SPMV) or its mutants (UAA-234 and U-91) probed with anti-SPMV CP polyclonal antiserum. Arrows indicate the SPMV CP-specific proteins and their molecular weights.

translated product from AUG2 was considerably lower in comparison with initiation of protein translation from the down-stream positioned AUG3 codon (Fig. III-1B). The absence of translation from AUG4 is most likely due to its relatively distant location from the 5'-end of SPMV RNA. To obtain additional evidence that translation can initiate from the downstream start codons AUG2 and AUG3 (Fig. III-1A), we suppressed the translational initiation of full-length SPMV CP from AUG1. For this purpose, a frame-shift mutation was introduced by insertion of a uracil (U) [thymidine (T) in cDNA clone] immediately after AUG1 at position nt 91 (SPMV/U-91 mutant), resulting in the generation of a stop codon at position nt 96. This resulted in efficient initiation of translation from AUG2 and even higher level of translation from the AUG3 codon, likely by leaky scanning (Fig. III-1B). SPMV/U-91 transcripts were infectious and in proso millet a 9.4 kDa truncated CP corresponding to translation initiation from AUG3 was detected (Fig. III-1C). The migration of CP products produced in vitro and in vivo was also verified by mixing in vitro translated products with extracts from infected plants followed by SDS-PAGE and immunoblot detection (not shown).

The protein predicted to be expressed from AUG2 was not detected in PMV plus SPMV/U-91 infected proso millet plants (Fig. III-1C). The G-rich region surrounding AUG2 (GGGGAUGGGGG) might prevent or interfere with translational initiation from this codon in vivo. To test this, we replaced the authentic sequence (5'-AAGGGGAUG-3') immediately up-stream of AUG2 (underlined) with 5'-UGAUAAAUG-3' (SPMV/UAA-234 mutant). SDS-PAGE followed by western blotting revealed the presence of an N-terminal truncated version of the ~12 kDa SPMV CP in infected proso millet plants (Fig. III-1C). Interestingly, the immunoblot did not reveal presence of the

9.4 kDa protein and infected plants did not develop severe mosaic (not shown). These data indicate that preferential initiation of translation occurred from AUG3, compared to AUG2, is most likely due to the unfavorable context surrounding AUG2. In vitro translation of capped and uncapped SPMV transcripts demonstrated identical patterns of protein synthesis in rabbit reticulocyte lysate and wheat germ extract (data not shown).

Differences in solubility and subcellular localization between full-length and the N-terminal truncated version of CP. The extraction of CP from PMV+SPMV infected plants under native and denaturing conditions enables reliable detection of the SPMV 17 kDa protein by western blot analysis. The 9.4 kDa protein expressed by SPMV/U-91 was not detected under native conditions (Fig. III-2), but the addition of 2% Triton X-100 to the extraction buffer allowed for its solubilization. The application of an anionic detergent (1% SDS) to the extraction solution also significantly increased the amount of protein detection by western blot assay. Interestingly, and similar to the full-length CP protein extraction, the addition of SDS resulted in immunodetection of a second slightly higher molecular weight protein, while Triton X-100 yielded a single protein band (Fig. III-2B).

To study how differences in solubility might direct SPMV CP subcellular localization we fractionated protein extracts from PMV+SPMV infected proso (Fig. III-3) and foxtail millet plants by differential centrifugation. We found that a considerable amount of SPMV CP was localized to the cytosol, but the greatest accumulation was observed in membrane- and cell wall-associated fractions (Fig. III-3A). Even more interestingly, the fractionation of extracts from plants infected with SPMV/U-91 (expressing the 9.4 kDa C-terminal version of CP) showed that the protein was

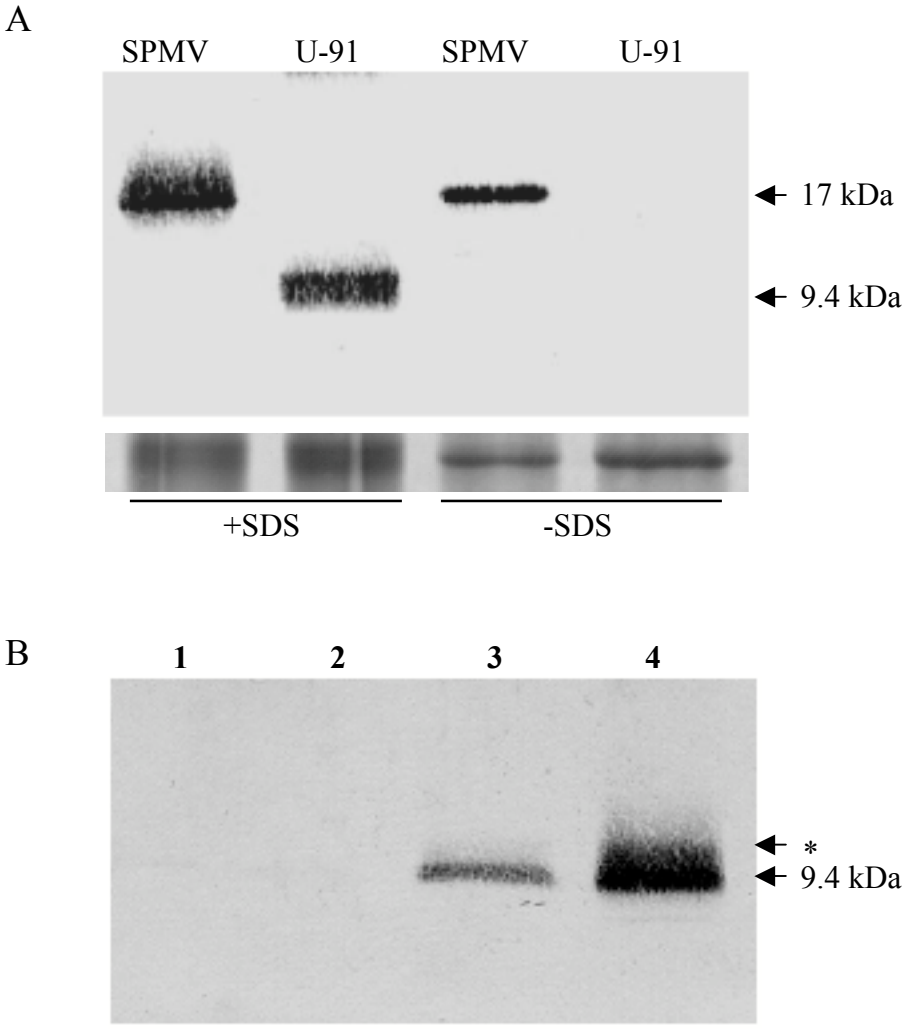

FIG. III-2. Differences in solubility of the 17 kDa SPMV CP and the 9.4 kDa N-terminally truncated SPMV/U-91 CP isolated from millet plants co-inoculated with *Panicum mosaic virus*. (A) Extraction and immunoblot detection of the capsid protein from SPMV and SPMV/U-91 under native (–SDS) and denaturing conditions (+SDS). The lower panel represents a SDS-PAG stained with Coomassie Brilliant Blue R to verify equal protein loading. (B) Extractions of the 9.4 kDa CP from SPMV/U-91 infected tissue were made in buffer alone (100 mM Tris-Hcl, pH7.5) (lane 1) and buffer plus 1 M NaCl (lane 2), 2% Triton X-100 (lane 3) or 1% SDS (lane 4). In lane 4, an asterisk (*) indicates an SPMV CP-specific protein, perhaps due to posttranslational modification, that was consistently observed.

exclusively associated with membrane- and with cell wall- enriched fractions (Fig. III-3B). Similar results were obtained for foxtail millet (not shown). These results suggest that cell wall- and membrane- co-fractionation of SPMV CP is determined by the C-terminal portion of the protein. This would support a separate role for this region, which is in agreement with our finding that this truncated protein can be translated separately. The co-fractionation of the capsid protein with the cell wall and membranes may indicate CP localization within these cell structures and designate protein involvement in systemic spread of the virus. To examine this possibility in some detail we studied the effects of the protein expression on systemic accumulation of SPMV, as described in the following section.

Capsid protein facilitates SPMV RNA systemic accumulation in millet plants. Previously we reported that although SPMV CP deletion mutants were competent for replication and spread when co-infected with PMV, the titer was often greatly reduced (172). From this we made a series of N- and C- terminal CP derivatives to more closely evaluate the contribution of the capsid in SPMV RNA systemic accumulation. The construct SPMV/Δ*Bsm*I-*Msc*I has a deletion from nt 248 to 456, representing the majority of the C-terminal region of the CP ORF (Fig. III-1A). Transcripts of this mutant were infectious, although the accumulation in the upper noninoculated leaves was host-dependent (Fig. III-4). Foxtail millet plants accumulated significantly less SPMV/Δ*Bsm*I-*Msc*I RNA compared to proso millet (Fig. III-4A), yet the SPMV CP deletion did not have any profound effect on PMV accumulation (Fig. III-4C). This suggested that expression of the full-length CP (or at least its C-terminal part) is essential for efficient SPMV systemic spread in foxtail plants. To examine more precisely the effect of CP

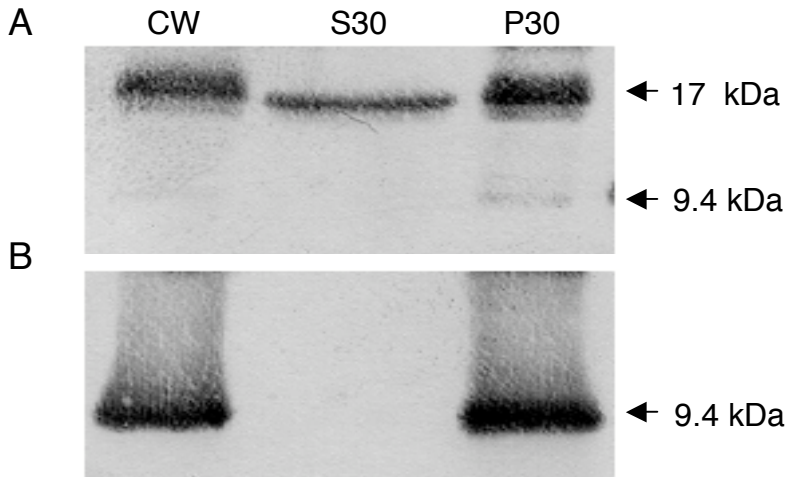

FIG. III-3. Serological detection of SPMV CP in proso millet plants collected 14 days after inoculation of PMV plus SPMV or SPMV/U-91 transcripts. The fractionation of cellular proteins by differential centrifugation is represented by CW (cell wall proteins), S30 (cytosolic proteins), P30 (membranes). The proteins (indicated by arrows) were separated by SDS-PAGE and analyzed by western blot using SPMV CP-specific antiserum. (A) Plants infected with PMV+SPMV wild type. (B) Plants infected with PMV+SPMV/U-91.

inactivation, we introduced a double frame-shift mutation (SPMV/U-301) on the SPMV cDNA. This fully suppressed SPMV CP translation, as was evident when transcripts were assayed by in vitro translation in both wheat germ extract and rabbit reticulocyte lysate (data not shown). As predicted, the SPMV CP was not present in plants infected with PMV plus SPMV/U-301 (Fig. III-5A). PMV RNA (not shown) and CP accumulation (Fig. III-5A) were not affected by SPMV/U-301. SPMV/U-301 RNA in was detected the upper noninoculated leaves of proso and foxtail millet plants but at lower levels than for SPMV wild-type infections (Fig. III-5B). Interestingly, the amount of SPMV/U-301 RNA in the upper leaves was not host-dependent, in contrast to the results for SPMV/Δ*Bsm*I-*Msc*I (Fig. III-4).

The implications of these data are that the removal of portions of the SPMV RNA (as in Fig. III-4) does not have a non-specific beneficial effect on systemic accumulation of the virus, e. g. due to size-selective permeability of the plasmodesmata (compare results of proso millet in Figures III-4 and 5). Moreover, SPMV CP, especially the C-terminal portion, significantly enhanced systemic accumulation of SPMV RNA (Fig. III-5) and this influence in conjunction with its RNA deletion is host-specific (Fig. III-4). This implies that the 9.4 kDa protein (either as a component of the full-length CP or as a separate unit) contributes in a host-dependent manner to virus spread.

SPMV CP contributes to systemic movement in foxtail plants in association with the SPMV 5'-UTR. It was found previously (172) that deletions from nt 67 to 104 (SP4) or nt 67 to 311 (SP5) on the SPMV genome did not affect systemic movement in proso millet plants while the same mutations effectively impaired systemic movement of SPMV in foxtail plants. Since the deletions also removed the SPMV start codon at nt 88,

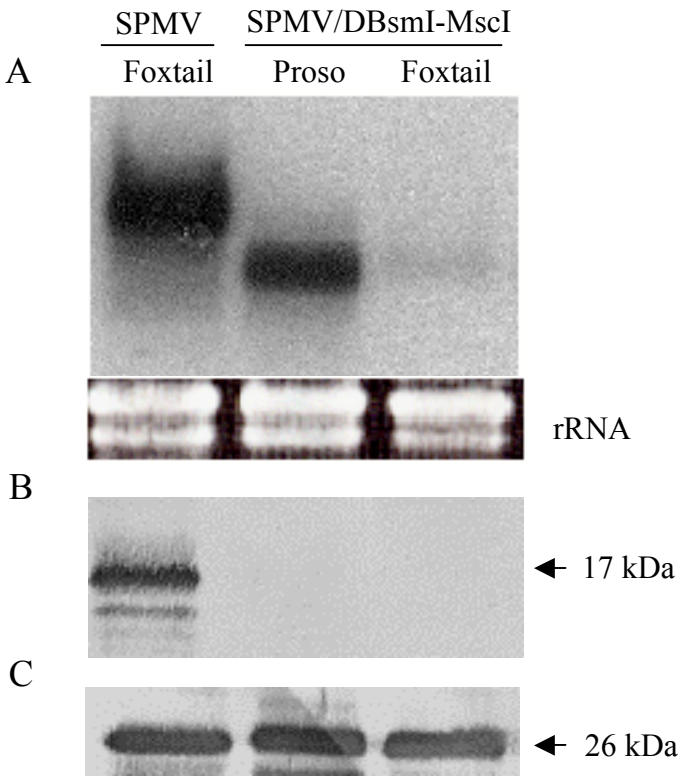

FIG. III-4. Host-dependent movement of SPMV/Δ*Bsm*I-*Msc*I in millet following co-infection with PMV. (A) RNA was isolated from upper noninoculated leaves of infected foxtail and proso millet plants. The upper panel represents an RNA blot probed with ^{32}P-labelled SPMV. The lower panel represents an ethidium bromide-stained gel to verify equal loading of RNA, represented by rRNA, for each sample. (B and C) Western blots of SPMV CP (B) or PMV CP (C) isolated from upper leaves of infected millet plants. The expressed proteins are indicated by arrows.

translation of full-length SPMV CP was abolished. Thus, these circumstances raised the possibility of cooperative involvement of the SPMV CP and the 5'-UTR in systemic spread of SPMV RNA in foxtail millet plants. In order to examine this scenario, two sets of experiments were performed in parallel.

To ensure translation of the full-length version (17 kDa) of the CP, several mutants were constructed from the wild type SPMV cDNA. A unique *Bam*HI site, producing a silent mutation, was introduced at nt 78 on the 5'-UTR. This permitted access to a small region from *Spe*I and *Bam*HI (nt 63 to 78) for further manipulations (Fig. III-1A). The second set of mutants was constructed with SPMV-AUC, a construct that expresses an N-terminal truncated version of SPMV CP (173). Then, as in case with wild type SPMV, a *Bam*HI site was created at nt 78. Both SPMV/Δ*Spe*I-*Bam*HI, based on wild type SPMV, and SPMV/AUC/Δ*Spe*I-*Bam*HI (from SPMV/AUC) have a 15 nt deletion from *Spe*I to *Bam*HI (Fig. III-1A). An insertion of four nt by digestion with *Bam*HI at position nt 78 followed by Klenow treatment also creates a *Cla*I restriction site on mutants SPMV/insert*Cla*I (wild type SPMV backbone) and SPMV/AUC/insert*Cla*I from the SPMV/AUC construct. Proso and foxtail millet plants infected with the 5'-UTR deletion and insertion mutants expressing the full-length SPMV CP were indistinguishable from wildtype SPMV infections. This was concluded from comparison of SPMV RNA and capsid protein expression with RNA- and immuno-blot analyses, respectively (Fig. III-6A).

The deletion of the N-terminal end of the SPMV CP resulted in reduced RNA accumulation (Fig. III-5). In Figure III-4, a similar effect is observed in the absence of the C-terminal portion of the CP and in Figure III-5, when the expression of SPMV CP is

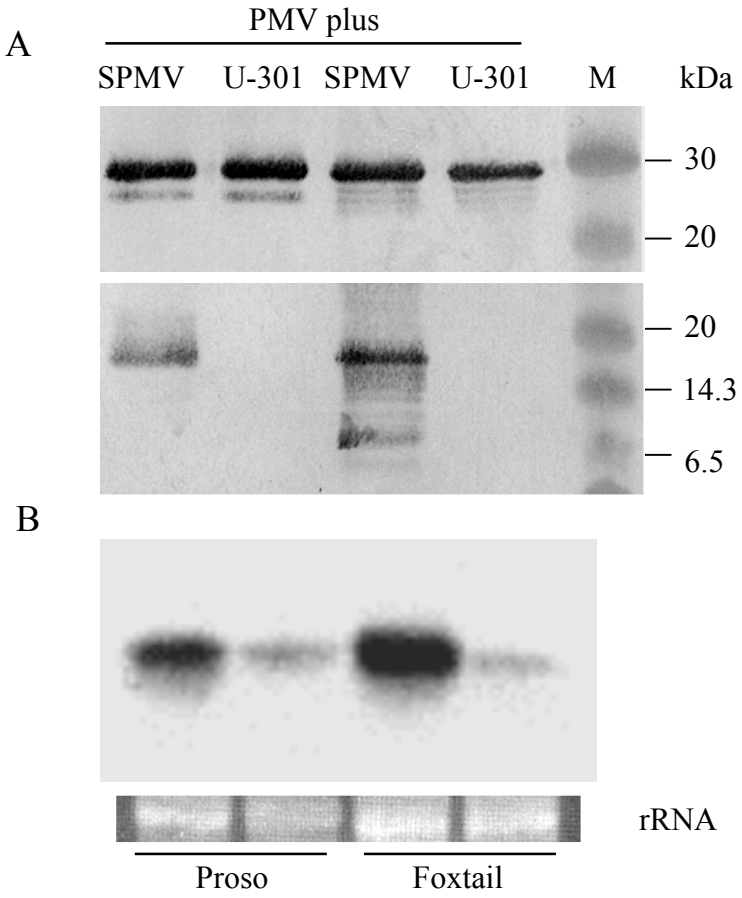

FIG. III-5. SPMV RNA accumulation in upper noninoculated leaves with SPMV/U-301, a mutant that does not express CP. (A) Immunodetection of the 26-kDa PMV CP (upper panel) and the 17-kDa SPMV CP (lower panel) in upper uninoculated leaves of proso and foxtail millet plants 14 dpi with PMV plus wild type SPMV or SPMV/U-301 (a double frame shift mutant to abolish CP expression). Molecular weight markers (kDa) are indicated on the rightmost side of the blot. (B) SPMV RNA accumulation as detected by northern blot using SPMV specific probe (upper panel). The lower panel is rRNA from an ethidium bromide-stained agarose gel representing the same volume for each sample.

completely abolished, the RNA accumulation also is perturbed. The amount of viral RNA and truncated CP detected in upper leaves of proso millet plants infected with the SPMV/AUC derived mutants (SPMV/AUC; SPMV/AUC/Δ*Spe*I-*Bam*HI and SPMV/AUC/insert*Cla*I) was significantly lower compared to plants inoculated with wild type SPMV transcripts (Fig. III-6B). In addition, we did observe host-specific effect of the 5'-UTR modifications. For example, although the parental SPMV/AUC mutant (with an intact 5'-UTR) accumulated in the upper noninoculated leaves of foxtail millet, mutants containing 5'-UTR insertions and deletions (nt 63-78) did not accumulate systemically in this host (Fig. III-6B).

Cumulatively, the data indicate that the capsid protein of SPMV facilitates systemic accumulation of SPMV in both proso and foxtail millet plants. However, the combination of CP truncation and the 5'-UTR modifications completely prohibited systemic accumulation of SPMV in foxtail millet plants.

SPMV CP specifically interacts with PMV CP. To examine interactions between the SPMV capsid protein and PMV-encoded proteins and to explore potential interactions with host proteins we conducted pull-down experiments. For this purpose, in vivo ^{35}S-methionine protein labeling of healthy and PMV+SPMV infected plants was followed by immunoprecipitation with SPMV CP specific antiserum. Extracts of PMV+SPMV-infected proso millet leaf tissue subjected to this procedure yielded three proteins. Along with the expected 17-kDa capsid protein of SPMV, two other proteins with molecular masses of approximately 26- and 40-kDa were detected (Fig. III-7). The precipitation of the ~40 kDa protein is most likely due a nonspecific reaction with SPMV CP antibody or the Protein-G agarose complex because this protein was also readily detectable in extracts

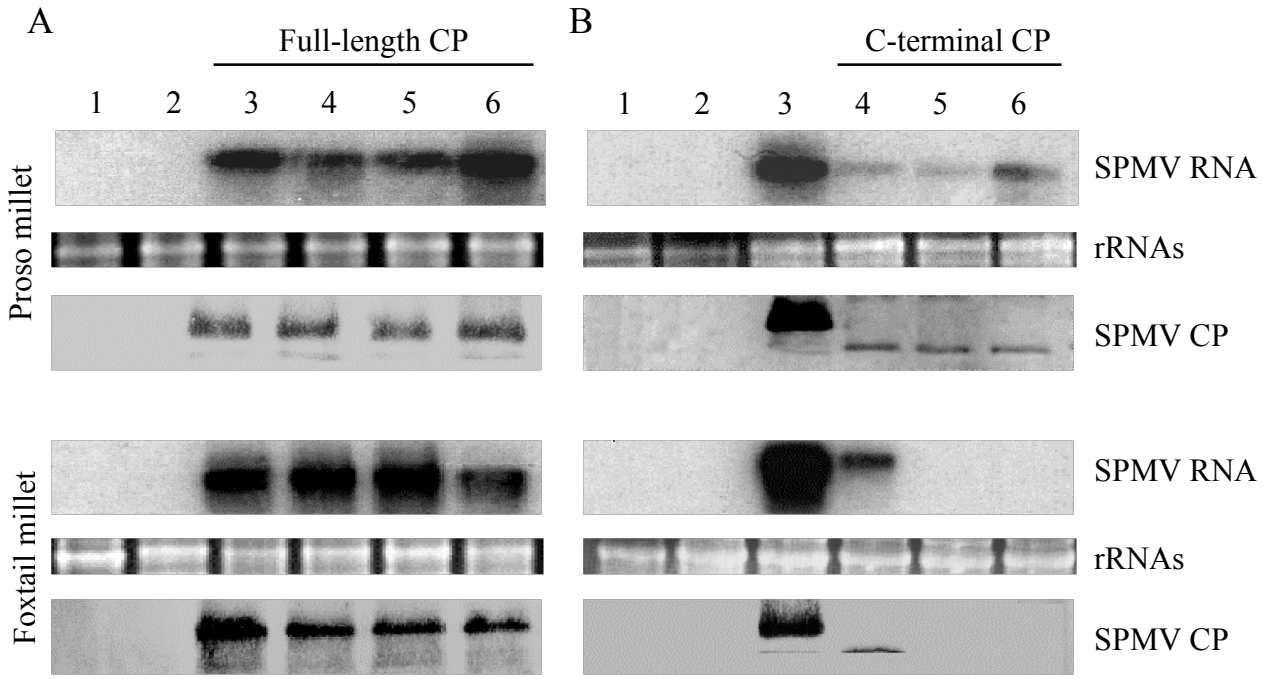

FIG. III-6. SPMV RNA and CP accumulation from 5'-UTR mutants of SPMV and SPMV/AUC. The upper noninoculated leaves of proso and foxtail millet plants co-infected with PMV and the respective mutants were used for western and northern blots. Equal loading of RNA was determined by visualizing rRNA levels on ethidium bromide-stained agarose gels, prior to transfer to membranes. Lanes 1, 2, and 3, represent mock inoculated, PMV inoculated, and PMV+SPMV infection. (A) SPMV 5'-UTR derivatives that retain the expression of the full-length CP (lanes 4 to 6), representing infections of PMV plus SPMV/*Bam*HI, SPMV/Δ*Spe*I-*Bam*HI, and SPMV/insert*Cla*I, respectively. (B) SPMV/AUC-derived constructs that express the 9.4 kDa C-terminal CP, but not wild type. Lanes 4 to 6 represent infections of PMV plus SPMV/AUC, SPMV/AUC/Δ*Spe*I-*Bam*HI, and SPMV/AUC/insert*Cla*I, respectively.

of mock inoculated (healthy) proso millet plants subjected to immunoprecipitation assay (Fig. III-7A).

In extracts from proso millet plants infected with helper virus alone, the capsid protein of PMV was immunoprecipitated exclusively by PMV but not SPMV CP antiserum (Fig. III-7B). The smaller (~26 kDa) protein was detected in plants infected with PMV+SPMV, but not mock inoculated plants. The molecular mass of the protein was identical to that of the capsid protein of helper virus (PMV). To confirm this, extracts of PMV+SPMV infected proso millet leaves were subjected to immunoprecipitation using separately, SPMV CP and PMV CP antiserum. The immunoprecipitated material was then cross-analyzed by western blot with SPMV CP or PMV CP antiserum as a probe. Our results show that pull-downs with SPMV CP antibody co-precipitated PMV CP and vice versa: immunoprecipitation with PMV CP antiserum also revealed a co-interaction with SPMV CP after western blot analysis (Fig. III-7). These data clearly show that a stable interaction occurs between PMV capsid protein and the satellite virus CP. This offers the possibility that the host-dependent effect of SPMV CP on movement may be partially related to its interaction with PMV CP.

Discussion

Initiation of translation in eukaryotes is regulated by several factors including mRNA length, the 5'-UTR, secondary structure, and the nucleotide context surrounding AUG start codons (59, 91, 117, 135). Eukaryotic mRNAs generally adhere to the first AUG rule—in most cases the AUG codon nearest the 5'-end is the sole site of initiation of translation (117). However, if the first AUG codon is positioned in suboptimal context,

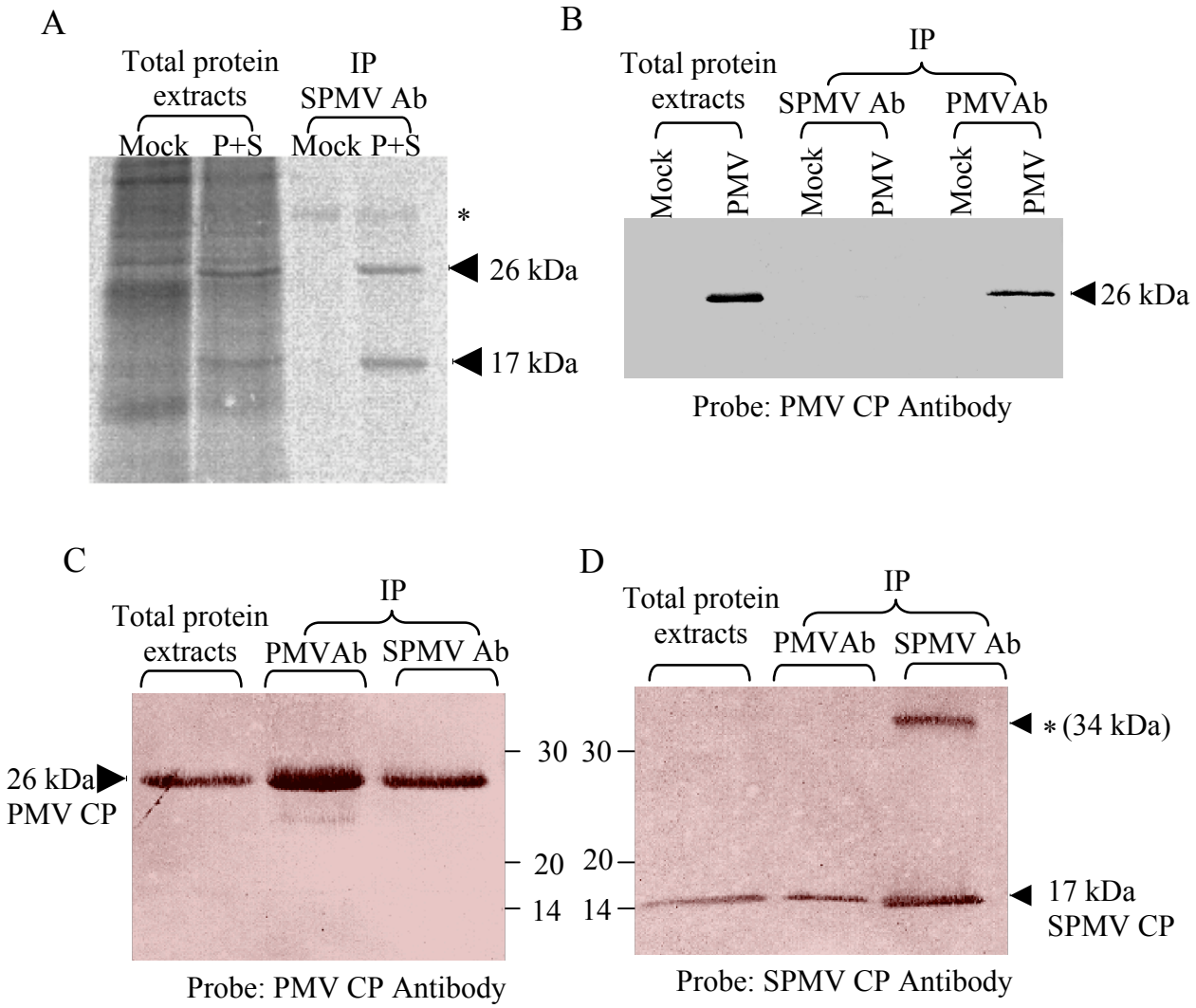

FIG. III-7. Biomolecular interactions between the PMV and SPMV capsid proteins. (A) Healthy (mock) and PMV+SPMV (P+S) infected proso millet plants were labeled in planta with [^{35}S]-methionine. The left panel shows total protein extracts and the right panel is an autoradiograph after pulldown assay using SPMV CP-specific antiserum for immunoprecipitation (IP). The asterisk indicates the position of a host protein (in healthy and infected plants). The PMV (26 kDa) and SPMV (17 kDa) capsid proteins are indicated with an arrow. (B) Immunoprecipitation and detection of PMV CP from extracts of infected proso millet leaves. PMV inoculated plants were subjected to immunoprecipitation, as separate assays, with SPMV CP or PMV CP antiserum. The resultant precipitate was eluted and subjected to western blot procedure and analyzed for the presence of PMV CP using PMV CP antibody as a probe. (C and D) Co-immunoprecipitation of SPMV and PMV capsid proteins from extracts of infected proso millet leaves. PMV+SPMV infected plants were subjected to immunoprecipitation using antiserum specific for either SPMV CP or PMV CP. The immunoprecipitates were eluted and separately subjected to western blotting and probed with polyclonal antiserum specific for PMV CP (C) or SPMV CP (D). The asterisk indicates position of dimeric form of SPMV CP (~34 kDa). The arrowheads show positions and molecular masses of precipitated proteins.

initiation may also occur from the second AUG codon, producing two proteins (118). Both cellular and viral mRNAs have been reported to produce two separately-initiated proteins by context-dependent leaky scanning (119). Our results show that the SPMV CP gene directs protein translation from the first (AUG1) and third (AUG3) start codons, both of which are in the same translational frame. The nucleotide sequence surrounding AUG1 (CUCCUGAUGG) is suboptimal; the optimal sequence context for translational initiation is GCCRCCAUGG ('R' is a purine).

Our experimental results suggest that G-rich regions immediately upstream and downstream of the AUG2 may prompt the ribosome to scan to AUG3. This was the case in planta, although the AUG2-encoded protein was weakly translated in vitro. The C-terminal portion of the SPMV CP is associated with a severe symptom phenotype in infected millet plants (173). Supportively, the results of this study revealed that the absence of 9.4 kDa C-terminal product expression in case of SPMV/UAA-234 mutant resulted in mild mosaic on millet plants when compared to severe symptoms caused by SPMV wild type and SPMV/U-91, which are both associated with C-terminal protein expression. This may further indicate a separate role of the 9.4 kDa truncated CP product in SPMV associated symptom modulation. Moreover, this phenomenon may be an effect of the biochemical properties of the C-terminal portion of SPMV CP, in that the 9.4 kDa protein associated exclusively with the cell wall- and membrane-enriched fractions of PMV+SPMV-infected millet plants. Perturbation of host membranes may play a pivotal role in the mechanism of severe symptoms induction associated with PMV+SPMV, compared to the very mild mosaic associated with PMV infection alone. More detailed

studies on protein subcellular localization are necessary to pinpoint the precise mechanism of the SPMV CP-mediated symptom modulation on millet host plants.

Recently it was shown that a satellite virus of *Macrobrachium rosenbergii*, a nodavirus that infects freshwater prawn, translates two proteins, a 17 kDa CP and an N-terminal truncated 16 kDa, from its plus-sense single-stranded RNA genome (246). Although the biological significance of this phenomena remains unclear, Widada and Bonami noted that the N-terminal domain of all satellite virus capsid proteins have a common motif containing hydrophilic amino acids and a positively charged arginine (246). This observation, along with data presented in the current work, suggests that the N-terminal domain of CP facilitates protein solubility, and as a result it is localized to the cytoplasm, where virions are assembled.

In addition to virion assembly, capsid proteins may contribute to other virus-related biological activities including replication, symptom modulation, cell-to-cell movement, and systemic spread reviewed in (28). For example, the *Brome mosaic virus* (BMV) CP is essential for systemic and cell-to-cell movement (167, 201). The very closely related *Cowpea chlorotic mottle virus* (CCMV) capsid protein is not required for cell-to-cell movement (181). However, CCMV CP is essential for systemic spread, although virion formation is not (204). Rod-shaped viruses such as *Potato virus X* (PVX) (47) and *Beet necrotic yellow vein virus* (BNYVV) (179) also require functional CP for systemic movement in plants.

The data presented in this paper demonstrate that SPMV capsid protein facilitates systemic spread of this satellite virus. The suppression of CP translation, with frame-shift and deletion mutants, significantly decreased the accumulation of SPMV RNA in upper,

noninoculated leaves of plants. Moreover, the results of this study also show that SPMV CP in association with a small portion of the 5'-UTR facilitates systemic SPMV RNA accumulation in a host-specific manner. The subcellular co-fractionation of SPMV CP to membrane- and cell wall-enriched fractions suggests a functional involvement as a movement-associated protein in systemic spread of the satellite virus.

It remains to be resolved why in foxtail millet the expression of the N-terminal domain of SPMV CP compensates for deletions or insertions of nucleotides in the 5'-UTR, while in proso millet the same mutations did not impair SPMV systemic spread regardless of the presence of CP. Interactions with viral RNA is another characteristic biochemical feature associated with movement proteins of plant viruses (43), one that we have also reported for SPMV CP (57). Perhaps systemic spread of SPMV in foxtail millet requires an interaction between the 5'-UTR and N-terminal region of the capsid protein. In contrast, the lack of such an interaction in proso millet may be provided by as yet unidentified host, biochemical and/or physiological factors.

Alternatively (or in addition), the compensatory effect of CP on SPMV systemic translocation in foxtail millet may involve a specific CP interaction with the capsid protein of the helper virus (PMV), while such interaction is not essential for systemic movement in proso plants. In support of this hypothesis is our observation that co-precipitation of PMV capsid protein using SPMV CP antiserum was detected exclusively when full-length SPMV CP was expressed in infected plants (not shown). The absence of interaction between the 9.4 kDa truncated SPMV CP and the PMV CP may lead to explanations for the decreased amount of SPMV RNA accumulation in upper leaves of proso and foxtail millet infected with SPMV/AUC mutants versus wild type (Fig. III-6).

The wild type CP may also protect the RNA from degradation via efficient RNA packaging and virion formation. Overall, the mechanism of host-specific systemic spread of SPMV likely involves a complex cross-specific interaction between SPMV RNA, host factors and movement proteins of the helper virus. SPMV RNA may direct synthesis of N-terminal truncated proteins as accessory factors to enhance SPMV infectivity, including replication and movement, by directing the RNA to the cell wall and membranes.

In summary, our results indicate that multifunctional features of SPMV CP are essential to sustain its robustness when supported by a PMV infection in a host plant. The specific interactions between PMV and SPMV capsid proteins also suggest that important molecular interactions occur between the satellite virus and helper virus in the plant. It is noteworthy to mention here, that the previously documented pattern of subcellular localization of PMV CP (232) is strikingly similar to results presented here on fractionation of SPMV CP at subcellular level. Interestingly, a recent study showed that contaminating virions of SPMV are incorporated into PMV crystals by insertion into the interstices between PMV virions in the crystal lattice (140). Is co-localization of PMV CP and SPMV CP important for SPMV (and PMV) movement? At the very least SPMV RNA must be in proximity to the PMV replicase proteins, perhaps the SPMV CP acts as a guide for intracellular localization.

CHAPTER IV

THE COMPLEX SUBCELLULAR DISTRIBUTION OF SATELLITE PANICUM MOSAIC VIRUS CAPSID PROTEIN REFLECTS ITS MULTIFUNCTIONAL ROLE DURING INFECTION

Introduction

Satellite viruses and satellite nucleic acids (satellite RNAs and satellite DNAs) represent a unique group of subviral agents that rely on a helper virus for replication and movement (210, 218). Unlike satellite nucleic acids, satellite viruses encode their own capsid protein (CP) to package the genome into virions. So far, four plant satellite viruses have been reported in pair-specific relationships with their helpers (61, 210, 218). A possible satellite virus has been reported associated with *Macrobrachium rosenbergii nodavirus* (MrNV) in freshwater prawn (246). Satellite panicum mosaic virus (SPMV) completely depends on its helper *Panicum mosaic virus* (PMV) (Genus *Panicovirus,* Family *Tombusviridae*) for replication and systemic spread in host plants (208, 232, 233). PMV has a positive-sense single-stranded RNA genome, which encodes six open reading frames (ORFs) (232, 233). The replicase components (p48 and p112) are expressed directly from the genomic RNA whereas the 26-kDa CP and three smaller proteins are translated from a polycistronic subgenomic RNA(232). Our previous studies demonstrated that synergism occurs in co-infection of SPMV and PMV in millet plants, which includes an increased infection rate of PMV, severe leaf mosaic symptoms, growth stunting and failure to set seed (208).

The virion crystal structure has been determined for three of the four known plant satellite viruses (7, 8). Although their CP monomers share a similar jelly-roll core structure of a ß-barrel, there is obvious difference in the organization of secondary structural elements, placement of subunits, and interactions among adjacent subunits (7). Amino acid sequence comparison analysis of the CPs of plant satellite viruses reveals very little similarity except that they all have a conserved N-terminal arginine-rich motif (N-ARM). In addition, SPMV CP shares a 46% identity to the nonstructural protein (P20) encoded by a satellite RNA (satRNA) associated with *Bamboo mosaic virus* (BaMV) (132, 133). The satRNA P20 protein also features an N-ARM region, which is required for its cooperative binding of the cognate RNA (231) and for its role in promoting the movement of BaMV satRNA.

SPMV has a small positive-sense single-stranded RNA genome of 824 nucleotides (nt), which directs the synthesis of a 17-kDa CP to assemble the T=1 virion (142). In addition to packaging its cognate RNA into virions, SPMV CP is able to encapsidate a PMV associated satellite RNA (57). As expected, SPMV CP binds SPMV RNA in a co-operative manner in gel mobility shift assays (57). However, SPMV CP performs in functions in addition to virion formation during co-infection with PMV. For instance, SPMV RNA moves systemically but very inefficiently without SPMV CP whereas the presence of SPMV CP significantly enhances the systemic accumulation of SPMV RNA as shown in chapter III. Furthermore, the deletion of a hairpin region in the 5'-UTR affects SPMV RNA movement in a host-specific manner (174), an effect that is complemented by the presence of full-length SPMV CP. Although not required for SPMV RNA replication, the absence of SPMV CP causes the generation of SPMV-

defective interfering RNA, suggesting its possible implication in SPMV RNA stabilization (173). In addition, SPMV CP is also involved in symptom exacerbation in host plants (172-174, 208). Taken together, SPMV CP plays a multi-functional role that is crucial for the establishment of a robust infection.

In this study we developed a series of experiments to differentiate some of the roles at the biochemical level. A domain responsible for SPMV CP self-interaction was identified and it was shown that SPMV CP accumulated in both cytosolic and noncytosolic fractions. However, chromatography studies and site-directed mutagenesis experiments indicated that virion formation is associated with the cytosolic accumulation of SPMV CP. The N-ARM of SPMV CP was crucial for SPMV genomic RNA binding and encapsidation. Successful systemic SPMV RNA accumulation also requires the functional N-ARM of SPMV CP, but surprisingly this was independent of SPMV particle formation. Subcellular fractionation study of SPMV infected tissues and fluorescent microscopy of GFP-tagged SPMV CP indicated that the noncytosolic SPMV CP is localized in the cell wall, nucleolus/other membranous organelles, and the membrane system. Taken together, SPMV CP plays a multifunctional role in viral infection, including but not limited to encapsidation and facilitating SPMV RNA movement and it is reasonable that a complex, but coordinated, subcellular localization process of SPMV CP is important for the fulfillment of its multifunctional roles.

Material and methods

Plant inoculation and maintenance. Proso millet plants (*Panicum miliaceum* L. cv. Sunup) were grown in climate controlled growth chambers (25°C, 14 h of light; 20°C,

10 h of dark). A PMV cDNA construct linearized with *Eco*ICRI, and SPMV cDNA constructs linearized with *Bgl*II were used as templates for in vitro transcription, as previously described (173). Proso millet plants at the two-leaf stage were mechanically rub inoculated with mixture of equal volumes of uncapped RNA transcripts (SPMV and PMV) and RNA inoculation buffer. *Nicotiana benthamiana* Domin. plants were grown under the same conditions and mechanically rub-inoculated at the three-leaf stage with the mixture of equal volume of corresponding RNA transcripts and RNA inoculation buffer.

Co-immunoprecipitation. All tested SPMV CP derivatives were labeled with [^{35}S]-methionine using a transcription-translation coupled wheat germ extract system (Promega, Madison, WI) according to the manufacturer's instructions. Equal volumes of labeled and unlabeled in vitro translation products were mixed and incubated at room temperature (RT) for 2 hr. The final volume was brought up to 500 µl with washing buffer [150 mM HEPES (pH 7.5), 1% Triton X-100, 150 mM NaCl, 5 mM EDTA, 2 mM dithiothreitol (DTT)] and 2 µl of HA-specific rabbit monoclonal antibodies (Sigma, St. Louis, MO) were added and gently mixed for 2 hr at RT. Following the addition of 30 µl ImmunoPure immobilized protein G agarose beads (Pierce, Rockford, IL), the mixtures were then shaken another 2 hr at RT. The beads were washed six times with ice-cold washing buffer and the immunoprecipitated material was separated by sodium dodecyl sulfate-15% polyacrylamide gel electrophoresis (SDS-PAGE) followed by autoradiography. The specificity of anti-HA antibodies was verified by immunoprecipitation of [^{35}S]-methionine-labeled WT capsid protein as a negative control.

Western blot assays. Protein samples were separated by SDS-PAGE in 15% polyacrylamide gels and transferred to nitrocellulose membranes (Osmonics, Westborough, MA). SPMV CP or PMV CP specific polyclonal antibodies were applied at a dilution of 1:2,000 (173). Alkaline phosphatase conjugated to goat anti-rabbit antiserum (Sigma, St. Louis, MO) was used as a secondary antibody at a dilution of 1:1,000. The immune complexes were visualized by the addition of tetrazolium-5-bromo-4-chloro-3-indolyl phosphate as described before (173).

Construction of SPMV mutants. The QuikChange kit (Stratagene, La Jolla, CA) was used to make R7/8, R7-12, 130D and ΔC6 via site-directed mutagenesis. The primers were designed following the manufacturer's instructions. The primers for R7/8 are: forward as 5'-ctaagggtaccagCGCatctaatcgtcggg-3' and reverse as 5'-cccgacgattagatGCGctggtacccttag-3'. The primers for R7-12 are: forward as 5'-agcgcatctaatcTCTcggcgggctcc-3' and reverse as 5'-ggagcccgccgAGAgattagttgcgct-3'. The primers for 130D are: forward as 5'-gacggactcgtgGAtaccaagggtga-3' and reverse as 5'-tcacccttggtaTCcacgagtccgtc-3'. All mutated nucleotides are indicated in capitals. The primers for ΔC6 are: forward as 5'-taggctggcgcct**TAA**agcgagcttcag-3' and reverse as 5'-ctgaagctcgct**TTA**aggcgccagccta-3'. The premature stop codon and its complementary sequence are shown in bold uppercase. *E. coli* transformed with pDEST17 (Invitrogen, Carlsbad, CA) based constructs permissive for over-expression of SPMV CP derivatives, deletion mutants (A, B, C and D), substitution mutant (NHA) and insertion mutant (82F), were acquired in the demonstration for a novel modified recombination PCR protocol in chapter II.

RNA analyses. Total RNA from 300 mg of inoculated or systemically infected leaves of millet plants were extracted at 14 dpi. Symptomatic leaf tissues were pulverized in 1 ml of ice-cold extraction buffer [100 mM Tris-HCl (pH 8.0), 1 mM ETDA, 0.1 M NaCl, and 1% SDS] and extracted twice with phenol-chloroform (1:1, vol/vol) at RT. Total RNA was precipitated with 8 M lithium chloride (1:1, vol/vol) at 4°C for 30 min. The resulting pellets were washed with 70% ethanol, resuspended in 300 μl RNase-free distilled water, and used for RNA blot hybridization. Approximately 5μg of total plant RNA was electrophoretically separated in 1% agarose gels and transferred to nylon membranes (Osmonics). SPMV RNA was detected by hybridization with α-[^{32}P]-dCTP-labeled -SPMV-specific probes as previously described (173).

Gel-filtration and ion-exchange chromatography. Infected proso millet leaf tissue (3 g) was homogenized in 3 ml extraction buffer [200 mM Tris-HCl (pH 7.4), 5 mM DTT, 150 mM NaCl] and centrifuged twice for 10 min at 10,000 × *g* at 4°C. For gel filtration chromatography, the supernatant (approximately 1 ml) was loaded and fractionated on a 2.5 × 80 cm column packed with Sephacryl S-200 high-resolution resin (Amersham, Piscataway, NJ) at a flow rate of 1.3 ml/min. The column was equilibrated with elution buffer [50 mM Tris-HCl (pH 7.4), 100 mM NaCl] and calibrated with gel filtration MW standards (12–200 kDa) (Sigma, St. Louis, MO). For anion-exchange chromatography, 10 g infected leaf tissue was homogenized in 25 ml of loading buffer [50 mM sodium phosphate (pH 7.4), 5 mM DTT]. The extract was centrifuged twice for 10 min at 10,000 × *g* at 4°C. The supernatant was loaded onto a 15 × 2.5 cm column packed with MacroPrep DEAE Support (Bio-Rad, Hercules, CA). The column was washed with 200 ml of loading buffer and the bound proteins were subsequently eluted

with a gradient of increasing concentrations of NaCl from 50 to 1000 mM. For both chromatography assays, every 3 fractions were combined (total = 9 ml) and checked for the presence of either SPMV CP or PMV CP by western blot.

Whole virion gel assay. Symptomatic leaf tissue (500 mg) was ground in 2 ml extraction buffer [0.2 M sodium acetate (pH 5.2)]. The homogenate was incubated at 37°C for 30 min to degrade any unprotected RNAs, including host cell RNA and unbound viral RNAs, using the endogenous plant RNases. The extract was then centrifuged at 10,000 rpm, 4°C, for 10 min and the supernatant was transferred to a new tube. PMV and SPMV virions were precipitated on ice for 30 min in the presence of 12% polyethylene glycol (PEG)-8000 and 300 mM NaCl. The virions were then pelleted by centrifugation at 10,000 rpm, 4°C, for 10 min. After resuspension of pelleted virions in 0.05 M sodium acetate (pH 5.5), a second precipitation was performed overnight at 4 ^{O}C as described above. The final virion pellet was dissolved in 50 µl of 0.05 M sodium acetate (pH 5.5) and 5 µl was resolved on a 1% Tris-glycine agarose gel in 2 × Tris-glycine buffer [10 mM Tris (pH 8.0), 76 mM glycine]. Whole virions were visualized by ethidium bromide staining and transferred to nylon membrane for the SPMV-specific RNA assays (173).

Northwestern blot. A 1.5 ml culture of induced *E. coli* BL21 (DE3) (Stratagene, La Jolla, CA] cells over-expressing SPMV CP and its derivatives were pelleted and boiled in 2% SDS-sample buffer, electrophoresed by 15% SDS-PAGE and transferred to nitrocellulose membrane as previously described (209). The membrane was then blocked for 2 hr at RT in binding buffer [10 mM Tris-HCl (pH 7), 1 mM EDTA, 1 × Denhardt's reagent] containing 300 mM NaCl and 50 µg/ml total RNA extracted from healthy plants.

The [^{32}P]-labeled SPMV transcript was added and incubated with the blot for 2 hr at RT. The membrane was washed three times with binding buffer plus 300 mM NaCl and exposed to X-ray film overnight.

Subcellular fractionation. Differential centrifugation was conducted using a slightly modified method previously described (63, 209). Briefly, 1 g tissue was homogenized in 1 ml extraction buffer [200 mM Tris-HCl (pH 7.4), 5 mM DTT, 50 mM NaCl] and filtered through double layers of cheesecloth. The extract was centrifuged at 1,000 × *g*, 4°C, for 15 min. The pellet was washed with extraction buffer and centrifuged several times until a white residue remained which contained the cell wall-enriched fraction. The used extraction buffer was combined with the supernatant and centrifuged at 8,000 × *g*, 4°C for 15 min. This enriched the organelles in the pellet, including nuclei, chloroplasts, mitochondria and lysosomes. The supernatant was then centrifuged at 30,000 × *g*, 4°C for 20 min to collect the pellet of membrane debris and the supernatant representing cytosolic material.

Microscopic imaging. A *Tomato bushy stunt virus* (TBSV) based vector (207) was used to deliver GFP (a kind gift from Dr. A. O. Jackson) or GFP-tagged SPMV CP into *N. benthamiana* plants. The ORFs of GFP and GFP:SPMV CP fusion protein were inserted in-frame with the original start codon of TBSV CP respectively for the optimal translation (206). Leaf epidermis of green fluorescent regions under UV (wavelength = 365 nm) was carefully peeled and used for fluorescence microscopy (211) to visualize the subcellular localization of GFP-fused SPMV CP. Microscopic observations were made using an Olympus BX51 microscope (Olympus America, Melville, NY) equipped with Olympus DSU spinning disc confocal imaging system. A motorized stage allowed for

optical sectioning along the Z-axis. An Olympus DP70 camera was used for image acquisition of DIC and wide field fluorescence images. A Q-imaging MicroPublisher RTV 5.0 camera (Q-Imaging, Burnaby, B.C., Canada) was used for Z-sectioning imaging. The GFP signal was excited and detected at the wavelength of 488 and 507 nm, respectively. Pictures were processed by Image J (http://rsb.info.nih.gov/nih-image).

Results

SPMV CP exists in both cytosolic and non-cytosolic fractions and can be detected as SDS-resistant dimers. In chapter III, we observed that the addition of detergent (Triton X-100 or SDS) to the protein extraction buffer increased the amount of SPMV CP detected by western blot assay. This led to an assumption that SPMV CP may be represented in both soluble (cytosol) and insoluble (mainly cell wall and organelles) fractions. To test this, protein extracts from SPMV+PMV infected millet plants were centrifuged twice at 10,000 × *g* at 4°C for 10 min, after which the non-cytosolic fractions (pellet) and cytosolic fractions (supernatant) were collected and tested for the presence of SPMV CP. As expected, SPMV CP was consistently detected in both the non-cytosolic and cytosolic fractions (Fig. IV-1A).

Interestingly, SPMV CP was detected as both monomers and SDS-resistant dimers (Fig. IV-1A). Studies of genomic RNA packaging of spherical plant viruses indicate that encapsidation proceeds as cooperative addition of CP dimers (41, 180, 263). From this, CP dimers are deemed the basic building blocks for viral capsid (263). To determine the regions on SPMV CP that mediate self-interaction and dimerization, we created a series of sequential deletion mutants of SPMV CP, each of which contained an in-frame step-

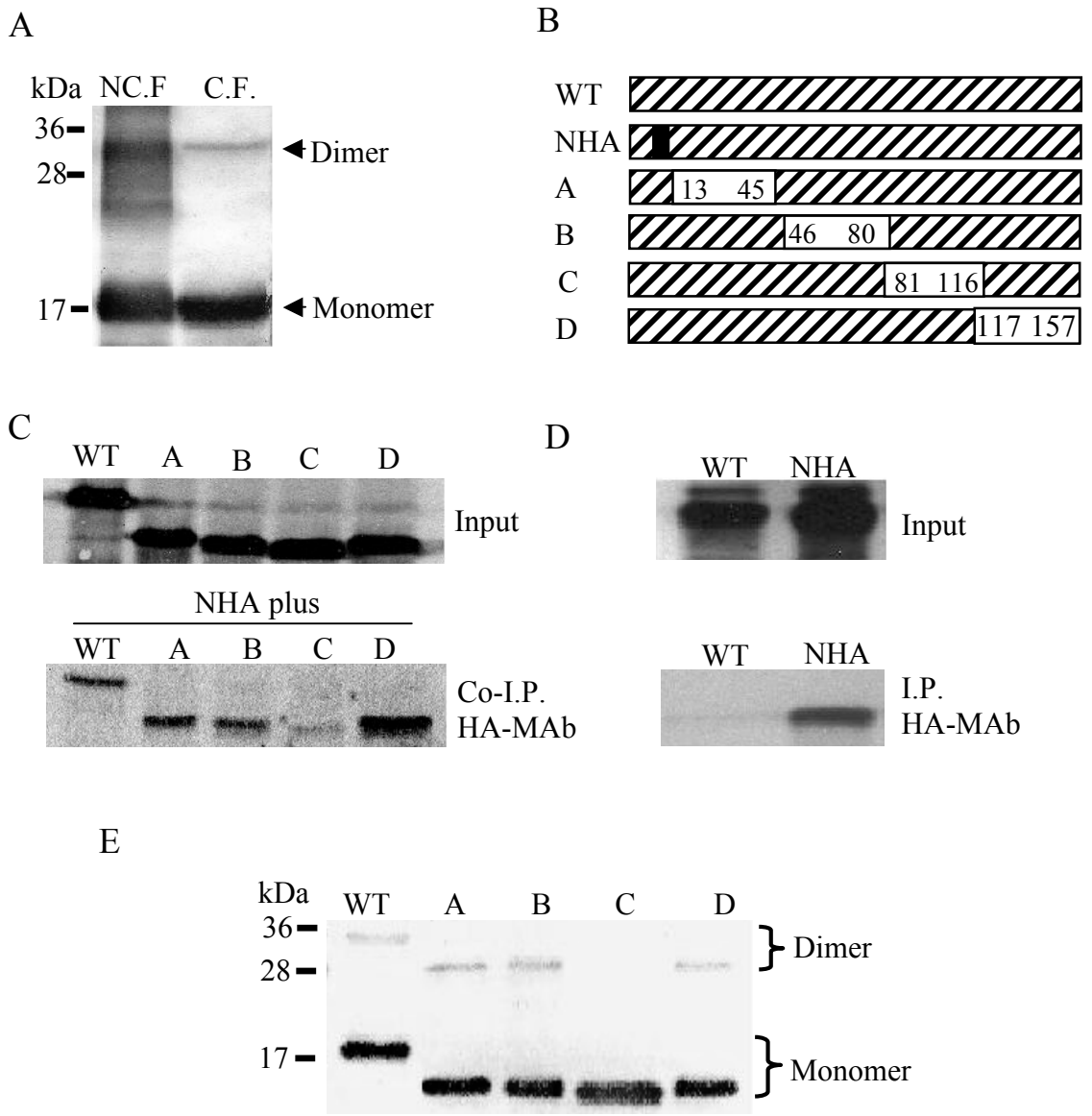

FIG. IV-1. Distribution and self-interaction of SPMV CP. (A) Immunodetection of SPMV CP in non-cytosolic (NC.F.) and cytosolic (C.F.) fractions of PMV+SPMV infected proso millet plants. The relative positions of SPMV CP dimers and monomers are indicated by arrows. (B) Schematic representation of SPMV CP mutants analyzed by co-immunoprecipitation. WT represents the CP open read frame (ORF) of SPMV type strain. Mutant NHA contains the sequence substitution of SPMV CP amino acids (AA) 4 to 12 with an HA epitope (YPYDVPDYA). A, B, C, and D represent mutants with four different regions of SPMV CP truncated: AA 13 to 45, AA 46 to 80, AA 81 to 116 and AA 117 to157, respectively. (C) Co-immunoprecipitation assays of SPMV CP deletion mutants to identify regions associated with self-interaction. All tested SPMV CP derivatives are [^{35}S]-methionine-labeled using a wheat germ extract in vitro translation system and are normalized for equal amount of application (upper panel). Each [^{35}S]-methionine labeled SPMV CP derivative is mixed with unlabeled NHA and then subjected to co-immunoprecipitation with anti-HA monoclonal antibodies (HA-MAb) (lower panel). (D) Analysis of the anti-HA monoclonal antibody specificity. [^{35}S]-methionine labeled WT- and NHA- SPMV CP (upper panel) were subjected to precipitation with HA-MAb and subsequent detection by autoradiography (lower panel). (E) Immunodetection of SDS-resistant SPMV CP dimers. Designation of WT SPMV CP and derivative mutants is listed above the blot. The relative positions of SPMV CP dimers and monomers are indicated. Molecular weight markers in kilodaltons (kDa), are indicated on the left of panels A and E.

wise deletion of ~30 AA from the N- to the C- terminus of the ORF (Fig. IV-1B). These mutants were first analyzed for their ability to interact with full-length SPMV CP using co-immunoprecipitation assays. Wild type (WT) SPMV CP and each of the four truncated derivatives (A, B, C, and D) were labeled by in vitro translation with methionine. An equal amount of [^{35}S]-labeled SPMV CP derivatives was mixed and incubated with the unlabeled CP of mutant NHA (Fig. IV-1C, upper panel). The NHA CP derivative contained the sequence exchange of amino acid (AA) 4-12 (KRSRRSNRR) of SPMV CP for the 9 AA hemagglutinin (HA) epitope (YPYDVPDYA) (Fig. IV-1B). Then each paired mixture (NHA with WT SPMV CP or each of A, B, C, D) was subjected to co-immunoprecipitation with anti-HA antibodies. Full-length WT SPMV CP was successfully precipitated, indicating its interaction with the unlabeled NHA CP derivative (Fig. IV-1C, lower panel). Similar results were obtained for the CP truncation derivatives A, B and D when tested using co-immunoprecipitation (Fig. IV-1C, lower panel). However, a significantly weaker signal was reproducibly detected for CP truncation derivative C, which indicated its compromised interaction with the NHA mutant (Fig. IV-1C, lower panel). The biological importance of region C (AA 81-116) was suggested by our previous observation that a SPMV mutant with deletions involving this region became more liable for the rapid accumulation of defective interfering RNAs (DIs) (173). As a control, [^{35}S]-methionine labeled WT SPMV CP was subjected to immunoprecipitation with anti-HA antibodies. As predicted, no signal was detected in the following autoradiography (Fig. IV-1D). Having confirmed the importance of CP-CP interaction, each SPMV CP truncation mutant was overexpressed in *E. coli* BL21 (DE3)

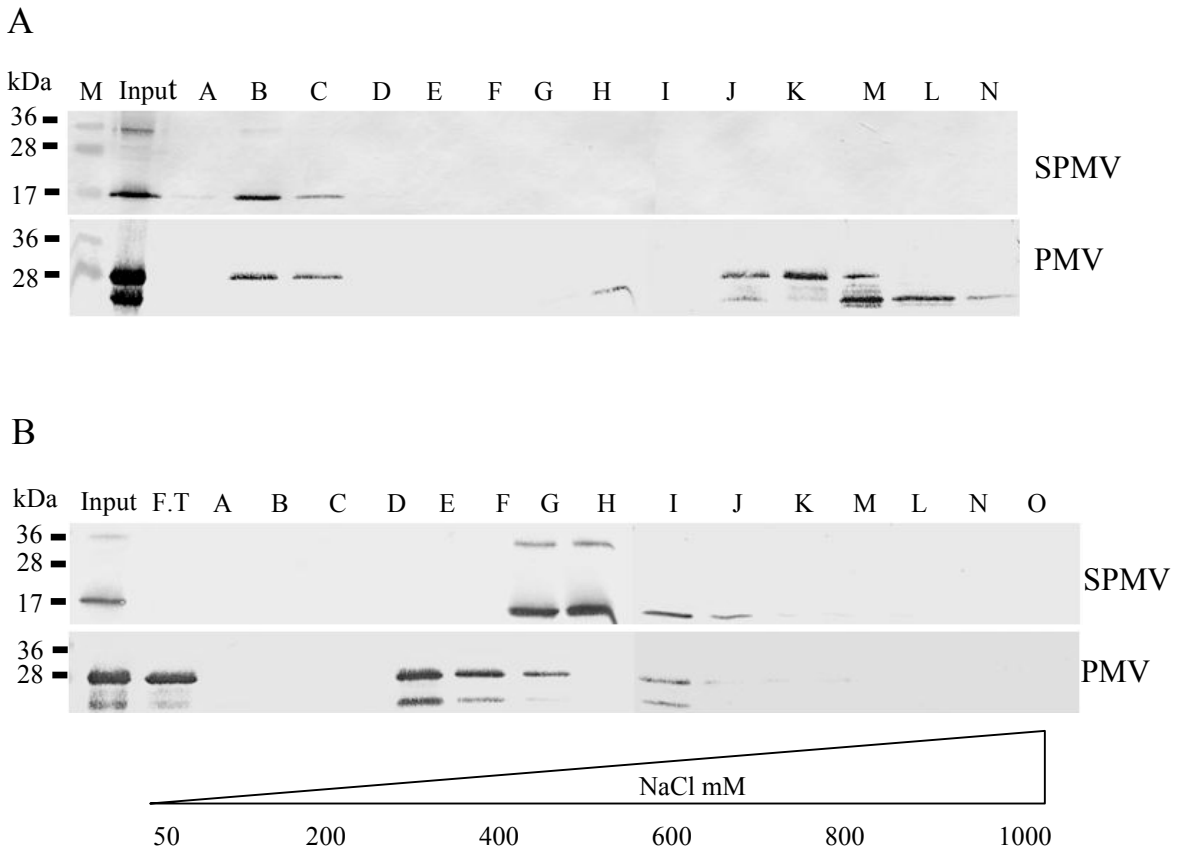

FIG. IV-2. Chromatography study of cytosolic protein extracted from proso millet plants infected with PMV and SPMV. (A) Gel filtration chromatography on a Sephacryl S-200 column. Each of the alphabetically annotated lanes (A through N) contains three adjacent fractions and each fraction is approximately 3 ml. Input is included as the positive control. The distribution of 17-kDa SPMV CP (upper panel) and 26-kDa PMV CP (lower panel) was monitored by western blots with the appropriate specific polyclonal antibody. Protein markers (M), in kilodalton (kDa), were indicated on the leftmost sides of the blots. (B) Anion-exchange chromatography of PMV and SPMV infected proso millet plants on DEAE column. Fractions (A through O) are analyzed for the presence SPMV CP and PMV CP in the same manner as described in (A). Input and flowthrough (F.T.) are indicated. The bottom panel represents the NaCl gradient (from 50 mM to 1 M) used to elute proteins from the DEAE column.

cells from a pDEST17-based vector to further analyze the formation of SDS-resistant dimers. As expected, the deletion of AA 81-116 (mutant C) disrupted the formation of SDS-resistant SPMV CP dimers (Fig. IV-1E) in agreement with the result of co-immunoprecipitation assays (Fig. IV-1C). In contrast, full-length SPMV CP and other truncation derivative (A, B and D) were readily detected as dimers (Fig. IV-1E).

Soluble SPMV CP exists in the form of a high molecular weight complex. To study the biological and biochemical importance of SPMV CP dimers, we attempted to purify these using gel-filtration chromatography through a Sephacryl S-200 packed column. Surprisingly, SPMV CP was eluted exclusively in the form of high molecular weight complexes (>600 kDa) (Fig. IV-2A, upper panel). In addition, SPMV RNA co-eluted with SPMV CP (data not shown). Together, these indicate that the cytosolic SPMV CP is in the form of SPMV virions and/or other high molecular weight ribonucleic-protein (RNP) complexes but not as monomers or dimers. In contrast, CP of the helper virus (PMV) was detected as a high molecular weight complex as well as dimers and monomers (Fig. IV-2A, lower panel).

To exclude the possibility that SPMV CP was not detectable in the form of dimers or monomers due to the dilution effect during gel-filtration chromatography, DEAE ion-exchange chromatography was performed and the distribution of SPMV CP and PMV CP was monitored. Based on amino acid composition, SPMV CP is a basic, positively charged protein (pI=10.12). However, SPMV CP could only be detected as a single elution peak at NaCl concentrations exceeding 350 mM. In addition, we found SPMV RNA also co-eluted with SPMV CP in DEAE ion-exchange chromatography (data not shown). In contrast, no SPMV CP was detected in the flow-through (fraction containing

positively charged proteins) after DEAE fractionation (Fig. IV-2B, upper panel). This indicates that cytosolic SPMV CP existed as an acidic, negatively charged protein complex. This apparent conundrum may be explained by a recent report whereby in the encapsidation process, the heavily positively charged regions of SPMV CP are buried as the interior capsid surface to bind SPMV RNA whereas the negatively charged regions are exposed as exterior capsid surface (139). This hypothesis is supported by the observation that the recombinant movement protein (MP) of *Tobacco mosaic virus* (pI=8.91) was eluted in the flow-through as free dimers but in the fractions of high NaCl concentrations as ssRNA associated complex in anion-exchange chromatography (22). In contrast, PMV CP displayed a more complicated distribution profile after DEAE fractionation (Fig. IV-2B, middle panel). One elution peak of PMV CP was detected in the flow-through and another two distinct peaks were detected at concentrations of 250 mM NaCl and 550 mM NaCl (Fig. IV-2B, lower panel). Taken together, we conclude that cytosolic (soluble) SPMV CP is present either as virions and/or in the form of negatively charged high molecular weight RNP complexes but not as free subunits. Furthermore, the first set of experiments provide evidence that the robust CP self-interaction mediated by a specific C-proximal region leads to the formation of stable SPMV CP dimers which are the basic building unit of the viral capsid and can not be totally disrupted even in the presence of strong ionic detergents such as SDS.

CP mutants defective in encapsidation are compromised in solubility in the cytosol/cytosolic accumulation. To study the correlation between in vivo RNA encapsidation and SPMV CP solubility in the cytosol, we introduced specific mutations at different sites of the SPMV CP and the resulting mutants were analyzed (Fig. IV- 3A).

The N-ARM of SPMV CP contains two arginine (R) pairs at amino acids 7/8 and 11/12. Mutant R7/8 was generated by changing the codons for arginine residues 7 and 8 into those for serine and alanine, respectively. Using R7/8 as parental construct, mutant R7-12 was created by changing the codons for the other arginine pair (RR 11/12) into those for serine and alanine as well. The CP derivative encoded by mutant 82F contained the coding sequence of a six amino acid FLAG epitope (DYKDDD) inserted between the codons of AA 81 and 82. Mutant 130D contained the substitution of the serine codon with an aspartic acid codon (D) at the site of AA 130. Mutant ΔC6 was created by introducing a premature stop codon before the coding sequence of the last six amino acids of SPMV CP.

The positions of these five target sites were selected based on the X-ray crystallography data (8). The N-ARM plunges into the interior of virions where it engages the SPMV genomic RNA, AA 82 is in the middle of a loop region, and AA130 is at the five-fold symmetry center also within a loop. The last 6 amino acids on SPMV CP are not essential for the "jelly-roll" core structure of SPMV CP and presumably not essential for virion assembly.

Transcripts of each SPMV derivative construct were co-inoculated with infectious PMV transcripts onto proso millet plants. At 14 dpi, symptomatic upper leaves were harvested and subjected to whole virion gel assays. As expected, PMV virions were detected in all infected plants (Fig. IV-3B, lower panel) and SPMV virions were detected in plants infected with PMV plus WT SPMV (Fig. IV-3B, upper panel). Of the five tested mutants, SPMV virions could be detected only for R7/8 and ΔC6 infected plants as a band moving toward the position corresponding to WT SPMV virions, though the

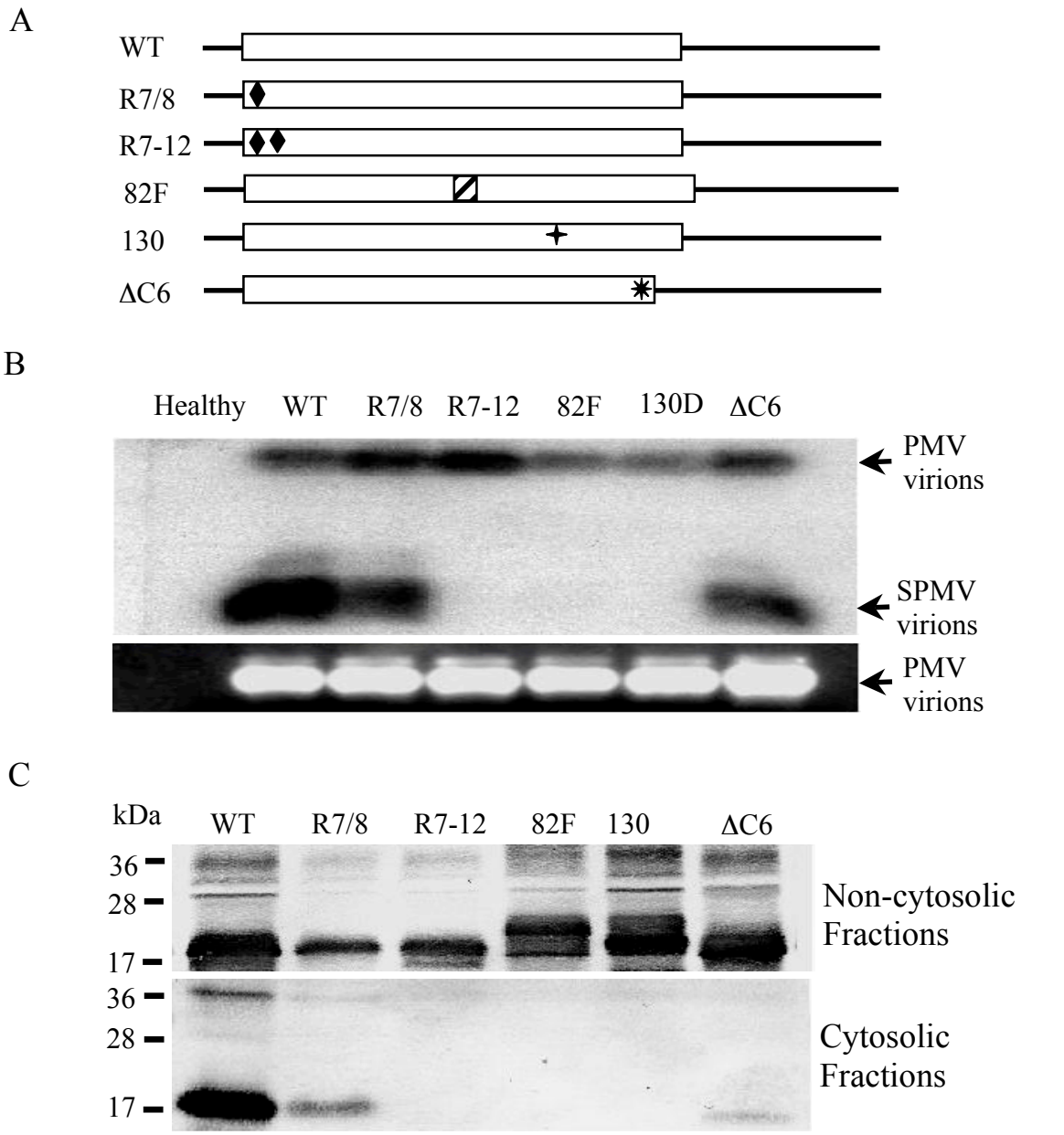

FIG. IV-3. Encapsidation and distribution analyses of SPMV CP mutants. (A) Schematic representation of SPMV CP mutants tested. Mutant R7/8 represents the exchange of arginine codons at amino acid (AA) residues 7 and 8 for serine and alanine codons (indicated by a diamond). Mutant R7-12 has the additional exchange of arginine codons at AA residues 11 and 12 for serine and alanine codons (two diamonds). Mutant 82F contains a FLAG epitope (striped box) inserted between AA residues 81 and 83. Mutant 130D contains substitutionthe of the serine codon of AA residue 130 with an aspartate codon (star). ΔC6 represents the truncation of the last 6 amino acids by introducing a premature stop codon (asterisk). (B) Encapsidation assay by whole virion agarose gel electrophoresis. Encapsidated RNAs are transferred to a nylon membrane for hyridization with ^{32}P-labeled SPMV cDNA-specific probes (upper panel). The positions of PMV and SPMV virions are indicated by arrows. SPMV-specific RNAs migrate to both PMV virions and SPMV virions if present. The presence of PMV virions is confirmed in the ethidium bromide-stained gel (lower panel). (C) Distribution of SPMV CP WT and derivatives. Non-cytosolic fractions and cytosolic fractions were prepared as in Figure IV-1A. Protein markers, in kilodaltons (kDa), are indicated on the left. Designation of WT SPMV and each mutant is listed above each blot.

relative amount of virions was reduced (Fig. IV-3B, upper panel). Our observation that mutants R7/8 and R7-12 were defective in forming virions confirmed the predicted function of N-ARM in SPMV RNA encapsidation (8). Furthermore, the loss of virion formation was additive, in that R7-12 was more compromised than R7/8. The reduced amount of SPMV virions associated with mutant ΔC6 suggested that the C-terminal extremity played an auxiliary but important role for efficient SPMV RNA encapsiation, despite its predicted dispensability for the "jelly-roll" core structure. Mutants R7-12, 82F and 130D did not form any detectable virions in the whole virion gel assay (Fig. IV-3B, upper panel). We consistently observed that SPMV RNA was also encapsidated into PMV virions, detected as a band of SPMV specific RNA that migrated to the position of PMV virions in autoradiography (Fig. IV-3B, upper panel) as previously described (173). This was not unexpected since PMV CP displayed some affinity for SPMV RNA using in vitro RNA binding assays (57).

To analyze the possible correlation between virion formation and the cytosolic accumulation of SPMV CP for these mutants, we tested the presence of SPMV CP in cytosolic and non-cytosolic fractions of proso millet plants infected with PMV and each mutant as mentioned above (Fig. IV-1A). As predicted, SPMV CP was present as monomers and dimers in non-cytosolic fractions for WT and all the tested mutants (Fig. IV-3C, upper panel). However, there was an obvious decrease in CP titer for mutants R7/8 and R7-12. Mutant 82F directed the synthesis of a protein of a slightly higher molecular weight compared to WT. In contrast, the ΔC6 mutant directed the synthesis of a smaller product. SPMV CP was detected in cytosolic fractions for WT as well as for mutants R7/8 and ΔC6 but at much reduced levels (Fig. IV-3C, lower panel), which was

coincident with the reduced amount of encapsidated SPMV RNA detected for R7/8 and 82F in the whole virus gel assay (Fig. IV-3B, upper panel). There was no detectable SPMV CP in the cytosolic fractions for encapsidation incompetent mutants R7-12, 82F and 130D (Fig. IV-3C, lower panel) indicating the correlation between compromised CP cytosolic accumulation and defective virion assembly. In summary, the chromatography assays and site-direct mutagenesis experiments both support the conclusion that virion formation is required for the cytosolic accumulation of SPMV CP.

The N-terminal arginine-rich motif (N-ARM) of SPMV CP is essential for successful in vivo SPMV RNA accumulation and in vitro SPMV RNA binding independent of virion formation. Having elucidated the correlation between SPMV CP cytosolic accumulation and virion assembly, we focused on the properties of RNA binding and movement facilitation associated with SPMV CP. An obvious target is the N-ARM, which is conserved among the CPs of the four known plant satellite viruses. As shown above, manipulation of the two arginine pairs (R7/8 and R7-12) in the N-ARM caused a significant decrease of SPMV CP titer (Fig. IV-3C). This effect was additive, as R7-12 representing a change of four arginine codons was more impaired than R7/8 for CP accumulation. Accordingly, plants infected with mutants R7/8 and R7-12 displayed much more attenuated symptoms compared to plants infected with WT SPMV (data not shown). This was consistent with our previous observations that SPMV CP was implicated in symptom exacerbation in millet plants (173, 208).

In addition, SPMV CP was demonstrated to facilitate long distance movement of SPMV RNA and inhibit the generation of DIs (173). In the present study, we extended our understanding of these properties by showing that manipulation of the N-ARM of

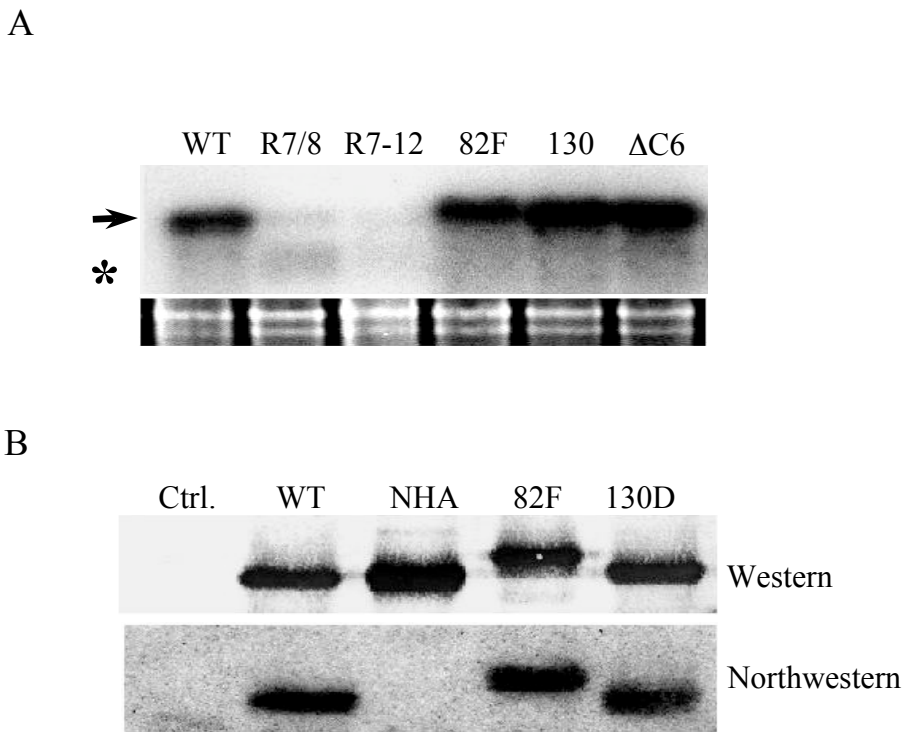

FIG. IV-4. The involvement of N-terminal arginine-rich motif (N-ARM) of SPMV CP in systemic SPMV RNA accumulation and CP:RNA interactions. (A) Systemic RNA accumulation analysis of SPMV CP mutants. All mutants are as in Figure 3A. RNA blot analyses were performed with [^{32}P]-dCTP labeled SPMV specific probes (upper panel). The positions of SPMV defective interfering RNAs (DIs) and full-length RNA are indicated by an asterisk and an arrow respectively. The lower panel shows rRNA from each sample on an ethidium bromide-stained agarose gel as loading control. (B) Northwestern blot assay of SPMV CP derivatives. All proteins are over-expressed in *E. coli* and transferred to a nitrocellulose membrane followed by probing with [^{32}P]-UTP labeled SPMV RNA (lower panel). SPMV CP mutant NHA is diagramed in Figure 2A; 82F and 130D are of the same amino acid sequence as in Figure 3A, except that they are expressed in *E. coli*. A duplicate blot was probed with SPMV CP specific polyclonal antibodies and included as the loading control (upper panel). The control lane (Ctrl) represents the total protein extract from *E. coli* cells expressing no SPMV CP. Designation of SPMV cDNA mutants or CP derivatives is listed above each blot.

SPMV CP significantly reduced the SPMV RNA titer in systemic leaves. Although the R7/8 mutant could still form detectable virions, it behaved the same as the R7-12 mutant in symptom modulation (data not shown) and systemic RNA accumulation (Fig. IV-4A, upper panel). In addition, it allowed the generation of defective interfering SPMV RNAs in infected proso millet plants (Fig. IV-4A, upper panel). Mutants 82F, 130D and ΔC6 were also defective in encapsidation (Fig. IV-3B) but they were as potent as the WT in both symptom modulation (data not shown) and systemic RNA accumulation (Fig. IV-4A, upper panel). These experiments provide evidence that the ability of SPMV CP to enhance systemic RNA accumulation is independent of the process of virion assembly but requires the presence of a functional N-ARM of SPMV CP.

The importance of the N-ARM was further analyzed by northwestern blot assays. For this purpose, mutant NHA (Fig. IV-2A) was used instead of R7-12 as it displayed the same phenotype in plants as R7-12 mutant (data not shown). All SPMV CP derivatives (WT, NHA, 82F and 130D) were over-expressed in *E. coli* BL21 (DE3) cells. A western blot was performed first to ensure equal loading of each SPMV CP derivative (Fig. IV-4B, upper panel). A duplicate membrane was used for northwestern blot assays. Interestingly, the recombinant CPs of WT SPMV, mutant 82F, and mutant 130D all efficiently bound α-^{32}P-UTP labeled SPMV RNA, which was detected as an autoradiography signal co-localized to the positions of corresponding SPMV CP derivatives in western blot (Fig. IV-4B, lower panel), even though mutants 82F and 130D were unable to encapsidate SPMV RNA in whole virus gel assays (Fig. IV-3B, upper panel). In contrast, the NHA CP derivative did not bind any detectable radiolabeled SPMV RNA (Fig. IV-4B, lower panel). To rule out the possibility of nonspecific SPMV

RNA binding by bacterial proteins, untransformed *E. coli* expressing no SPMV CPs was employed as the negative controls and we did not detect any SPMV RNA binding activity (Fig. IV- 4B, upper panel).

In summary, defective systemic RNA accumulation and in vitro RNA binding caused by manipulating the N-ARM of SPMV CP indicates that an N-ARM-mediated CP:RNA interaction (Fig. IV-4B) is crucial for successful SPMV infection and SPMV RNA encapsidation. However, virion formation does not necessarily ensure efficient systemic RNA accumulation and *vice versa* (Fig. IV-3B and Fig. IV-4A), supporting the existence of differential control.

SPMV CP has a complex subcellular localization profile. Since the biological experiments suggest that the presence of SPMV CP in different subcellular fractions is a crucial factor to specify its multiple functions at different stages of infection, we decided to perform a further study of SPMV CP subcellular localization. First, we conducted subcellular fractionation of SPMV infected plant tissue using differential centrifugation. Four fractions were acquired by this procedure: CW, P8, P30 and S30. Based on our previous studies (209, 232), the CW was enriched in cell wall material; P8 was enriched in membranous organelles such as nuclei, mitochondria, and plastids; P30 was enriched in membrane fragments generated during leaf tissue homogenization and S30 contained soluble cytosolic proteins. Western blot analyses revealed that WT SPMV CP was present in each of the 4 fractions (Fig. IV-5, left panel). As expected, the CP derivative of mutant 130D, which was present in non-cytosolic fractions (Fig. IV-3C, upper panel), was detected in cell wall- and organelle- enriched fractions but not in the (S30) cytosolic fraction (Fig. IV-5, right panel). Interestingly, the CP of 130D was present in the (P30)

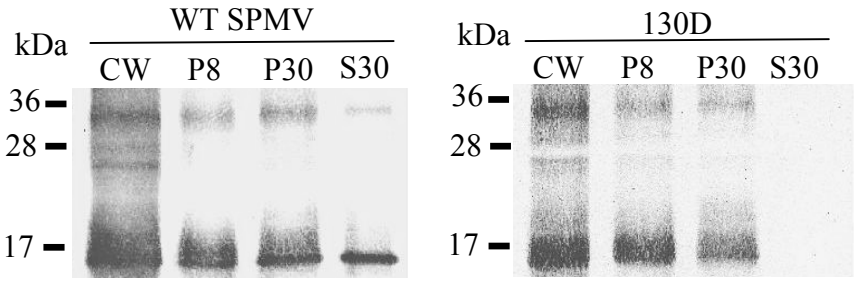

FIG. IV-5. Subcellular fractionation of SPMV CP in proso millet plants infected with PMV plus SPMV wild type (WT) or 130D. Fractions prepared by differential centrifugation are represented as CW (cell wall), P8 (organelle enriched fraction), P30 (membrane fragments) and S30 (cytosolic fraction) and are analyzed for the presence of SPMV CP by western blot. Protein markers, in kilodaltons (kDa), are indicated on the leftmost side of the blots.

membrane-enriched fraction (pellet of 30,000 × *g*) but it was not detectable in the soluble fractions following centrifugation at 10,000 × *g* (Fig. IV-3C, lower panel). This was probably because the membrane associated (correlated to fraction P30) SPMV CP was too diluted to be detected (Fig. IV-3C, lower panel) until concentrated during the ultracentrifugation at 30,000 × *g* (Fig. IV- 5). Therefore, the absence of SPMV CP for 130D in fraction S30 (Fig. IV-5) strongly correlated with its inability to form virions (Fig. IV-3B).

The biochemical data pointed to crucial differential roles for SPMV CP in different subcellular fractions. To acquire more detailed information about SPMV CP subcellular localization, a *Tomato bushy stunt virus* (TBSV) based vector (Fig. IV- 6A) was used to deliver GFP-tagged SPMV CP into *N. benthamiana* plants by rub-inoculation. At 2 dpi, the epidermis of infected regions (green under UV light) was peeled off and observed by fluorescent microscopy. Unfused GFP was distributed throughout the whole cell in a diffusive manner (Fig. IV-6B, upper left panel). When fused to SPMV CP, GFP was preferentially localized to the nucleolus and to cell walls where it formed fine puncta (Fig. IV-6B, upper right panel). When sequential sections at 1 μm intervals were stacked, we also observed some irregular shaped structures apparently localized in the cytoplasm for GFP-fused SPMV CP (Fig. IV-6B, lower left panel). This suggested that SPMV CP also localized in the membrane or to membranous organelles. A close-up view of the nucleus clearly showed the nucleolar localization of GFP-tagged SPMV CP and the GFP-SPMV CP fusion protein was also found to form some small round puncta inside the nucleus (Fig. IV-6B, lower right panel). The subcellular localization of SPMV CP in *N. benthamiana* plants (Fig. IV-6B) is in perfect agreement with the results of the

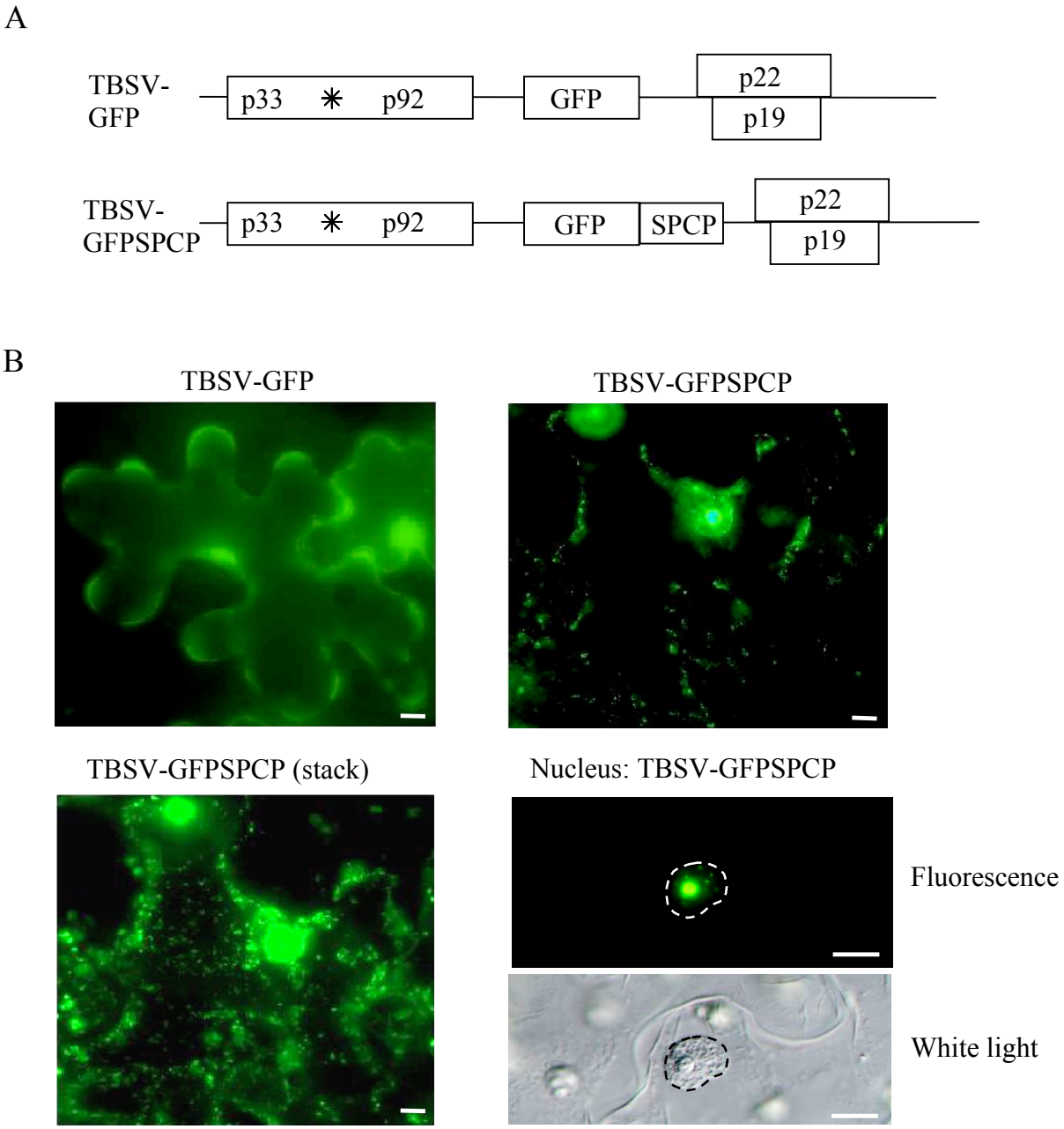

FIG. IV-6. Fluorescence microscopic study of SPMV CP subcellular localization. (A) Diagram of the TBSV based vector used for delivering GFP or GFP-tagged SPMV CP in *N. benthamiana* plants. The TBSV CP gene is replaced with the ORF of either GFP (TBSV-GFP) or GFP fused at the N-terminal end of SPMV CP (TBSV-GFPSPCP). (B) Fluorescent microscopy of TBSV-GFP and TBSV-GPFSPCP infected *N. benthamiana* epidermal cells. Free GFP is distributed throughout the infected cell (left upper panel). GFP-tagged SPMV CP is localized along the cell wall and in the nucleolus (indicated by the arrow) (right upper panel). The stack [TBSV-GFPSPCP (stack)] is generated by overlaying 7 sequential sections at 1 μm intervals of TBSV-GFPSPCP infected cells (left lower panel). In addition to localization in the nucleolus, a close-up view of the nucleus (enclosed by a white dashed curve and a black one under fluorescence and white light respectively) shows that GFP-tagged SPMV CP also localizes to some smaller structures in the nucleus as well (right lower panel). Even though *N. benthamiana* is not a host plant for PMV+SPMV infection, the images suggest that the subcellular distribution of SPMV CP in *N. benthamiana* plants is not an artifact of ectopic expression from the viral vector. All bars are 10 μm in each panel.

biochemical subcellular fractionation assays on infected proso millet plants (Fig. IV-5).

Discussion

A C-proximal region on SPMV CP contributes to stable dimer formation. Virus genome encapsidation is an intricate and highly orchestrated process, which involves various dynamic molecular interactions. In the case of plant RNA viruses, these interactions can be grouped into three major categories: RNA-protein interaction, protein-protein interaction, and ion-protein interactions (180). Encapsidation studies on *Brome mosaic virus* (BMV) and its related viruses indicated that virion assembly of spherical viruses begins with nucleation by CP pentamers and proceeds by the cooperative addition of CP dimers (180, 263). Therefore, CP dimers are considered as the basic building blocks of most plant spherical RNA viruses. Dimerization is also a signature feature of many plant virus movement proteins (MP) such as the MP of *Tobacco mosaic virus* (TMV) (21, 22) and the ORF3 protein of *Groundnut rosette virus* (GRV), an *Umbravirus* (226). From this, MP dimers may also serve as the basic building blocks in the cooperative binding of viral RNA by viral MPs. SDS-resistant SPMV CP dimers were consistently detected in our routine western blot assays (Fig. IV-1A). To understand the functional mechanism of SPMV CP in encapsidation and movement facilitation, we analyzed a series of deletion mutants to identify SPMV CP regions responsible for self-interaction (Fig. IV-1B). Using co-immunoprecipitation, such a region was mapped within a 35 amino-acid region, from AA81 to AA116, of SPMV CP (Fig. IV-1C). The deletion of this region also abolished the detection of SDS-resistant dimers in western blot (Fig. IV-1E). These results agree with earlier observations of the importance of this

region because the deletion of a region from AA76 to AA124 caused early accumulation of DIs and disappearance of full-length SPMV genomic RNA (173).

In order to study the biochemical property of SPMV CP dimers, we attempted to purify these by different kinds of chromatography. However, both gel filtration and anion-exchange chromatography indicated that free SPMV CP dimers were not accumulating within the cytosol, where SPMV CP mainly existed in the form of virions (Fig. IV-2). In contrast, PMV CP of the helper virus was detected as dimers and monomers in our chromatography assays (Fig. IV-2), which is similar to other small RNA plant viruses (70). These results suggest that the assembly of free SPMV CP dimers into whole virions is a very rapid process and SPMV CP dimers are very stable basic building unit of virions, which cannot be totally disrupted even in the presence of strong ionic detergents such as SDS.

The cytosolic accumulation of SPMV CP depends on virion formation. The results of our chromatography experiments raised a question whether virion formation is the prerequisite for cytosolic (soluble) accumulation of SPMV CP. To test this, we introduced a series of mutations at different sites of SPMV CP (Fig. IV-3A) and analyzed the effects on SPMV RNA encapsidation and CP accumulation profile. Of the five tested mutants, R7-12, 82F and 130D were completely defective in SPMV RNA encapsidation in whole virus gel assays (Fig. IV-3B) and could no longer be detected in the cytosol (Fig. IV-3C, lower panel). Mutants R7/8 and ΔC6 displayed intermediate phenotypes of reduced accumulation of SPMV virions (Fig. IV- 3B) and CP in the cytosol (Fig. IV-3C, lower panel). We also noticed that R7/8 mutant displayed a much lower protein titer in the noncytosolic fractions (Fig. IV-3C, upper panel) and a significantly reduced RNA

level compared to WT (Fig. IV-4A). Therefore, the compromised SPMV virion accumulation for R7/8 could not be solely attributed to encapsidation defect but at least partially to the decreased pools of SPMV CP and SPMV RNA for encapsidation.

The last six amino acids of SPMV CP located within a non-structural loop region and were predicted not to interact with other regions of SPMV CP (8). However, the deletion of the last 6 amino acids (ΔC6) did have a major effect on the function of SPMV CP in virion assembly. The ΔC6 SPMV virion titer was even as low as that observed for the R7/8 mutant (Fig. IV-3B) though it was as competent as WT in CP and RNA accumulation (Fig. IV-3C and Fig. IV-4A). This suggested that the C-terminal region of SPMV CP, though not required, played a crucial role in encapsidation possibly by stabilizing virions via quarternary interactions.

Our results indicate that the proper RNA:CP interactions, essential for virion formation, also dictate the appropriate conformation and the stability in solution. This observation may provide an explanation for our previous finding that SPMV CP prepared by dissociating SPMV virions was very unstable in solution and usually precipitated as aggregates within days (57). However, intact purified SPMV virions remained infectious in solution for several months (data not shown). Studies on the SPMV virion structure showed that during encapsidation, CP subunits are arranged in such a way that negatively charged regions are located at the exterior capsid surface and positive charged regions are located at the interior capsid surface where CPs bind the viral RNA (139). This results in the strong negative charge of SPMV virion and explains the elution of SPMV CP in the fractions containing heavily negative charged protein (Fig. IV-2B). Therefore, it is reasonable to suggest that the coordinated process of encapsidation also locates the

hydrophilic regions of SPMV CP at the exterior surface of SPMV virions and confers SPMV virions its solubility in the cytosol. Larson and McPherson proposed a replication-coupled encapsidation model for satellite tobacco mosaic virus (STMV), which was also valid for SPMV (123, 139). According to this model, the progeny RNA exposes its local CP dimer binding elements sequentially while emerging from the replicase complex (usually associated with the host cell membranes) so that CP dimer binding is controlled temporally by the arrangement of CP binding elements on the viral RNA. This is believed to stabilize these structural elements until enough CP dimers bind to the progeny RNA to initiate the CP-CP interactions required for productive capsid assembly (123). Therefore, the viral RNA also plays a crucial active role in virion assembly. The effect of viral RNA on virion assembly by directing CP subunit binding has been demonstrated by the RNA-controlled capsid polymorphism observed for BMV (120). Interestingly, it was reported that the phosphorprotein (P) of rabies virus can mimic the phosphate diester backbone of RNA to interact with its nucleoprotein (N) and prevent N from aggregating, binding cellular mRNA and immature encapsidation to ensure the appropriate assembly of infectious virions (146).

In conclusion, the cytosolic accumulation of SPMV CP depends on the coordinated RNA:CP and CP:CP interactions which lead to productive virion assembly. Coat protein units not participating in encapsidation may either form insoluble disordered CP/RNA aggregates and/or an alternative RNP complex translocating to cell wall-, organelle-, and membrane-enriched fractions for the other functions associated with SPMV CP such as systemic movement.

Successful systemic accumulation of SPMV RNA requires the presence of an intact N-ARM of SPMV CP. Chapter III demonstrated that SPMV CP, though not required, could enhance systemic SPMV RNA movement and accumulation. Accordingly, SPMV CP displays some signature properties of plant virus movement proteins (MP). For example, SPMV CP is localized to the membrane- and cell wall-enriched fractions similarly as the MP of *Tobacco mosaic virus* (TMV) (18), the 3a protein of the *Brome mosaic virus* (BMV) (72), and the TGBp2/3 proteins of *Potato virus X* (PVX) (68, 222). CP-assisted cell-to-cell and long-distance movement has been reported for various plant virus genera (14, 111, 112, 138, 167, 244). Based on the functional form of CP in movement, they have been be divided into three groups in a recent review by Scholthof (205). The first group includes members from *Tobamovirus*, *Carmovrius*, and *Hordeivirus*, which encode specialized MPs and do not depend on CPs for cell-to-cell movement (205). In the second scenario, optimal movement requires the presence of functional CP but virion formation is dispensable. For example, CMV forms a MP-CP-RNA complex to move from cell to cell (14). The third movement strategy requires the formation of virions that necessitates encapsidation competent CP. Viruses in this category include *Cowpea mosaic virus* (111) and BMV (112, 167). Our results with SPMV CP appear to provide a fourth exemplar where a virus CP has discrete and distinct role as a movement protein.

To understand the functional mechanism of SPMV CP in promoting long distance movement, we analyzed the systemic accumulation of SPMV RNA in upper leaves for mutants R7/8, R7-12, 82F, 130D and ΔC6. Mutants 82F, 130D and ΔC6 were as competent as WT in RNA and CP accumulation (Fig. IV-3C and Fig. IV-4A). However,

these mutants were either completely (82F and 130D) or partially (ΔC6) defective in virion assembly (Fig. IV-3B) and did not accumulate in the cytosol as WT (Fig. IV-3C). This observation indicates that the movement facilitation property of SPMV CP is independent of encapsidation and the "insoluble" SPMV CP in non-cytosolic fractions is not a non-functional disordered aggregate but actively involved in the infection and pathogenesis of SPMV. In contrast, alteration of the N-ARM in mutants R7/8 and R7-12 rendered these very inefficient in promoting systemic SPMV RNA accumulation (Fig. IV-4A) suggesting the requirement of an intact N-ARM of SPMV CP for systemic SPMV RNA movement. An N-ARM is found present on the CP of many plant icosahedral RNA virus including BMV, CMV, TBSV, and all 4 known plant satellite viruses (107, 196, 246, 248). A series of genetic studies have demonstrated the importance of N-ARM in encapsidation, movement, and pathogenicity in different systems (107, 182, 201). Likewise, our results also show that SPMV CP N-ARM was essential for RNA encapsidation (Fig. IV-3B) and protein/RNA accumulation (Fig. IV-3C and Fig. IV-4A). In addition, mutations in the N-ARM of SPMV also led to rapid generation of SPMV DIs (Fig. IV-4A).

Northwestern blots further confirmed that the N-ARM is absolutely required for in vitro SPMV RNA binding (Fig. IV-4B), which suggests that the N-ARM mediated SPMV CP:RNA interaction is essential for efficient systemic SPMV RNA movement. This is supported by the studies about the P20 protein encoded by a BaMV associated satellite RNA. P20 and SPMV CP share a 46% identity (132, 133). The P20 protein also features an N-ARM region and alterations of this region affect both its RNA binding ability (231) and movement of the cognate RNA (240). Interestingly, mutants defective in

encapsidation (82F and 130D) displayed a WT-like affinity for SPMV RNA in northwestern in vitro RNA binding assay (Fig. IV-4B). This suggests that the interaction between SPMV CP and SPMV RNA leads to the formation of not only virions but also some alternative ribonucleoprotein (RNP) complexes targeted to cell wall-, organelle-, and membrane-enriched fractions for movement facilitation. Since mutants 82F and 130D were totally defective in SPMV virion assembly, which requires a cooperative binding of RNA by CP, it was very likely that the N-region of SPMV CP mainly mediated a basal level RNA binding. Our previous gel mobility shift assays revealed a two-phase cooperative binding of SPMV RNA by SPMV CP - a cooperative binding phase that is liable for the presence of non-SPMV competitor RNA and a basal binding phase is more specific and unaffected by the addition of competitor RNA (57). Thus, N-ARM mediated RNA binding may also serve as a specificity filter for SPMV virion assembly.

Thus, N-ARM mediated SPMV CP:RNA interaction seems to be absolutely required for every aspect of the function of SPMV CP in infection. However, biological assays indicate that it is not SPMV virions in cytosol but the “insoluble” SPMV CP or CP complex in the non-cytosolic fractions that is involved in the facilitation of SPMV RNA movement and the inhibition of DI generation.

SPMV CP features a complex subcellular localization profile corresponding to its multi-functional role. As mentioned above, “insoluble” SPMV CP mutants 82F and130D still retained the full competence for a robust infection as WT. Nevertheless, “insoluble” is not a precise reflection of SPMV CP distribution in the cells and provides no insights about its biological activity during infection and pathogenesis. To determine

this, we explored the subcellular localization of SPMV CP by differential centrifugation and GFP-tagging. To our surprise, WT SPMV CP was detected in cytosol, cell wall-, organelle-, and membrane- enriched fractions but seemed the most abundant in the cell wall-enriched fraction (Fig. IV-5, left panel). An important signature property of plant virus movement proteins is their co-localization with the cell wall material (18, 68, 113, 222) and the enrichment of SPMV CP in the cell wall containing fraction supports our premise that it is associated with SPMV RNA movement. Mutant 130D displayed a similar subcellular fractionation profile as WT except that it was absent in the cytosol fraction corresponding to its defect in encapsidation (Fig. IV-5, right panel). Using fluorescent microscopy, we observed fine punctate structures for GFP-SPCP fusion along the cell wall (Fig. IV-6B). Presumably, these structures represented SPMV CP aggregates at the plasmodesmata and were reminiscent of the similar structures observed for MPs of TMV, CMV and PVX (14, 67, 222).

In addition to the association with cell wall, GFP-fused SPMV CP showed a preferential localization to the nucleolus and other organized structures in the nucleus (Fig. IV-6B, right low panel). Recently, the nucleolar localization of viral proteins has been realized as a pan-virus phenomenon, which is observed for positive-sense RNA viruses such as Coronaviruses (92), Alphaviruses (151), and Flaviviruses (242), and for negative-sense RNA viruses including Paramyxoviruses (171) and Influenza viruses (45). The exact biological significance of viral protein nucleolar localization is not yet understood. One suggested role is the recruitment of nucleolar host factors that are essential or beneficial for virus multiplication (9). Protein nucleolar localization has also been reported for plant viruses including the CP of *Potato leaf roll virus* (Genus:

Polerovirus, Family: *Luteoviridae*) (84) and the ORF3 protein of *Groundnut rosette virus* (GRV), an *Umbravirus* (114, 194). The GRV ORF3 protein was reported to interact with GRV RNA in vivo, which is required for its function to promote the long distance movement through phloem (195). Recently, it is shown that GRV ORF3 protein entered the nucleolus by interacting with Cajal bodies (CBs) and inducing their fusion with the nucleolus (114). It is also demonstrated that the nucleolar localization of ORF3 protein is required for its activity in promoting long distance movement (114). Based on these findings, a model is proposed that the GRV ORF3 protein utilized the CBs-nucleolus trafficking pathway to recruit host factors such as fibrillarin to form functional RNP complexes required for long distance viral RNA movement (114).

The nucleolar localization of SPMV CP (Fig. IV-6B), together with its RNA binding activity (Fig. IV- 4B), and involvement in systemic movement (Fig. IV-4A), suggests that SPMV CP uses a similar mechanism as the GRV ORF3 protein to facilitate the systemic movement of SPMV RNA. The nucleolus is the site of ribosome maturation that requires modifications of pseudouridylation and 2'-O-ribose methylation mediated by small nucleolar ribonucleoprotein (snoRNP) (115, 163). CBs contain high concentrations of various RNP particles including snoRNP and are involved pre-rRNA processing (143). The nucleolus and CBs are associated both physically and functionally (42). As we noticed, GFP-SPMV CP fusion protein was predominantly localized in the nucleolus and CB-like subnuclear bodies (Fig. IV-6B). Therefore, it is likely that SPMV CP targets the nucleolus either by inducing CB-nucleolus fusion like the ORF3 protein of GRV (114) or by interacting with host factors involved in the CB-nucleolus snoRNP trafficking pathway. After recruiting the appropriate host factors in the nucleolus, SPMV CP forms

the functional RNA:protein complexes required for movement, which circulates along the membrane system to the plasmodesmata and finally into adjacent cells. Perhaps, the "insoluble" SPMV CP in non-cytosolic fractions (cell wall-, membrane- and nucleolus-enriched) is actually required and sufficient for optimal SPMV RNA movement instead of the "soluble" CP in the cytosol (capsids of the virions). However, a functional N-ARM is still required to bind SPMV RNA and form the RNP complexes. This could explain why encapsidation defective mutants 82F and 130D behave like WT in systemic accumulation of RNA and protein (Fig. IV-3C and Fig. IV-4A). If this is true, the nucleolus-involved RNP-trafficking pathway might be of common importance for plant RNA virus movement. However, it is very likely that GFP-tagged SPMV CP cannot form virions due to steric constraint. Therefore, there was still a lack of visual evidence about the subcellular localization of SPMV virions in infected cells.

In conclusion, we demonstrated that SPMV CP has a complex subcellular distribution profile correlated with its multiple functions in movement and encapsidation. It is logical to surmise that these multiple functions of SPMV CP should be appropriately regulated for a successful infection. Phosphorylation has been shown to be a signature property of plant virus MPs and regulate the RNA binding activity of viral proteins (125). Despite of the lack of experimental evidence, phosphorylation may be implicated in regulating these functions. Using NetPhos 2.0 (http://www.cbs.dtu.dk/services/NetPhos), we have identified several sites with high probability of being phosphorylated on SPMV CP. The challenge of our future investigation will be to identify and understand the regulation mechanism of SPMV CP functions, to identify host factors interacting with

SPMV CP in its trafficking to the nucleolus, and to understand the relevance of such interactions to SPMV infection and to the biology of its helper virus PMV.

CHAPTER V

MULTIPLE ACTIVITIES ASSOCIATED WITH THE CAPSID PROTEIN OF SATELLITE PANICUM MOSAIC VIRUS ARE CONTROLLED SEPARATELY BY THE N- AND C- TERMINI

Introduction

The mixed infection of *Panicum mosaic virus* (PMV) and satellite panicum mosaic virus (SPMV) is the cause of St. Augustinegrass decline diseas (27, 208). SPMV depends on its helper virus PMV (genus *Panicovirus*; family *Tombusviridae*) for replication as well as systemic movement in host plants (142, 210). PMV has the unique feature of supporting the multiplication of two distinct subviral agents, SPMV and a satellite RNA (27). PMV has a positive-sense, single-stranded genomic RNA (gRNA) of 4,326 nucleotides (nt), which encodes six open reading frames (ORF) (233). The p48 and p112 protein are required for replication and expressed directly from the genomic RNA (233). The 26-kDa capsid protein (CP) and three smaller proteins (p8, p6.6 and p15) are translated from a single subgenomic RNA (sgRNA). These proteins are required for local and systemic movement of PMV in millet plants (232). Compared to the mild symptoms associated with PMV infection alone, the co-infection of PMV and SPMV induces exacerbated symptoms including a severe chlorotic mottle with bleaching effects, stunting, and failure to set seeds (208).

SPMV has a positive-sense, single-stranded RNA genome of 824 nt which encodes a 17-kDa CP to assemble 16 nm T=1 icosahedral satellite virus particles (142). Several *cis*-acting elements involved in replication and movement were identified within the 5'-untranslated region (UTR) and 3'-UTR of SPMV genomic RNA (168, 174). Interestingly, the SPMV CP ORF contains four in-frame start codons on the gRNA and more than one of them can be recognized for translation in vitro as well as in vivo (168). In addition to SPMV genomic RNA encapsidation, SPMV CP is implicated in symptom exacerbation in millet plants (173, 208). Although SPMV CP is not absolutely required for SPMV RNA replication and systemic movement (174), the absence of CP stimulates the rapid accumulation of SPMV defective interfering RNAs (DIs) (173). In contrast, the presence of full-length CP can greatly enhance systemic SPMV RNA accumulation (168). Though multiple biological roles have been reported for SPMV CP, the precise mechanisms behind these functions remain largely unknown.

SPMV CP has a distinct N-terminal arginine-rich motif (N-ARM), which is predicted to extend into the interior of virions and interacts with the SPMV genomic RNA (8, 139). This was confirmed by our observation that N-ARM mutants are defective in virion assembly in chapter IV. In addition, mutations of the N-ARM impair the virion-independent systemic SPMV RNA accumulation and lead to rapid accumulation of SPMV DIs. In vitro RNA binding assays indicate that the N-ARM is essential for SPMV CP:RNA interactions. Collectively, these results suggest that the N-ARM mediated SPMVCP:RNA interactions are indispensable for all the reported functions associated with SPMV CP.

The present study was initiated to investigate the contribution of the C-terminal region (CTR) that is predicted to be exposed on the CP for intermolecular interactions and to further refine the role of the N-ARM during infection. The results show that mutations in the CTR reduced SPMV RNA and CP titers in systemically infected leaves, stimulated the accumulation of DIs, attenuated symptoms, and impaired virion formation even though in vitro RNA binding activity was solely controlled by the N-ARM. Both N-ARM and CTR mutants accumulated poorly in inoculated leaves, yet replication in protoplasts occurred effectively, providing evidence for an ancillary role of SPMV CP in cell-to-cell movement. Intriguingly, the N-ARM and CTR were also essential for RNA maintenance in infected plants at high temperatures. Combined with previous data, the results strongly suggest that SPMV CP has multiple roles during infection, including the cell-to-cell movement by non-virion CP:RNA complexes. The stability of these complexes seems to be controlled in a biological relevant manner by viral RNA-CP and alternative CP-mediated interactions that are separately controlled by the N- and C-termini of the CP. In vitro PMV RNA binding activity of SPMV CP suggest that the formation of such complexes comprising SPMV CP, PMV RNA, and other PMV- or host-encoded factors may account for the synergistic interactions between PMV and SPMV in co-infections.

Materials and methods

Host plants and inoculation. Proso millet plants (*Panicum miliaceum* cv. “Sunup”) were grown in a growth chamber (25 °C, 14 h of light; 20 °C, 10 h of dark) or in the greenhouse (temperature range of 30-38 °C). Plants were mechanically rub inoculated

with the mixture of equal volumes of uncapped RNA transcripts (SPMV and PMV) and RNA inoculation buffer (0.05 M K_2HPO_4, 0.05 M glycine; 1% bentonite; 1% celite, pH 9.0) at the three-leaf stage. Visual symptoms of systemically infected leaves were monitored and compared for 3 weeks post inoculation. Each biological assay was repeated three times. Protoplasts were isolated from foxtail millet (*Setaria italica* cv. 'German R') seedlings two weeks after germination in a growth chamber. The preparation and transfection of foxtail millet protoplasts were performed as described before (206) except that millet protoplasts were centrifuged at 210 × *g* instead of 70 × *g* in a clinical centrifuge (International Equipment Co., Needham Heights, Mass.). Approximately 5×10^6 protoplasts were transfected with ca. 6 μg of PMV RNA transcripts alone or in combination with in vitro-synthesized SPMV transcripts (ca. 6 μg each) derived from either the type strain or mutant cDNA clones through a polyethylene glycol procedure (206). The transfected protoplasts were incubated in the growth cabinet (28 °C, 14 h of light; 24 °C, 10 h of dark) for ~48 hr prior to the extraction of total RNA or protein.

Construction of SPMV mutant cDNA. The QuikChange kit (Stratagene, La Jolla, CA) was used to make R7/8, R7-12, 130D, ΔC6, and ΔC9 via site-directed mutagenesis. The primers for R7/8 are: forward as ctaagggtaccagCGCatctaatcgtcggg, and reverse as cccgacgattagatGCGctggtacccttag. The primers for R7-12 are: forward as agcgcatctaatcTCTcggcgggctcc and reverse as ggagcccgccgAGAgattagttgcgct. The primers to generate mutant 130D are: forward as gacggactcgtgGAtaccaagggtga and reverse as tcacccttggtaTCcacgagtccgtc. All mutated nucleotides are in capitals and affected codons are underlined. The primers to create mutant ΔC6 are: forward as

taggctggcgcct**TAA**agcgagcttcag and reverse as ctgaagctcgct**TTA**aggcgccagccta. The primers to create mutant ΔC9 are: forward acgggttgctttagg**TAA**ctggcgcctagcgag and reverse ctcgctaggcgccag**TTA**cctaaagcaacccgt. The premature stop codons are in bold uppercase. Deletion mutants (A, B, C and D), insertion mutant (82F) and substitution mutant (NHA) were obtained in the demonstration for the modified recombination PCR protocol in chapter II. Primers to create ΔC-APS are designed following the rationale desribed in chapter II: the forward primer sequence is as *tttaggctggcgcttc*agtcttcataaagtatc and the reverse primer sequence is *ctgaagctccagcctaaa*gcaacccgtaacaat. Primers to create silent mutant R7-12' and C-APS' are designed following the principle as described in (261). The primers for R7-12' are: the forward primer sequence as *ag**a**cg**t**tctaatcg**ca**ggg*cgggcgcccgggcta and the reverse as *cc**tg**cgattaga**a**cg**t**ct*ggtacccttagg. The primers of C-APS' are: the forward as *aggttagc**a**cc**gtc**cgag*cttcagtcttcttaa and the reverse as *ctcg**gac**ggt**g**ctaacct*aaagcaacccgtaaca. Complimentary regions of the primers are in italic lowercase and mutated nucleotides are bolded.

In vitro transcription and translation. A PMV cDNA construct linearized with *Eco*ICRI and SPMV cDNA construct or mutated SPMV cDNA constructs linearized with *Bgl*II were used as templates for in vitro transcription. In vitro translation was carried out using T'N'T-coupled wheat germ extract system according to the manufacturer's instructions (Promega, Madison, WI).

RNA and protein analysis. Total RNA from 300 mg of inoculated or systemically infected leaves of millet plants were extracted at 14 days post-inoculation (dpi). Symptomatic leaf tissues were pulverized in 1 ml of ice-cold extraction buffer [100 mM Tris-HCl (pH 8.0), 1 mM ETDA, 0.1 M NaCl, and 1% SDS] and extracted twice with

phenol-chloroform (1:1, vol/vol) at room temperature. Total RNA was precipitated with 8 M lithium chloride (1:1, vol/vol) at 4 °C for 30 min. The resulting pellets were washed with 70% ethanol, resuspended in RNase-free distilled water, and used for northern blot hybridization. Approximately 5 µg of total plant RNA was electrophoretically separated in 1% agarose gels and transferred to nylon membranes (Osmonics, Westborough, MA). SPMV RNAs were detected by hybridization with α-[^{32}P]-dCTP-labeled SPMV specific probes. Protein samples were separated by SDS-PAGE in 15% polyacrylamide gels and transferred to nitrocellulose membranes (Osmonics, Westborough, MA). The SPMV CP or PMV CP antibodies were applied at a dilution of 1:2,000. Alkaline phosphatase conjugated to goat anti-rabbit antiserum (Sigma, St. Louis, MO) was used as a secondary antibody at a dilution of 1:1,000 and the immune complexes were visualized by hydrolysis of tetrazolium-5-bromo-4-chloro-3-indolyl phosphate as the substrate. Densitometric analysis of RNA and CP titeres were conducted using NIH ImageJ (http://rsb.info.nih.gov/ij/).

Minipurification of virions and encapsidation assays. Symptomatic leaf tissue (0.5 g) was ground in 2 ml extraction buffer (0.2 M sodium acetate, pH 5.2). The homogenate was incubated at 37 °C for 30 min to utilize the endogenous plant RNases to degrade any unprotected RNAs, including host cell RNA and unencapsidated viral RNAs. The extract was then centrifuged at 10,000 rpm, 4 °C, for 10 min. The supernatant was transferred to an empty tube and the virions were precipitated on ice for 30 min in the presence of 12% polyethylene glycol (PEG)-8000 and 300 mM NaCl (PEG-NaCl). The virions were then pelleted by centrifugation at 10,000 rpm, 4 °C, for 10 min and resuspended in 0.05 M sodium acetate (pH 5.5) for a second precipitation overnight at

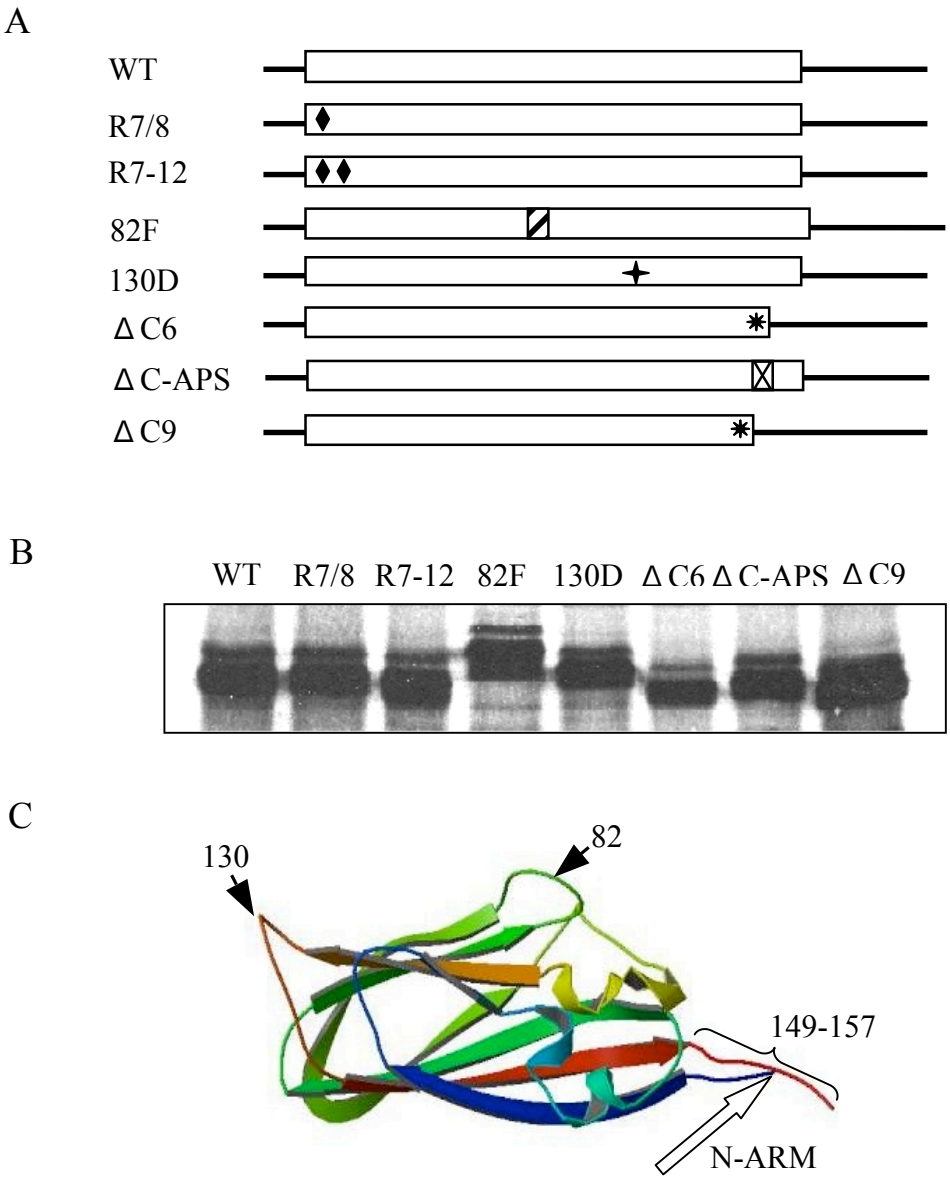

FIG. V-1. Schematic representations and in vitro translation analyses of SPMV derivatives. (A) Schematic representations of the SPMV cDNA constructs. SPMV CP ORF is indicated by the open box. WT represents the SPMV type strain. Mutants R7/8, R7-12, 82F, 130D and ΔC6 are described as in Chapter IV. Mutant ΔC9 represents the truncations of the last nine amino acid (AA) codons, which was performed by introducing premature stop codons (asterisks) at the relevant positions. Mutant ΔC-APS contained the deletion of AA codons of 149-151, which is indicated by a crossed box. (B) In vitro translation assays of SPMV derivatives illustrated in (A) using a transcription-translation coupled wheat germ extract system. All tested constructs direct the translation of proteins with predicted sizes. SPMV WT, R7/8, R7-12, and 130D produce proteins of 17 kDa. 82F directs the synthesis of a protein with a molecular weight slightly higher than 17 kDa. ΔC6, ΔC-APS, and ΔC9 produce proteins of different molecular weights but all lower than 17 kDa. All proteins are [^{35}S]-methionine labeled and detected by autoradiography. Designation of WT SPMV and each mutant is listed above the blot. (C) The spatial distribution of mutated regions on SPMV CP. The original X-ray crystallography analysis was accomplished by Ban and McPherson (8). AA residues 82 and 130 are indicated by arrows. The last 9 AA residues are indicated by the bracket. The N-ARM is composed of the first 16 AAs and represented as an open arrow box here. Its detailed structure has not been completely resolved.

4 °C with PEG-NaCl, as described above. The final virion pellet was resuspended in 50 µl of 0.05 M sodium acetate (pH 5.5) and 5 µl of resuspended virions was resolved on a 1% Tris-glycine agarose gel in 2 × Tris-glycine buffer [10 mM Tris (pH8.0), 76 mM glycine]. Whole virions were transferred to nylon membrane for the SPMV-specific RNA hybridization assays.

In vitro SPMV and PMV RNA binding assays. All SPMV CP derivatives were over-expressed in *E. coli* BL21(DE3) cells (Stratagene, La Jolla, CA) using a pDEST17 based vector (Invitrogen, Carlsbad, CA). An 1.5 ml culture of induced *E.coli* BL21(DE3) cells were pelleted and boiled in 2% SDS-sample buffer, electrophoresed through 15% polyacrylamide gels and transferred to nitrocellulose membrane. The membrane was then blocked for 2 h room temperature (RT) in binding buffer [10 mM Tris–HCl (pH 7), 1 mM EDTA, 1 × Denhardt's reagent] containing 300 mM NaCl and 400 µg/ml total RNA extracted from healthy plants. The [^{32}P]-labeled SPMV RNA probe was added and incubated with the blot for 2 hr at RT. The membrane was washed three times with binding buffer plus 300 mM NaCl and exposed to X-ray film overnight as previously described (57).

Results

Biological activity of SPMV mutants. To elucidate the functional mechanisms of SPMV CP, various mutations were introduced at different sites of SPMV CP ORF (Fig. V-1A). Mutants R7/8, R-12, 82F, 130D, and ΔC6 were described and partially characterized in chapter IV. They were further analyzed in this study and included as controls in some assays. In brief, the arginine codons of amino acid (AA) residues 7th

Table V-1. Phenotype summary of SPMV wild type and mutants

Construct	RNA [a]	Virion [b]	RNA binding [c]	High temperature sensitivity [d]	Chlorosis [e]	CP titer [f]
SPMV	*****	+	+	-	*****	*****
R7/8	*/DI	+	-	+	**	**
R7-12	*/DI	-	-	+	**	**
82F	*****	-	+	-	*****	*****
130D	*****	-	+	-	*****	*****
ΔC6	*****	+	+	-	*****	*****
ΔC-APS	***/ DI	-	+	+	***	***
ΔC9	**/ DI	-	+	+	*	*

[a] The number of asterisks indicates the arbitrarily estimated titer of genome-sized SPMV RNA detected; DI indicates the accumulation of SPMV defective interfering RNAs (DI).

[b] + and – indicate the presence or absence of SPMV virions on the agarose gels analyzed for SPMV RNA.

[c] + and – indicate the presence or absence of SPMV RNA binding activity. The lack of SPMV RNA binding in mutants R7-12 is deduced from CP derivative NHA. Mutants 82F and 130D were tested in Chapter IV. The binding activities of mutants ΔC6, ΔC-APS, and ΔC9 are predicted based upon SPMV CP deletion derivative D (Fig. V-5).

[d] + and – indicate whether high temperature treatment affected the viral RNA accumulation of SPMV WT and derivative mutants.

[e] The number of asterisks indicates the arbitrarily estimated leaf symptom severity of infected plants.

[f] The number of asterisks indicates the arbitrarily estimated titers of SPMV CP detected in infected plants.

and 8th were replaced with a serine and an alanine codons respectively in mutant R7/8. Mutant R7-12 was created based upon R7/8 and contains the additional substitutions of the arginine codons of AA residues 11th and 12th with a serine and an alanine codons respectively. Mutant 82F contains an in-frame insertion of a six amino acid FLAG epitope (DYKDDD) between AA 82 and AA 83. Mutant 130D contains the substitution of the serine codon at the AA residue 130 with an aspartate codon. Mutant ΔC6 and ΔC9 contain truncations of the last 6 AAs and the last 9 AAs respectively, which is accomplished by introducing premature stop codons into SPMV CP ORF. The three residues (alanine, proline, and serine) from 149 to 151 were deleted in the mutant ΔC-APS. The seven SPMV derivatives direct the synthesis of SPMV CP products of predicted sizes as efficiently as SPMV wild-type (WT) in the wheat germ extract in vitro translation system (Fig. V-1B). According to the X-ray crystallography of SPMV CP (8), the N-terminal ARM plunged into the interior of virions where it engaged the SPMV genomic RNA (Fig. V-1C). AA82, AA130, and the last 9 AAs were all within loop regions and not essential for the general "jelly-roll" structure of SPMV CP (Fig. V-1C).

Uncapped transcripts of each SPMV derivative and PMV transcript were inoculated onto proso millet plants (*Panicum miliaceum* cv. Sunup) and the inoculated plant were maintained in a growth chamber. An infection of PMV alone caused mild chlorotic mottle and a barely visible vein-clearing on infected leaves (Fig. V-2). In contrast, plants co-infected with PMV+SPMV developed a typical severe chlorotic mottle with bleaching effects (Fig. V-2 and Table V-1) and severe stunting (data not shown). Among the seven mutants analyzed in this study, 82F, 130D, and ΔC6 induced a chlorotic mottle similar to SPMV WT (Fig. V-2 and Table V-1) and stunting (data not shown). In contrast, plants

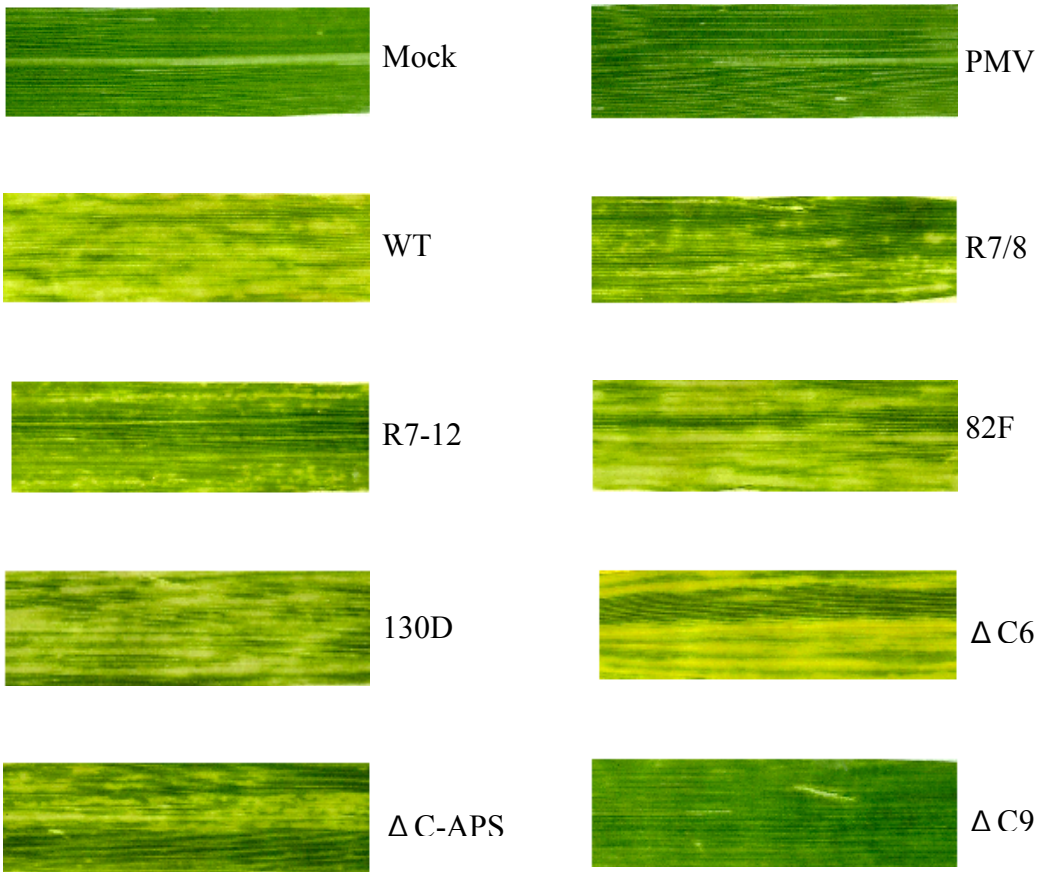

FIG. V-2. Phenotypic comparison of symptom severity induced by SPMV WT and its mutants represented in Fig. V-1A. Upper systemic leaves from proso millet plants (*Panicum miliaceum* cv. Sunup) co-infected with *Panicum mosaic virus* (PMV) and respective SPMV derivatives are monitored and scored for symptom severity. PMV infected and mock-inoculated plants are included as controls. All leaves are harvested and photographed 3 weeks post inoculation.

co-infected with PMV+ΔC9 displayed a mild mottle symptom almost indistinguishable from that caused by PMV infection alone (Fig. V-2). Compared with the severe chlorotic mottle caused by SPMV WT and the mild mottle caused by ΔC9, mutants R/8, R7-12, and ΔC-APS induced leaf symptoms of intermediate levels (Fig. V-2 and Table V-1), but no obvious stunting.

Replication and encapsidation competence of SPMV derivatives. To figure out what causes the symptom attenuation by mutations in the N-ARM and the C-terminal proximity, we first evaluate the replication competency of our SPMV mutants. Transfections of foxtail millet protoplasts with transcripts of PMV and each of mutants R7/8, R7-12, ΔC-APS and ΔC9 led to significant accumulation of progeny RNA after ~ 48 hr incubation in a growth chamber (Fig. V-3A). Each of these four mutants were replicated in protoplasts to a similar level as SPMV WT except that the RNA titer of ΔC-APS was approximately 20% lower than SPMV WT (Fig. V-3A). No DIs were observed for the N-ARM mutants though our previous results demonstrated in planta DI generation for mutants R7/8 and R7-12 in chapter IV. Mutants 82F, 130D, and ΔC6 were tested for their replication efficiency in foxtail protoplasts with similar results (data not shown.)

Encapsidation assays were performed as described in chapter IV. As predicted, PMV virions were present in all infected plants and SPMV virions were detected for SPMV WT (Fig. V-3B). Among the seven tested mutants, SPMV virions were detected only for R7/8 and ΔC6 as a signal migrating toward a position corresponding to WT SPMV virions (Fig. V-3B, upper panel) and no SPMV virions were observed for R7-12, 82F, 130D as described in chapter IV. Densitometric analysis using NIH ImageJ indicated that

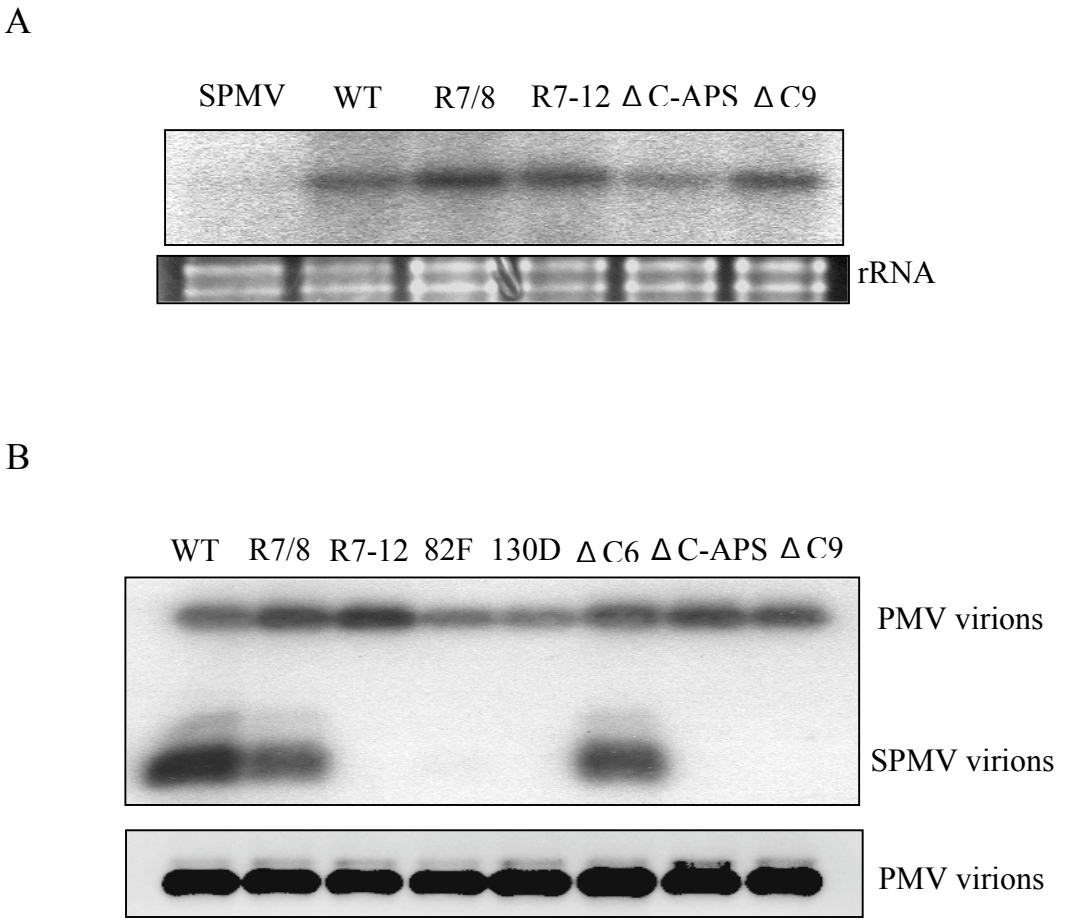

FIG. V-3. Replication and encapsidation assays of SPMV mutants. (A) Replication competency assays of SPMV WT and derivative mutants described in Fig. V-1A in foxtail millet protoplasts coinfected with PMV. Total RNA is extracted approximately 48 hr posttransfection. An ethidium bromide stained agarose gel is included as the loading control. (B) Encapsidation assay of SPMV derivatives using whole virion gels. Encapsidated RNAs are transferred to nylon membrane followed by detection with ^{32}P-labeled SPMV cDNA-specific probe (upper panel). The positions of PMV and SPMV virions are indicated on the right side of the panel. SPMV-specific RNAs migrate to the positions of both PMV virions and SPMV virions if present. The ethidium bromide-stained gel is included as a negative image to demonstrate the presence of PMV virions in all infected proso millet plants (lower panel). Designation of SPMV constructs is listed below the panels.

the virion titers of R7/8 and ΔC6 were ~35% lower than that of SPMV WT. Interestingly, ΔC-APS and ΔC9 were also defective in virion assembly (Fig. V-3B) though the C-terminal extremity of SPMV CP is predicted not essential for its "jelly-roll" core structure (8). In addition, we consistently detected SPMV RNA encapsidated into PMV virions as SPMV RNA specific signals migrating to the position of PMV virions (Fig.V-3B) as previously reported (173). In summary, the encapsidation study indicates that the C-terminus of SPMV CP is of crucial importance for SPMV virion assembly despite their dispensability for the core structure of SPMV CP as shown for the N-ARM. Since mutants 82F and 130D induced typical chlorotic mottle symptom associated with SPMV infection (Fig. V-2) but were incapable of encapsidation, it is evident that SPMV virion or the process of virion assembly is not essential for symptom modulation (Table V-1).

Manipulation of SPMV CP N-ARM and C-terminal extremity impairs SPMV CP and RNA accumulation in planta. It has been reported that SPMV CP promotes the systemic movement of SPMV RNA (168, 173) and this activity depends on a functional N-ARM. However, the contribution of SPMV CP C-terminu is not known. It is also not clear whether SPMV CP is involved in cell-to-cell movement and/or local accumulation of SPMV RNA and CP. Therefore in this study, we analyzed SPMV CP and RNA accumulation for each SPMV derivative (Fig. V-1A) in the inoculated leaves of plants co-infected with PMV+SPMV derivatives respectively. SPMV WT accumulated a substantial amount of CP in inoculated leaves (Fig.V-4A, upper panel). In contrast, the CP titers of mutants R7/8 and R7-12 were reduced by 67% and 80% respectively compared to SPMV WT (Fig. V-4A, upper panel). Mutants 82F, 130D, and ΔC6 displayed similar levels of CP titers as SPMV WT (Fig. V-4A, upper panel).

Interestingly, mutations of the C-terminal extremity of SPMV CP also severely impaired CP accumulation in inoculated leaves with the CP titers of ΔC-APS and ΔC9 reduced to 40% and 17% of SPMV WT, respectively (Fig. V-4A, upper panel).

RNA analysis by northern blot revealed a similar profile for SPMV RNA accumulation of each derivative in the inoculated leaves (Fig. V-4A, middle panel). Manipulation of the N-ARM led to the reduction of SPMV genomic RNA titer by ~80% for mutants R7/8 and R 7-12 compared to SPMV WT (Fig. V-4A, middle panel). The genomic RNAs of mutants 82F, 130D and ΔC6 accumulated to a similar level as SPMV WT (Fig. V-4A, middle panel). However, alterations of the C-terminal extremity of SPMV CP resulted in compromised SPMV RNA accumulation in inoculated leaves. The genomic RNA titers of mutants ΔC-APS and ΔC9 were decreased by 50% and 75% respectively (Fig. V-4A, middle panel). In addition, manipulations of the N-ARM and the C-terminal extremity of SPMV CP caused the *de novo* generation of SPMV DIs (Fig. V-4A, middle panel). Collectively, RNA analysis of inoculated leaves indicates that SPMV CP enhances viral RNA accumulation in inoculated leaves. Above all, this activity is tightly associated with the presence of a functional N-ARM and C-terminal extremity of SPMV CP. In addition, this activity is probably implicated in the process of cell-to-cell movement because replication efficiency in the protoplasts is not affected by the alterations in the N-ARM and C-terminal extremity (Fig. V-3A).

At the same time, parallel protein and RNA analyses were performed on the systemically infected leaves of proso millet plants inoculated with PMV plus each SPMV derivative shown in Figure V-1A. As described in chapter IV, mutations in the N-ARM region of SPMV CP compromised systemic accumulation of CP, yet mutants 82F, 130D,

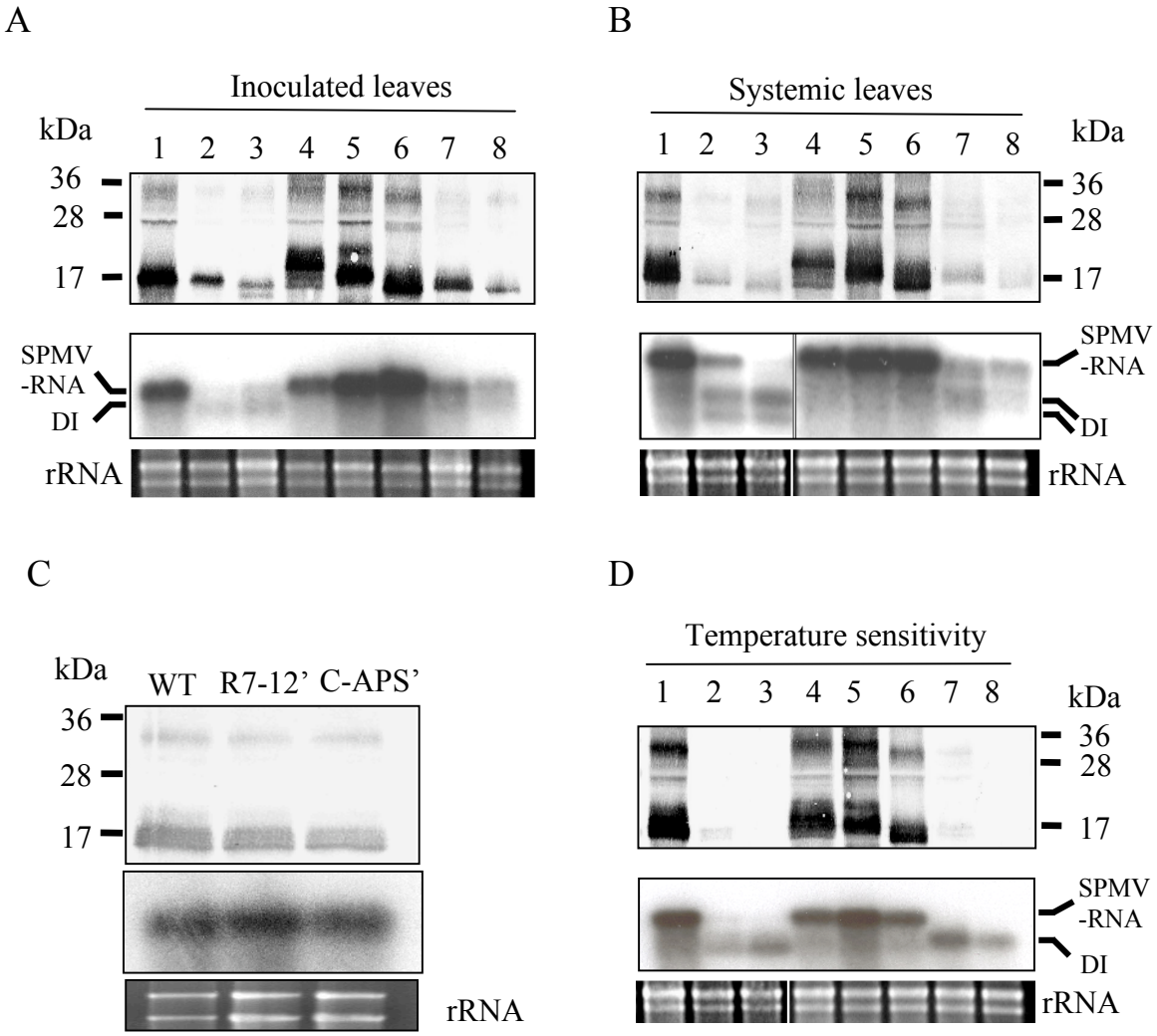

FIG. V-4. CP and RNA analysis of proso millet plants co-infected with uncapped transcripts of PMV and each SPMV derivative. Lanes 1to 8 represents the mixed infection of PMV with SPMV WT, R7/8, R7-12, 82F, 130D, ΔC6, ΔC-APS, and ΔC9 respectively. (A) SPMV CP (upper panel) and RNA (middle panel) accumulation in inoculated leaves of infected plants maintained in the growth chamber (20-25 °C). Immuno-detection of SPMV CP is by western blots using polyclonal specific antibodies. Protein molecular weight markers in kilodalton (kDa) are indicated on the left side of the panel. Northern blots of total RNA extracted from inoculated leaves are performed using with ^{32}P-labeled SPMV cDNA-specific probe. The relative positions of full-length SPMV RNAs and associated DIs are indicated on the right. The ethidium bromide stained agarose gel is included as the loading control. (B) SPMV CP (upper panel) and RNA (middle panel) accumulation in systemic leaves of infected plants maintained in the growth chamber (20-25 °C). Protein and RNA analyses are performed as described in (A). Note the DIs of different sizes observed for mutants R7/8 and R7-12. (C) Mutations of the N-ARM and C-terminal extremity of SPMV CP do not affect *cis*-acting elements. R7-12' and C-APS' contain codon changes at the corresponding sites in mutants R7-12 and ΔC-APS but retain the wild type amino acid sequence. Protein (upper panel) and RNA analyses are as described in (A). Designation of SPMV derivatives is listed above the blots. (D) SPMV CP (upper panel) and RNA (middle panel) accumulation in systemic leaves of infected proso millet plants maintained in the green house (ambient temperature 30-38 °C). RNA and protein analyses are the same as in (A). Note the decreasing amount of CP and full-length genomic RNA and increasing amount of DIs in R7/8, R7-12, ΔC-APS and ΔC9 infected proso millet plants.

and ΔC6 were barely affected in their CP accumulation (Fig. V-4B, upper panel). The same as in the inoculated leafs (Fig. V-4A, upper panel), mutations in the C-terminal extremity also resulted in defective accumulation of CP for ΔC-APS and ΔC9 in systemic leaves (Fig. V-4B, upper panel). Densitometric analysis indicated that the CP titer of ΔC9 was reduced by 95% and those of R7/8, R7-12, and ΔC-APS were reduced by ~80% compared to SPMV WT. Therefore, there is a obvious dosage effect of SPMV CP on symptom severity (Table V-1), which is in agreement with its reported function as the pathogenicity factor (173, 175). RNA analysis revealed that viral RNA accumulation of R7/8, R7-12, ΔC-APS, and ΔC9 in systemic leaves (Fig. V-4B, middle panel) displayed the same defects as in inoculated leaves (Fig. V-4A, middle panel). These include reduced SPMV gRNA titers and the generation of DIs. Interestingly, we noticed that mutations of the N-ARM (mutants R7/8 and R7-12) resulted in the generation of DIs of two different sizes unlike our previous observation of DIs of only one size in chapter IV. As predicted, mutants 82F, 130D and ΔC6 accumulated viral RNA as efficiently as SPMV WT in systemic leaves (Fig. V-4B, middle panel).

To rule out a possible disruption of *cis*-acting elements in the N-ARM and C-terminal extremity of SPMV CP, silent mutations were introduced at the positions of the corresponding amino acid codons altered in mutants R7-12 and ΔC-APS. In mutant R7-12', the arginine codons of residue 7t, 8, 11 and 12 were changed from AGG, CGA, CGT, and CGG into AGA, CGT, CGC, and AGG on a full-length infectious SPMV cDNA clone. Similarly, the original alanine, proline and serine codons were changed from GCG, CCT, and AGC into GCA, CCG, and TCC in mutant C-APS'. Therefore, these mutations changed the RNA sequence but not the amino acid sequences. Western

blot and northern blot assays showed that the CP and RNA accumulation was not affected for these two derivatives (Fig. V-4C), indicating that it was not the mutation of *cis*-acting RNA elements but the mutation of amino acids that impaired the in planta accumulation of SPMV RNA and CP. In summary, the RNA assays suggest that the capability of SPMV CP in promoting local and systemic SPMV RNA accumulation and maintaining viral RNA integrity requires functional N-ARM and C-terminal extremity regions but not the formation of SPMV virions (Table V-1).

Mutation of the N-ARM and C-terminal extremity regions renders SPMV sensitive to high temperature. A parallel biological analysis was performed on plants inoculated with PMV plus each SPMV derivative and maintained in the greenhouse with ambient temperatures ranging from 30 to 38 °C. Co-infection of PMV plus SPMV WT, 82F, 130D, or ΔC6 still induced typical chlorotic mottle symptoms with bleaching effects similar to what was shown in Figure V-2 (data not shown). However, the symptoms induced by the N-ARM mutants (R7/8 and R7-12) and C-terminal extremity mutants (ΔC-APS and ΔC9) were greatly attenuated and indistinguishable from the mild vein clearing and chlorotic mottle induced by PMV infection alone (data not shown). As predicted, the CP levels of these mutants were either barely detectable (R7/8 and ΔC-APS) or undetectable (R7-12 and ΔC9) by western blot assays (Fig. V-4D, upper panel). In contrast, the CP accumulation of mutants 82F, 130D and ΔC6 resembled that of SPMV WT (Fig. V-4D, upper panel). The high-temperature sensitive property was also observed for systemic RNA accumulation of the N-ARM and C-terminal extremity mutants (Fig. V-4D, middle panel). The gRNA of mutant R7/8 was barely detectable and no genomic RNA was detected for R7-12, ΔC-APS, and ΔC9 mutants (Fig. V-4D, middle panel).

However, there was an obvious increase in the amount of DIs detected for these SPMV derivatives (Fig. V-4D, middle panel) compared to infected plants maintained in the growth chamber (Fig. V-4B, middle panel). In contrast, no DIs were detected for SPMV WT or 82F, 130D, and ΔC6 (Fig. V-4D, middle panel), whose genomic RNA accumulated as efficiently as when corresponding infected proso millet plants were maintained in the growth chamber with ambient temperature 20-25 °C (Fig. V-4B, middle panel).

SPMV CP binds both SPMV and PMV genomic RNAs in vitro. It was shown that SPMV CP binds SPMV RNA in sequence-specific manner (57). In this study, we further analyzed the RNA binding property of SPMV CP by northwestern blot assays. For this purpose, a series of SPMV CP derivatives were over-expressed in *E. coli* (Fig. V-5A). WT and R7/8 were the corresponding recombinant capsid proteins of SPMV WT and mutant R7/8 (Fig. V-1). The NHA SPMV CP derivative contained the substitution of the amino acid sequence from 4 to 12 with the nine-amino-acid HA epitope (YPYDVPDYA) and was shown incapable of binding SPMV RNA in vitro in chapter IV. Its corresponding SPMV mutant displayed the same phenotype as R7-12 (Fig. V-1) in biological assays (data not shown). A, B, C, and D were recombinant SPMV CP derivatives with different regions deleted as illustrated (Fig. V-5A).

A western blot was first performed to ensure equal loading of each SPMV CP derivative (Fig. V-5B, upper panel). Duplicate membranes were used for the northwestern blot and probed with α-^{32}P-UTP labeled SPMV (Fig. V-5B, middle panel) and PMV RNA (Fig. V-5B, lower panel). As expected, SPMV WT CP efficiently bound the radio-labeled SPMV RNA, which was detected as an autoradiography signal co-

localized to the position of SPMV CP in western blot (Fig. V-5B, middle panel). Surprisingly, SPMV WT CP also bound PMV RNA significantly (Fig. V-5B, lower panel). In contrast, the R7/8 CP derivative failed to bind detectable SPMV RNA (Fig. V-5B, middle panel) though it was still capable of virion assembly (Fig. V-3D). As reported in chapter IV, the NHA CP derivative did not bind SPMV RNA (Fig. V-5B, middle panel). Neither the R7/8 CP derivative nor the NHA CP derivative could bind PMV RNA (Fig. V-5B, lower panel) as predicted. CP derivatives with deletions (A, B, C, and D) bound SPMV and PMV RNAs with different affinities, which became weaker with the deleted regions in increasing proximity to the N-terminal ARM (Fig. V-5B, upper panel and middle panel). To rule out the possibility of nonspecific SPMV RNA binding by bacterial proteins, untransformed *E. coli* expressing no SPMV CP was employed as the negative control and no SPMV or PMV RNA binding activity was detected (Fig. V-5B, upper panel and lower panel). In summary, the N-terminal ARM of SPMV CP plays an essential role in CP:RNA interactions.

Discussion

Satellite viruses and satellite nucleic acids comprise the group of molecular parasites that depend on a helper virus for replication and movement (210, 218). Satellite viruses differs from satellite nucleic acids in their capacity of directing the synthesis of their own CP to package cognate RNAs. SPMV is one of four reported satellite viruses associated with plants (61, 210, 218). The presence of SPMV accelerates the movement and enhances the titer of PMV (208). In addition, co-infection of PMV with SPMV exacerbates the symptoms including severe leaf chlorotic mottle, stunting, and failure to

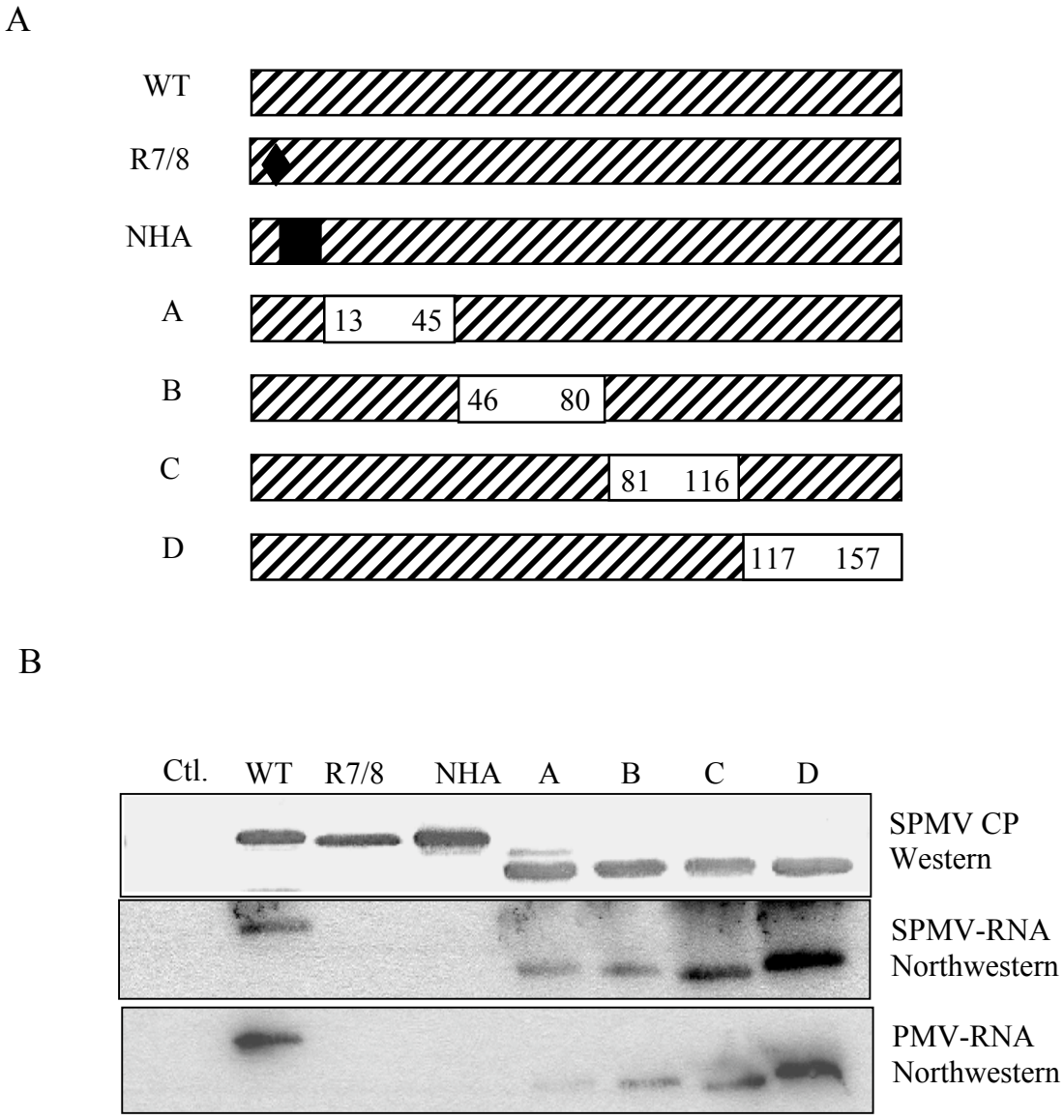

FIG. V-5. In vitro RNA binding analysis of SPMV CP derivatives. (A) Schematic representation of SPMV CP derivatives analyzed in northwestern blot assays. The amino acid (AA) sequence of R7/8 is the same as illustrated in Fig. 1A. NHA contains the substitution of AA from 4 to 12 with an HA epitope (YPYDVPDYA). A, B, C, and D are four mutants with sequential deletions in SPMV CP ORF from AA 13 to 45, AA 46 to 80, AA 81 to 116, and AA 117 to 157, respetively. (B) Northwestern blot analysis of SPMV CP derivatives illustrated in (A). All SPMV CP derivatives tested are over-expressed in *E. coli* and transferred to nitrocellulose membranes followed by probing with ^{32}P-labeled SPMV (middle panel) or PMV (lower panel) transcripts. A blot probed with SPMV CP specific polyclonal antibodies is included to ensure equal loading of proteins for each sample (lower panel). The negative control (C) represents total proteins extracted from *E coli* cells lacking the construct for expressing recombinant SPMV CP.

set seeds. The property of symptom exacerbation is attributed to SPMV CP (168, 173). This conclusion was further supported by our observation of the dosage effect of SPMV CP on leaf symptom severity in this study (Table V-1 and Figs. V-2 and V-4B). SPMV CP accumulation was compromised to different extents by manipulation of the N-ARM (R7/8 and R7-12) and the extreme C-terminal regions (CTR) (ΔC-APS and ΔC9) of SPMV CP (Fig. V-4). Correspondingly, these derivatives were associated with symptom attenuation phenotypes ranging from mild mottle (ΔC9) to moderate chlorotic mottle (R7/8, R7-12 and ΔC-APS) (Fig. V-2).

In contrast, the mutants (82F, 130D and ΔC6) that had a WT-like CP accumulation in infected plants induced the typical chlorotic mottle associated with PMV+SPMV infections (Fig. V-2). Interestingly, these mutants were either partially (ΔC6) or completely (82F and 130D) defective in virion formation (Fig. V-3B), suggesting that SPMV virions are not essential for the property of symptom modulation. Thus far, the possible pathogenicity mechanism of SPMV CP still remains largely unknown. However, a cytopathology study revealed an obvious disruption of mitochondria and tonoplast membrane in association with co-infections of PMV+SPMV (247). This is consistent with the results of our subcellular fractionation study that SPMV CP co-fractionated with the cell wall- and membrane-enriched fractions where as well as the cytosol (Chapter III and IV). However, the cytosolic accumulation of SPMV CP depends on successful SPMV virion assembly and non-virion SPMV CP is exclusively associated with the cell wall- and membrane-enriched fractions (Chapter IV). Taken together, these observations suggest that the noncytosolic SPMV CP targeted to the membranes or membranous organelles are responsible for the symptom modulation property instead of SPMV

virions. This would explain why encapsidation defective mutants (82F, 130D and ΔC6) were able to induce the typical symptoms associated with PMV+SPMV infections.

SPMV CP houses a distinct N-terminal ARM composed of 6 arginines and 1 lysine. X-ray crystallography of SPMV virions shows that this N-terminal region extends into the interior of virions and presumably interacts with the encapsidated SPMV gRNA (8, 139). This prediction is supported by our observation that manipulations of the N-ARM regions impaired both virion assembly (Fig. V-3B) and SPMV RNA binding ability (Fig. V-5B, upper panel). N-terminal ARMs is found present on the CPs of many plant icosahedral RNA viruses such as *Brome mosaic virus, Cucumber mosaic virus* (107, 196) and the four reported plant satellite viruses (246). Furthermore, a series of genetic studies have demonstrated the importance of an N-ARM in encapsidation and movement (107, 182, 201). In addition to encapsidation, SPMV CP is capable of enhancing the systemic accumulation of SPMV gRNA (168). However, there is very little knowledge about the functional mechanism of this activity except that it requires a functional N-ARM (Fig. V-4B, middle panel) (in chapter IV). Furthermore, the present study also demonstrats that SPMV CP facilitates the accumulation of SPMV RNA in the inoculated leaves and this activity also depended on a functional N-ARM (Fig. V-4A, middle panel). Collectively, the RNA accumulation assays indicate that SPMV CP participates in both long-distance and cell-to-cell movement. This is supported by the studies of the 20-kDa protein encoded by *Bamboo mosaic virus* satellite RNA (BMV satRNA). There is a 46% sequence identity between the SPMV CP and the BMV satRNA 20-kDa protein (142, 231). The satBMV 20-kDa protein is required for systemic movement and contains an N-ARM, which has been shown to be required for its functions in movement and the

cooperative binding of satBMV RNA in vitro (133, 231). A recent study shows that the N-ARM of the satBMV 20-kDa protein also mediates self-interaction, intracellular localization and cell-to-cell movement (240).

Although the functional N-ARM mediated RNA binding is essential for both successful local (Fig. V-4A, middle panel) and systemic SPMV RNA accumulation (Fig. V-4B, middle panel), it is unlikely that SPMV virions are required for this activity because encapsidation defective mutants (82F and 130D) were able to enhance SPMV RNA accumulation as SPMV WT in the inoculated leaves (Fig. V-4A, middle panel) and systemic leaves (chapter IV). Therefore, some alternative ribonucleoprotein (RNP) complexes of SPMV RNA and CP, rather than SPMV virions, must be required for efficient long-distance (chapter IV) and cell-to-cell movement of SPMV. Interestingly, the N-ARM of SPMV CP also mediated the in vitro interactions between SPMV CP and PMV genomic RNA (Fig. V-5B, middle panel). PMV CP displays a noticeable affinity for SPMV RNA in vitro as well (57). Therefore, it is not surprising that SPMV RNA is consistently detected in PMV virions (Fig. V-3B). PMV CP is involved in systemic movement as well (232). Taken together, the reciprocal interactions between the CPs and RNAs of PMV and SPMV may provide some insights about the mechanism of the synergistic interaction between PMV and SPMV in co-infections (208).

The SPMV CP has the core structure of an eight-stranded “jelly roll” β-barrel and the last nine amino acids were predicted as not critical for this core structure (Fig. V-1C) (8). However, we found that the deletion of the last six amino acids (in mutant ΔC6) caused reduced SPMV virion accumulation (Fig. V-3B). This indicates that the C-terminal extremity of SPMV CP plays an important auxiliary role during encapsidation to

stabilize the virions possibly by contributing to the quarternary interactions of adjacent subunits. The deletion of the last six amino acids had no effect on symptom modulation (Fig. V-2) or local (Fig. V-4A) and systemic (Fig. V-4B) CP and RNA accumulation when compared to SPMV WT. However, deletions that involved the three amino acids immediately upstream of this region (mutants ΔC-APS and ΔC9) resulted in defective phenotypes similar to those caused by mutations in the N-ARM of SPMV CP including attenuated symptoms on infected plants (Fig. V-2), failure of virion assembly (Fig. V-3B), and compromised local and systemic CP and RNA accumulation (Fig. V-4). These defects cannot be explained merely by the defective SPMV CP:RNA interactions because SPMV CP retained a strong affinity in binding SPMV and PMV gRNA even with a substantial deletion at its C-terminal region (CTR) (in CP derivatives C and D) (Fig. V-5B). On the other hand, it is likely that the CTR of SPMV CP is required for interactions with host- or PMV-encoded factors. The interactions between CPs and other viral factors or host factors have been reported for many plant viruses. For example, interactions between CP and 2b protein of *Tobacco rattle virus* participate in its nematode vectored transmission among host plants (96); the CP of *Alfalfa mosaic virus* (AlMV) activates genome replication by physically interacting with the viral replicase protein (183); and interactions between the CP of *Brome mosaic virus* and a host factor are absolutely required to initiate infections (166). It is found that SPMV CP interacts with PMV CP in the form of virions though the biological relevance of such an interaction remains unclear (Chapter III).

Another intriguing property of SPMV CP is it ability to inhibit the generation and accumulation of defective interfering RNAs (DIs). It is known that the absence of

functional SPMV CP triggers the *de novo* generation and accumulation of DIs (173). However, it is unclear how SPMV CP functions to ensure the synthesis of full-length SPMV gRNA though Chapter IV indicates that the N-ARM mediate SPMV CP:RNA interaction is essential for this purpose. This was further confirmed by our observations that mutations of the N-ARM also resulted in the *de novo* accumulation of SPMV DIs in both inoculated and systemic leaves (Fig. V-4A and B, middle panels). Interestingly, alterations in the C-terminal extremity of SPMV CP also led to the *de novo* accumulation of SPMV DIs (Fig. V-4A and B, middle panels). A possible explanation is that SPMV CP acts as a processivity factor interacting with the RNA template via its N-ARM and with the replication machinery via its C-terminal extremity to bond them more tightly to ensure the synthesis of full-length progeny RNAs. Therefore, the impairment of SPMV CP:RNA interactions or possible CP interactions with the viral replicase complex would lead to a less processive replication by the RNA-dependent RNA polymerase of PMV and the rapid accumulation of SPMV DIs.

The importance of CP in replication has been reported for alfamoviruses and ilarviruses (16, 40, 98). A recent study has reported that AlMV CP increases the affinity between template RNA and AlMV RNA polymerase by interacting with them simultaneously (183). Therefore, a reasonable explanation for why mutants 82F and 130D were resistant to DI accumulation (Fig. V-4) is that their corresponding CPs still retain the functional domains (N-ARM and the C-terminal extremity) to interact with the template RNA and the replication machinery. Essentially, their appropriate “bridging” function was intact despite their defect in virion assembly (Fig. V-3B). Alternatively, SPMV CP may simply interact with cognate RNAs to prevent their possible recognition

by a cellular RNA surveillance pathway such as posttranscriptional gene silencing (241) and/or to inhibit the accumulation of aberrant RNAs that may serve as DI progenitors. However, it was perplexing that no DIs were detected for mutants R7/8, R7-12, ΔC-APS, and ΔC9 in transfected foxtail millet protoplast, nor did these mutants display any obvious defects of replication (Fig. V-3A). One possible explanation is that transfected foxtail millet protoplast can only be maintained for ~48 hours. This may be far less than the time needed for the *de novo* generation of DIs in nature or their detection. Alternatively, DIs may be selected for during cell-to-cell movement in millet plants.

The biological importance of the N-ARM and extreme CTR was also reflected by the high temperature-sensitivity phenotype observed for the mutants R7/8, R7-12, ΔC-APS, and ΔC9. When the infected plants were maintained in the greenhouse with ambient temperatures of 30-38 °C, we observed more compromised CP accumulation (Fig. V-4D, upper panel), the increasing amount of DIs, and the absence of full-length gRNA (Fig. V-4D, middle panel) for mutants R7/8, R7-12, ΔC-APS, and ΔC9 compared to infected plants maintained in the growth chamber (ambient temperature 20-25 °C). One plausible explanation is that the fast growth rate of proso millet plants in the green house may enable the host plants to outpace the infection front of these movement defective mutants to keep the new tissues free of the full-length parental SPMV RNA. Alternatively but not exclusively, the defective interactions of the mutated proteins of R7/8, R7-12, ΔC-APS and ΔC9 with SPMV RNA or other factors will become even less stable and result in the high temperature sensitive phenotype.

In summary, the results of this study show that both the N-ARM and the extreme CTR of SPMV CP are of crucial importance for virion formation and long-distance and

cell-to-cell movement of SPMV RNA. In addition, manipulation of these regions results in symptom attenuation as well as the accumulation of DIs. As we observed, in vitro RNA binding assays confirm the requirement of an intact N-ARM for SPMV and PMV RNA binding. However, SPMV virions are not essential for the functions of SPMV CP in enhancing movement and inhibiting DI generation (Table V-1). This observation raises an open question: why does SPMV CP maintain its ability of encapsidating SPMV RNA since virions does not provide obvious advantages to SPMV or PMV in this study? This property should be quickly lost in the absence of positive selective pressures due to mutations resulting from the error-prone nature of viral RNA polymerase. A possible function of SPMV virion assembly is to serve as the long-term reserves of inoculum for host-to-host transmission under natural conditions (perhaps vectored by a chytrid-like fungus). This hypothesis is supported by the observation that TMV virions have been reported to remain infectious in none-sterile extracts at room temperature for at least 50 years while its genomic RNA is no more stable than other single stranded RNAs (212). In addition, the interactions between SPMV and PMV virions (168) may lead to the uncoating of SPMV and PMV RNAs in close proximity upon the entry of new host cells. This would provide SPMV RNA a better chance to be recognized by PMV replicase complex for multiplication.

CHAPTER VI

CONCLUSIONS AND FUTURE EXPERIMENTS

Conclusions

We routinely use the reverse genetic strategy to study the functions of SPMV CP, which necessitates site-directed introduction or deletion of nucleotides into the ORF of SPMV CP. In the past, we used the traditional single primer method, which is time-consuming and inefficient (121). Therefore, a more efficient method for site-directed mutagenesis was developed at the beginning of this study. Chapter I presented a novel, straightforward primer design strategy, which allows for efficient fragment insertion, substitution, and deletion at target sites using the Quick-change mutagenesis (QCM) kit from Stratagene. My strategy centers on the use of a pair of 5'-partially complementary primers. By manipulating the combination of 5'-complementary sequences (foreign sequences vs. target flanking sequences) and 3'-annealing sequences (consequent full-length amplification vs. partial amplification), all three types of mutagenesis (insertion, substitution and deletion) can be accomplished using the standard QCM protocol.

This method enabled fast and accurate in-frame manipulations of the SPMV CP ORF. For example, I created a series of SPMV CP mutants with sequential deletions of ~30 AA at different sites (Fig. II-2A) simultaneously using the same PCR program. These mutants were used to identify the domain mediating the self-interaction of SPMV CP (Fig. IV-1C) and study the RNA binding activity of SPMV CP (Fig. V-5B). In addition, I successfully inserted the HA and FLAG epitopes into different sites of SPMV

CP as a tentative exploration of the possibility to develop a SPMV based vector for epitope display (Fig. II-2).

Previous studies in our laboratory revealed a multifunctional role of SPMV CP in infection (173). These functions include, but are not limited to, virion assembly, facilitation of the long-distance movement of SPMV RNA, symptom exacerbation, and inhibition of the accumulation of SPMV defective interfereing RNAs (DIs). Biological assays in this study show that SPMV CP is also involved in the cell-to-cell movement and local accumulation of SPMV RNA (Fig. IV-4A). This dissertation study also provided new confirmatory evidence for the previouly reported functions. For example, a predicted hairpin structure upstream the start codon of SPMV CP ORF was necessary for SPMV RNA movement in a host specific manner (174). However, the host specific movement defect caused by mutation of this region is fully compensated by the presence of full-length SPMV CPs (Fig. III-6). Since some SPMV CP mutants are defective in encapsidation (Fig. IV-3B) but behave like WT in the activities of promoting movement (Fig. IV-4A) and inhibiting DI generation (Fig. IV-4A), SPMV provides a good example where a virus CP has discrete and distinct functions other than encapsidation. Furthermore, I found that alterations of SPMV CP lead to a high temperature sensitive phenotype, including symptom attenuation, deterioration of RNA and CP accumulation and increased amount of SPMV DIs (Fig. V-4D).

SPMV CP has been shown to be responsible for the induction of exacerbated symptoms on infected plants including severe chlorotic mottle, stunting and failure to set seed. Its capacity as a pathogenicity factor is further supported the observation of a dosage effect of SPMV CP on symptom severity in this study (Table V-1). In addition,

we find that SPMV virions or the process of virion assembly is not required for the property of symptom modulation. So far, the exact pathogenicity mechanism of SPMV CP still remains largely unknown except that the mitochondria and tonoplast membranes are disrupted in plant cells infected by PMV+SPMV (247). This is in agreement with the results of the subcellular fractionation assays in this dissertation study where SPMV CP co-fractionated with the organelle- and membrane-enriched fractions (Fig. IV-5) and especially the visualization of GFP fused SPMV CP in membranous organelles using fluorescent microscopy (Fig. IV-6B).

Corresponding to its multi-functional role in infection, SPMV CP exhibits a complex subcellular localization profile. For instance, SPMV CP co-fractionates with cell wall- and membrane enriched materials, which is a signature property of plant virus movement proteins (18, 68, 72, 222). The fluorescent microscopy study demonstrates that GFP tagged SPMV CP forms fine puncta along the cell wall Fig. (IV-6B), which presumably represents SPMV CP aggregates at the plasmodesmata and are reminiscent of the similar structures observed for MPs of TMV, CMV and PVX (14, 67, 222). Subcellular fractionation studies show that virion assembly is required for the cytosolic accumulation of SPMV CP, which indicates that the coordinated RNA:CP interactions leading to productive virion assembly also dictate the appropriate conformation and stability of SPMV CP in the cytosol. Otherwise, SPMV CP is exclusively associated with cell wall-, organelle-, and membrane-enriched fractions (Fig. IV-5). Since SPMV virion formation is dispensable for the properties of movement facilitation, symptom modulation, and inhibition of SPMV DI generation (Fig. IV-4A), it is logical to assume that SPMV CPs associated with the cell wall, organells, and membranes direct these processes.

A significant finding of my dissertation study is that SPMV CP is localized to the nucleolus (Fig. IV-6B). Protein nucleolar localization has also been reported for plant viruses including the CP of *Potato leaf roll virus* (Genus: *Polerovirus*, Family: *Luteoviridae*) (84) and the ORF3 protein of *Groundnut rosette virus* (GRV), an *Umbravirus* (114, 194). Recently, it was shown that GRV ORF3 protein entered the nucleolus by interacting with Cajal bodies (CBs) and inducing their fusion with the nucleolus to recruit host factors such as fibrillarin to form functional RNP complexes required for long distance viral RNA movement of GRV (114). The nucleolar localization of SPMV CP (Fig. IV-5C), together with its RNA binding activity (Fig. IV-4B) (57), and involvement in systemic movement (Fig. III-5B) (173), suggests that SPMV CP uses a similar mechanism as the GRV ORF3 protein to facilitate the movement of SPMV RNA. If this is true, the nucleolus-involved RNP-trafficking pathway might be of common importance for plant RNA virus movement.

To understand the mechanisms of the multiple functions of SPMV CP, a series of biochemical and biological experiments were conducted in my dissertation study to identify possible functional domains on SPMV CP. SPMV CP houses a distinct N-terminal arginine-rich motif (N-ARM) composed of 6 arginines and 1 lysine. N-ARMs are found present on the CPs of many plant icosahedral RNA virus such as BMV and CMV and a series of elegant studies have shown the crucial importance of N-ARMs in the biology of these viruses (107, 182, 196, 201). Northwestern blot assays show that the N-ARM of SPMV CP is essential for the RNA binding ability of SPMV CP (Fig. IV-4B). Biological assays reveal that alterations of this N-ARM disrupt every known function of SPMV CP, including virion assembly (Fig. IV-3B), facilitation of local and systemic

movement (Fig. IV-4A and Fig. V-4A), and the maintenance of SPMV RNA integrity (Fig. IV-4A and Fig. V-4A).

Together, the results of this study show that the N-ARM-mediated SPMV CP:RNA interaction is essential for every reported function of SPMV CP. Since SPMV virions are not required for the properties of movement facilitation and inhibition of SPMV DI generation, the N-terminal ARM mediated SPMV CP:RNA interaction may also be involved in the formation of some alternative ribonucleoprotein (RNP) complexes for these purposes. Such RNP complexes may include host factors such as fibrillarin, as mentioned above, and PMV-encoded proteins. Interestingly, the N-ARM of SPMV CP also mediates the in vitro interactions between SPMV CP and PMV genomic RNA (Fig. V-5). PMV CP displays an obvious in vitro affinity for SPMV RNA (57) and is involved in systemic movement (232) as well. Therefore, the reciprocal interactions between the CPs and RNAs of PMV and SPMV may provide some insights into the mechanism of the synergistic interaction between PMV and SPMV in co-infections (208). For example, the interaction of SPMV CP with PMV RNA may help to recruit extra auxiliary host factors into the PMV RNP complexes and result in a more rapid virus movement and *vice versa*.

In routine western blots of SPMV CP, I consistently detected SPMV CP dimers. CP dimers are considered as the basic building blocks of most plant spherical RNA viruses and dimerization is also a signature feature of many plant virus movement proteins, such as the MP of TMV (21, 22) and the ORF3 protein of GRV (226). Co-immunoprecipitation assays on a series of SPMV CP deletion mutants successfully map a self-interaction domain within a 35 amino acid region (AA81 to AA116) of SPMV CP (Fig. IV-1C). The importance of this region is reflected by a previous observation that

deletions implicating this region lead to the accumulation of DIs and loss of full-length SPMV RNA (173).

Though the last nine amino acids are predicted not to be critical for the "jelly-roll" β-barrel core structure of SPMV CP (8), the C-terminal extremity of SPMV CP also seems to be required for every known function of SPMV CP. Deletions within the C-terminal extremity result in the same phenotypes as mutations of the N-ARM, such as defective virion assembly (Fig. V-3B), facilitation of local and systemic movement (Fig. V-4), and maintenance of SPMV RNA integrity (Fig. V-4). However, these defects associated with these CP C-terminal extremity mutants cannot be explained merely by compromised SPMV CP:RNA interactions because SPMV CP retains a strong affinity in binding both SPMV and PMV genomic RNAs even with a substantial deletion at its C-terminal region (Fig. V-5). One possible explanation is that the C-terminal extremity of SPMV CP plays an important auxiliary role to stabilize SPMV virions or some alternative RNP complexes possibly by contributing to the quarternary interactions of adjacent CP subunits. In addition, the C-terminal extremity of SPMV CP may be required for its interactions with host- or PMV-encoded factors and these interactions may be important for the appropriate SPMV CP functions. For example, SPMV CP interacts with PMV CP in the form of virions (Fig. III-7), though the biological relevance of such an interaction remains unclear. This idea is also supported by the observation that the PMV CP and P8, both are movement-associated proteins, co-fractionated with SPMV CP (Fig. III-3 and Fig. IV-5) (232). Furthermore, SPMV CP may interact with the PMV replicase complex and serve as a "processivity factor" to bind the RNA template with the replication machinery more tightly to ensure the synthesis of full-length progeny and inhibit the

generation of DIs. The implication of CP in replication has been reported for alfamoviruses and ilarviruses (17, 102). A recent study has reported that AlMV CP increases the affinity between template RNA and AlMV RNA polymerase by interacting with them simultaneously (183). Therefore, as long as SPMV CP retains the functional domains to interact with the template RNA and the replication machinery, it can bridge the RNA template with the replication machinery tightly for processive replication to inhibit DI accumulation. Similarly, the presence of functional CP domains to interact with SPMV RNA and host- or PMV-encoded factors might be sufficient for the formation of the required RNP complexes regardless of virions assembly.

This dissertation confirms and extends previous reports by our laboratory about the multifunctional role of SPMV CP in its co-infection with PMV with new biological and biochemical evidence. In addition, it is shown for the first time that SPMV CP is involved in cell-to-cell movement of SPMV RNA. In agreement with its multifunctional roles, SPMV CP features a complex subcellular localization profile. The identification of multiple functional domains on SPMV CP provides significant insight about the possible mechanism of the different activities of SPMV CP. However, this dissertation study also raises two significant questions. First, how are the multiple functions of SPMV CP regulated? And second, why does SPMV CP maintain its ability of encapsidation SPMV RNA since this function does not provide obvious advantages to SPMV or PMV in this study? This property should be quickly lost in the absence of positive selective pressures due to mutations resulting from the error-prone nature of viral RNA polymerase. It is reasonable to speculate that all the functions of SPMV CP should be coordinately regulated so that a robust infection can be established and phosphorylation can be such a

regulatory mechanism. Phosphorylation has been shown to regulate the RNA binding activity of viral proteins including MPs (44, 82, 113, 144, 230) and CPs (37, 100, 101, 124). Several residues with a high probability of being phosphorylated have been identified on SPMV CP using NetPhos 2.0. A possible function of SPMV virion assembly is to serve as the long-term reserves of inoculum for host-to-host transmission under natural conditions (perhaps vectored by a chytrid-like fungus). This hypothesis is supported by the observation that TMV virions have been reported to remain infectious in none-sterile extracts at room temperature for at least 50 years while its genomic RNA is no more stable than other single stranded RNAs (212). In addition, the interactions between SPMV and PMV virions may lead to the uncoating of SPMV and PMV RNAs in close proximity upon the entry of new host cells. This would provide SPMV RNA a better chance to be recognized by PMV replicase complex for replication. However, since infectious SPMV transcripts are always used as inoculum for biological studies under laboratory conditions, the exact function of SPMV virion in natural host-to-host transmission cannot be thoroughly evaluated.

Taken together, the results of this dissertation lead to my proposal of a model about the regulatory mechanism of SPMV CP functions (Fig. VI-1). According to this model, phosphorylated SPMV CP will traffic to the nucleolus of host cell to recruit the necessary host factors and then bind progeny SPMV RNA to form the SPMV RNP complexes required for movement. Alternatively, phosphorylated SPMV CP may first interact with progeny SPMV RNA to form the initial RNP complexes, which become mature while they traffic through the nucleolus to recruit host factors. In addition, PMV movement related proteins, such as P8 and P6.6, may also participate in this process of SPMV RNP

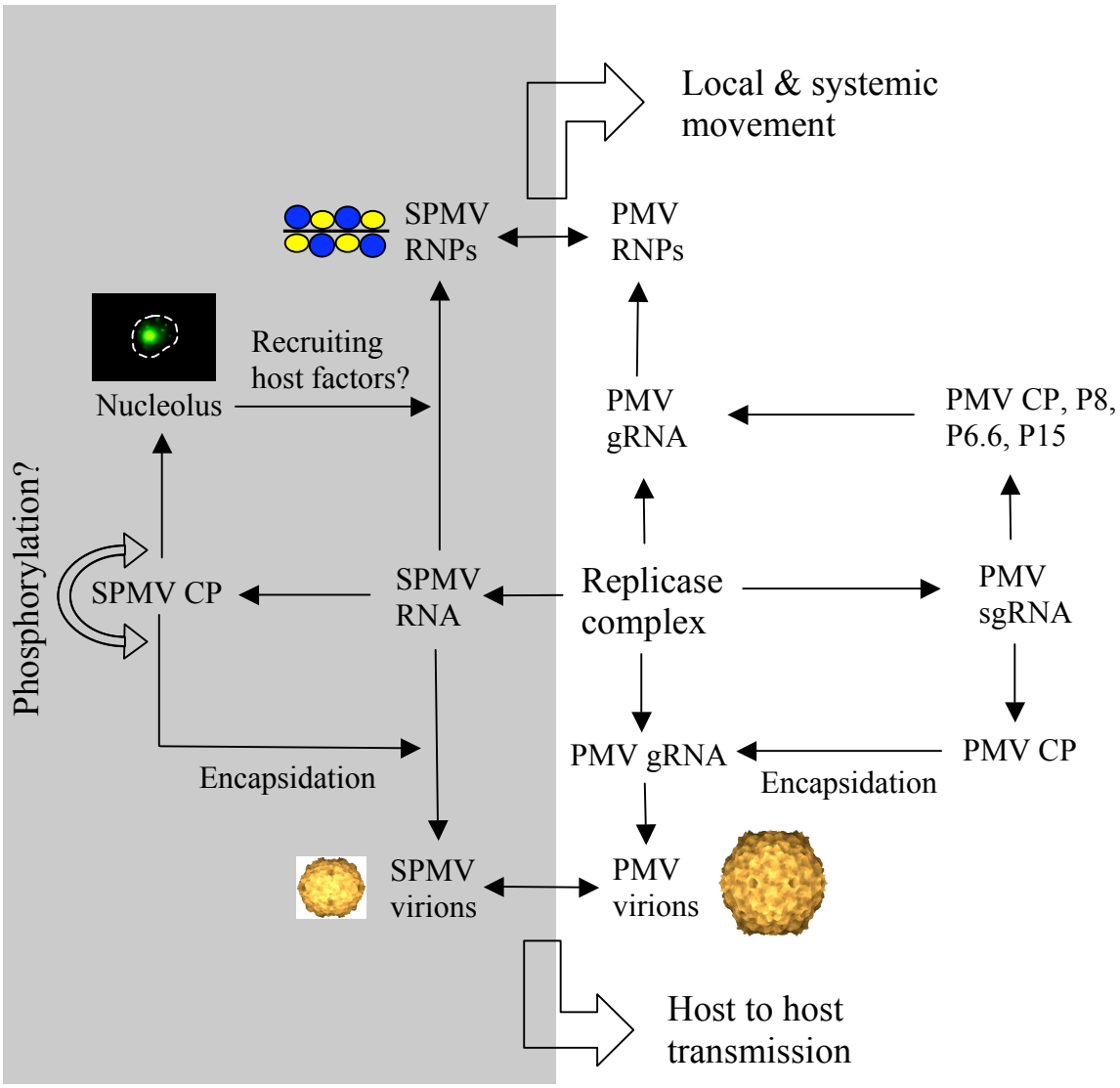

FIG. VI-1. A model for the multiple functions of SPMV CP and a possible regulatory mechanism. All processes involving SPMV CP are represented as shaded. After translation from SPMV RNA, SPMV CP, if phosphorylated, will traffic to the nucleolus of host cells and recruit the necessary host factors to form SPMV ribonucleoprotein (RNP) complexes essential for movement. A similar process is described for PMV except that the viral proteins of PMV are expressed from a subgenomic RNA (sgRNA) and whether PMV factors traffic to the nucleolus is unknown. Interactions between factors of these two pathways may be essential or facile for the movement of viruses. If not phosphorylated, SPMV CP will encapsidate SPMV progeny RNAs into the T=1 virions. SPMV and PMV virions will interact with each other and act as the inoculum for host-tohost transmission.

complex formation. Reciprocally, SPMV CP may also be incorporated into PMV RNP complexes for movement. If this is true, the consequent recruitment of extra auxiliary host factors will explain the observation of the faster movement of PMV RNA in co-infections with SPMV. If not phosphorylated, SPMV CP will encapsidate SPMV progeny RNAs into the T=1 virions, which will interact with PMV virions and act as the inoculum for future host-to-host transmission.

Future questions and experiments

The biochemical and cell biology studies of this dissertation have generated substantial information about the mechanisms of SPMV CP functions and resulted in the proposal of a tentative working model. In order to obtain a refined model of SPMV CP functions, more information should be gathered about other possible functional regions on SPMV CP, host- and PMV- encode factors interacting with SPMV CP, and the regulatory mechanism of its various functions.

One potential functional domain of SPMV CP to target is the putative nucleolar localization signal. This study has revealed a preferential nucleolar localization of SPMV CP. However, the nucleolar localization signal of SPMV CP still remains to be determined. Identification of the putative signal and the following mutagenesis studies will reveal the biological importance of SPMV CP nucleolar localization. For this purpose, the site-direct mutagenesis method I developed (Chapter I) can be used to introduce small deletions at different sites of SPMV CP, followed by confocal imaging of the GFP-tagged SPMV CP derivatives for the initial identification of the signal candidates. Once the signal candidates are identified, parallel biological studies using the

corresponding SPMV infectious transcript should be conducted to evaluate the relevance of these signal candidates.

To date, little is known about potential factors interacting with SPMV CP. In chapter III, it was demonstrated that SPMV CP interacted with PMV CP in the form of virions, using co-immunoprecipitation. However, the biological importance of such interactions is still unknown. To address this problem, mutagenesis experiments can be designed and conducted to identify the regions of SPMV CP that mediate this interaction (as described in Figure IV-1), followed by biological studies of the corresponding SPMV mutants. One technical obstacle in the identification of factors interacting with SPMV CP is that SPMV CP accumulates only as virions in the cytosol. Therefore, co-immunoprecipitation cannot be used to pull down host- or PMV- encoded proteins interacting with SPMV CP in the cell wall-, organelle-, and membrane-enriched fractions. An alternative is to use the yeast two-hybrid assay, which is a routine method in our laboratory. In addition, I have recently begun to test a yellow fluorescent protein (YFP) based bio-molecular fluorescence complementation (BiMFC) system. This can also be used in a similar way to the yeast two-hybrid assay for the identification of host- and PMV-encoded factors interacting with SPMV CP in the non-cytosolic fractions. In either case, it will be necessary to construct and screen a cDNA library of host- and PMV-encoded proteins. Once potential proteins are identified, it will be possible to map the domains of SPMV CP and these factors that participate in these interactions. Then mutagenesis experiments can be performed on these domains to understand the importance of these interactions in the infection cycle of SPMV.

As mentioned above, phosphorylation is a signature property of plant virus movement proteins and a common mechanism of regulating RNA:protein interactions. There have been reports about the importance of viral CP phosphorylation in the infection cycle of plant and animal viruses (37, 100, 101, 124). Therefore, it is very likely that phosphorylation is implicated in regulating functions of SPMV CP. The confirmation of whether SPMV CP is phosphorylated can be performed using in vitro phosphorylation assays (101). If the results are positive, the phosphorylation sites can be identified by 2D gel-electrophoresis of hydrolyzed ^{32}P-labeled SPMV CP, radioactive phosphorpeptide sequencing, and mass spectrometry (100). Mutations affecting the phosphorylation sites should be introduced into SPMV CP to study the biological importance of its phosphorylation. Meanwhile, phosphorylated SPMV CP or CP derivatives mimicking the phosphorylated status will be analyzed for their interactions with SPMV RNA and host- and PMV-encode proteins to understand the biochemical mechanism, by which phosphorylation regulates the different functions of SPMV CP.

REFERENCES

1. **Altenbach, S. B., and S. H. Howell.** 1981. Identification of a satellite RNA associated with turnip crinkle virus. Virology **112:**25-33.

2. **Alzhanova, D. V., Y. Hagiwara, V. V. Peremyslov, and V. V. Dolja.** 2000. Genetic analysis of the cell-to-cell movement of beet yellows closterovirus. Virology **268:**192-200.

3. **Alzhanova, D. V., A. J. Napuli, R. Creamer, and V. V. Dolja.** 2001. Cell-to-cell movement and assembly of a plant closterovirus: roles for the capsid proteins and Hsp70 homolog. EMBO J. **20:**6997-7007.

4. **Annamalai, P., Y. H. Hsu, Y. P. Liu, C. H. Tsai, and N. S. Lin.** 2003. Structural and mutational analyses of *cis*-acting sequences in the 5'-untranslated region of satellite RNA of bamboo mosaic potexvirus. Virology **311:**229-239.

5. **Argos, P.** 1988. A sequence motif in many polymerases. Nucleic Acids Res. **16:**9909-9916.

6. **Baer, M. L., F. Houser, L. S. Loesch-Fries, and L. Gehrke.** 1994. Specific RNA binding by amino-terminal peptides of alfalfa mosaic virus coat protein. EMBO J. **13:**727-735.

7. **Ban, N., S. B. Larson, and A. McPherson.** 1995. Structural comparison of the plant satellite viruses. Virology **214:**571-583.

8. **Ban, N., and A. McPherson.** 1995. The structure of satellite panicum mosaic virus at 1.9 Å resolution. Nat. Struct. Biol. **2:**882-890.

9. **Banerjee, R., M. K. Weidman, S. Navarro, L. Comai, and A. Dasgupta.** 2005. Modifications of both selectivity factor and upstream binding factor contribute to poliovirus-mediated inhibition of RNA polymerase I transcription. J. Gen. Virol. **86:**2315-2322.

10. **Batten, J. S., B. Desvoyes, Y. Yamamura, and K.-B. G. Scholthof.** 2006. A translational enhancer element on the 3'-proximal end of the Panicum mosaic virus genome. FEBS Lett. **580:**2591-2597.

11. **Batten, J. S., M. Turina, and K.-B. G. Scholthof.** 2006. Panicovirus accumulation is governed by two membrane-associated proteins with a newly identified conserved motif that contributes to pathogenicity. Virol. J. **3:**12-23.

12. **Baulcombe, D.** 2002. RNA silencing. Curr. Biol. **12:**82-84.

13. **Bernal, J. J., and F. Garcia-Arenal.** 1994. Complex interactions among several nucleotide positions determine phenotypes defective for long-distance transport in the satellite RNA of cucumber mosaic virus. Virology **200:**148-153.

14. **Blackman, L. M., P. Boevink, S. S. Cruz, P. Palukaitis, and K. J. Oparka.** 1998. The movement protein of cucumber mosaic virus traffics into sieve elements in minor veins of *Nicotiana clevelandii*. Plant Cell **10:**525-538.

15. **Blok, V. C., A. Ziegler, D. J. Robinson, and A. F. Murant.** 1994. Sequences of 10 variants of the satellite-like RNA-3 of groundnut rosette virus. Virology **202:**25-32.

16. **Bol, J. F.** 1999. Alfalfa mosaic virus and ilarviruses: involvement of coat protein in multiple steps of the replication cycle. J. Gen. Virol. **80:**1089-1102.

17. **Bol, J. F., L. van Vloten-Doting, and E. M. Jaspars.** 1971. A functional equivalence of top component a RNA and coat protein in the initiation of infection by alfalfa mosaic virus. Virology **46:**73-85.

18. **Boyko, V., J. van der Laak, J. Ferralli, E. Suslova, M. O. Kwon, and M. Heinlein.** 2000. Cellular targets of functional and dysfunctional mutants of tobacco mosaic virus movement protein fused to green fluorescent protein. J. Virol. **74:**11339-11346.

19. **Brault, V., S. Perigon, C. Reinbold, M. Erdinger, D. Scheidecker, E. Herrbach, K. Richards, and V. Ziegler-Graff.** 2005. The polerovirus minor capsid protein determines vector specificity and intestinal tropism in the aphid. J. Virol. **79:**9685-9693.

20. **Brault, V., J. F. van den Heuvel, M. Verbeek, V. Ziegler-Graff, A. Reutenauer, E. Herrbach, J. C. Garaud, H. Guilley, K. Richards, and G. Jonard.** 1995. Aphid transmission of beet western yellows luteovirus requires the minor capsid read-through protein P74. EMBO J. **14:**650-659.

21. **Brill, L. M., S. Dechongkit, B. DeLaBarre, J. Stroebel, R. N. Beachy, and M. Yeager.** 2004. Dimerization of recombinant tobacco mosaic virus movement protein. J. Virol. **78:**3372-3377.

22. **Brill, L. M., R. S. Nunn, T. W. Kahn, M. Yeager, and R. N. Beachy.** 2000. Recombinant tobacco mosaic virus movement protein is an RNA-binding, alpha-helical membrane protein. Proc. Natl. Acad. Sci. USA **97:**7112-7117.

23. **Brodersen, P., and O. Voinnet.** 2006. The diversity of RNA silencing pathways in plants. Trends Genet. **22:**268-280.

24. **Bruyere, A., V. Brault, V. Ziegler-Graff, M. T. Simonis, J. F. Van den Heuvel, K. Richards, H. Guilley, G. Jonard, and E. Herrbach.** 1997. Effects of mutations in the beet western yellows virus readthrough protein on its expression and packaging and on virus accumulation, symptoms, and aphid transmission. Virology **230:**323-334.

25. **Buzayan, J. M., W. L. Gerlach, and G. Bruening.** 1986. Satellite tobacco ringspot virus RNA: A subset of the RNA sequence is sufficient for autolytic processing. Proc. Natl. Acad. Sci. USA **83:**8859-8862.

26. **Buzen, F. G., C. L. Niblett, G. R. Hooper, J. Hubbard, and M. A. Newman.** 1984. Further characterization of panicum mosaic virus and its associated satellite virus. Phytopathology **74:**313-318.

27. **Cabrera, O., and K.-B. G. Scholthof.** 1999. The complex viral etiology of St. Augustine decline. Plant Dis. **83:**902-904.

28. **Callaway, A., D. Giesman-Cookmeyer, E. T. Gillock, T. L. Sit, and S. A. Lommel.** 2001. The multifunctional capsid proteins of plant RNA viruses. Annu. Rev. Phytopathol. **39:**419-460.

29. **Campbell, R. N., and P. R. Fry.** 1966. The nature of the associations between *Olpidium brassicae* and lettuce big-vein and tobacco necrosis viruses. Virology **29:**222-233.

30. **Canfield, V. A., and R. Levenson.** 1993. Transmembrane organization of the Na,K-ATPase determined by epitope addition. Biochemistry **32:**13782-13786.

31. **Carpenter, C. D., and A. E. Simon.** 1996. In vivo repair of 3'-end deletions in a TCV satellite RNA may involve two abortive synthesis and priming events. Virology **226:**153-160.

32. **Carpenter, C. D., and A. E. Simon.** 1996. In vivo restoration of biologically active 3'-ends of virus-associated RNAs by nonhomologous RNA recombination and replacement of a terminal motif. J. Virol. **70:**478-486.

33. **Carrington, J. C.** 1999. Reinventing plant virus movement. Trends Microbiol. **7:**312-313.

34. **Cascone, P. J., C. D. Carpenter, X. H. Li, and A. E. Simon.** 1990. Recombination between satellite RNAs of turnip crinkle virus. EMBO J. **9:**1709-1715.

35. **Celix, A., J. Burgyan, and E. Rodriguez-Cerezo.** 1999. Interactions between tombusviruses and satellite RNAs of tomato bushy stunt virus: a defect in satRNA B1 replication maps to ORF1 of a helper virus. Virology **262:**129-138.

36. **Celix, A., E. Rodriguez-Cerezo, and F. Garcia-Arenal.** 1997. New satellite RNAs, but no DI RNAs, are found in natural populations of tomato bushy stunt tombusvirus. Virology **239:**277-284.

37. **Champagne, J., M. E. Laliberte-Gagne, and D. Leclerc.** 2007. Phosphorylation of the termini of cauliflower mosaic virus precapsid protein is important for productive infection. Mol. Plant-Microbe Interact. **20:**648-568.

38. **Chen, H. C., Y. H. Hsu, and N. S. Lin.** 2007. Downregulation of bamboo mosaic virus replication requires the 5'-apical hairpin stem loop structure and sequence of satellite RNA. Virology **365**:271-284.

39. **Chiu, J., P. E. March, R. Lee, and D. Tillett.** 2004. Site-directed, Ligase-Independent Mutagenesis (SLIM): a single-tube methodology approaching 100% efficiency in 4 h. Nucleic Acids Res. **32:**e174.

40. **Choi, J., B. S. Kim, X. Zhao, and S. Loesch-Fries.** 2003. The importance of alfalfa mosaic virus coat protein dimers in the initiation of replication. Virology **305:**44-49.

41. **Choi, Y. G., and A. L. N. Rao.** 2003. Packaging of brome mosaic virus RNA3 is mediated through a bipartite signal. J. Virol. **77:**9750-9757.

42. **Cioce, M., and A. I. Lamond.** 2005. Cajal bodies: a long history of discovery. Annu. Rev. Cell. Dev. Biol. **21:**105-131.

43. **Citovsky, V., D. Knorr, G. Schuster, and P. Zambryski.** 1990. The P30 movement protein of tobacco mosaic virus is a single-strand nucleic acid binding protein. Cell **60:**637-647.

44. **Citovsky, V., B. G. McLean, J. R. Zupan, and P. Zambryski.** 1993. Phosphorylation of tobacco mosaic virus cell-to-cell movement protein by a developmentally regulated plant cell wall-associated protein kinase. Genes Dev. **7:**904-910.

45. **Compans, R. W., and N. J. Dimmock.** 1969. An electron microscopic study of single-cycle infection of chick embryo fibroblasts by influenza virus. Virology **39:**499-515.

46. **Crescenzi, A., F. Grieco, and D. Gallitelli.** 1992. Nucleotide sequence of a satellite RNA of a strain of cucumber mosaic virus associated with a tomato fruit necrosis. Nucleic Acids Res. **20:**2886.

47. **Cruz, S. S., A. G. Roberts, D. A. M. Prior, S. Chapman, and K. J. Oparka.** 1998. Cell-to-cell and phloem-mediated transport of Potato virus X: The role of virions. Plant Cell **10:**495-510.

48. **Cui, X. F., and X. P. Zhou.** 2005. Viral suppressor of RNA silencing. Prog. Biochem. Biophys. **32:**210-216.

49. **D'Arcy, C. J., and M. Mayo.** 1997. Proposals for changes in luteovirus taxonomy and nomenclature. Arch. Virol. **142:**1285-1287.

50. **Danthinne, X., J. Seurinck, F. Meulewaeter, M. Van Montagu, and M. Cornelissen.** 1993. The 3'-untranslated region of satellite tobacco necrosis virus RNA stimulates translation in vitro. Mol. Cell Biol. **13:**3340-3349.

51. **Danthinne, X., J. Seurinck, M. Van Montagu, C. W. Pleij, and J. van Emmelo.** 1991. Structural similarities between the RNAs of two satellites of tobacco necrosis virus. Virology **185:**605-614.

52. **Dawson, W. O.** 1992. Tobamovirus-plant interactions. Virology **186:**359-367.

53. **Dawson, W. O., P. Bubrick, and G. L. Grantham.** 1988. Modifications of the tobacco mosaic virus coat protein gene affecting replication, movement, and symptomatology. Phytopathology **78:**783-789.

54. **Degraaff, M., M. R. M. I. Tveld, and E. M. J. Jaspars.** 1995. In vitro evidence that the coat protein of alfalfa mosaic virus plays a direct role in the regulation of plus and minus RNA synthesis - implications for the life cycle of alfalfa mosaic virus. Virology **208:**583-589.

55. **Demler, S. A., and G. A. de Zoeten.** 1989. Characterization of a satellite RNA associated with pea enation mosaic virus. J. Gen. Virol. **70:**1075-1084.

56. **Demler, S. A., D. G. Rucker, L. Nooruddin, and G. A. de Zoeten.** 1994. Replication of the satellite RNA of pea enation mosaic virus is controlled by RNA 2-encoded functions. J. Gen. Virol. **75:**1399-1406.

57. **Desvoyes, B., and K.-B. G. Scholthof.** 2000. RNA:protein interactions associated with satellites of panicum mosaic virus. FEBS Lett. **485:**25-28.

58. **Devic, M., M. Jaegle, and D. Baulcombe.** 1990. Cucumber mosaic virus satellite RNA (strain Y): analysis of sequences which affect systemic necrosis on tomato. J. Gen. Virol. **71:**1443-1449.

59. **Dinesh-Kumar, S. P., and W. A. Miller.** 1993. Control of start codon choice on a plant viral RNA encoding overlapping genes. Plant Cell **5:**679-692.

60. **Ding, X., M. H. Shintaku, S. A. Carter, and R. S. Nelson.** 1996. Invasion of minor veins of tobacco leaves inoculated with tobacco mosaic virus mutants defective in phloem-dependent movement. Proc. Natl. Acad. Sci. USA **93:**11155-11160.

61. **Dodds, J. A.** 1999. Satellite tobacco mosaic virus. Curr. Top. Microbiol. Immunol. **239:**145-157.

62. **Dodds, J. A.** 1998. Satellite tobacco mosaic virus. Annu. Rev. Phytopathol. **36:**295-310.

63. **Donald, R. G., H. Zhou, and A. O. Jackson.** 1993. Serological analysis of barley stripe mosaic virus-encoded proteins in infected barley. Virology **195:**659-668.

64. **Doz, B., J. Dunez, and J. M. Bove.** 1977. Satellite RNA (RNA3) of tomato black ring virus is found with one of the 2 major RNAs (RNA2) in a new capsid nucleoprotein. C. R. Acad. Sci. Hebd Seances Acad. Sci. D. **285:**1573-1576.

65. **Dry, I. B., L. R. Krake, J. E. Rigden, and M. A. Rezaian.** 1997. A novel subviral agent associated with a geminivirus: the first report of a DNA satellite. Proc. Natl. Acad. Sci. USA **94:**7088-7093.

66. **Dunoyer, P., and O. Voinnet.** 2005. The complex interplay between plant viruses and host RNA-silencing pathways. Curr. Opin. Plant. Biol. **8:**415-423.

67. **Erhardt, M., M. Morant, C. Ritzenthaler, C. Stussi-Garaud, H. Guilley, K. Richards, G. Jonard, S. Bouzoubaa, and D. Gilmer.** 2000. P42 movement protein of beet necrotic yellow vein virus is targeted by the movement proteins P13 and P15 to punctate bodies associated with plasmodesmata. Mol. Plant-Microbe Interact. **13:**520-528.

68. **Erhardt, M., C. Stussi-Garaud, H. Guilley, K. E. Richards, G. Jonard, and S. Bouzoubaa.** 1999. The first triple gene block protein of peanut clump virus localizes to the plasmodesmata during virus infection. Virology **264:**220-229.

69. **Esau, K., and L. L. Hoefert.** 1972. Development of infection with beet western yellows virus in the sugarbeet. Virology **48:**724-738.

70. **Espinha, L. M., and J. O. Gaspar.** 1999. Subcellular localization of the coat protein in tobacco cells infected by cucumber mosaic virus isolated from *Catharanthus roseus*. Cytobios. **100:**119-126.

71. **Fuchs, M., M. Pinck, M. A. Serghini, M. Ravelonandro, B. Walter, and L. Pinck.** 1989. The nucleotide sequence of satellite RNA in grapevine fanleaf virus, strain F13. J. Gen. Virol. **70:**955-962.

72. **Fujita, M., K. Mise, Y. Kajiura, K. Dohi, and I. Furusawa.** 1998. Nucleic acid-binding properties and subcellular localization of the 3a protein of brome mosaic bromovirus. J. Gen. Virol. **79:**1273-1280.

73. **Garret, A., C. Kerlan, and D. Thomas.** 1993. The intestine is a site of passage for potato leafroll virus from the gut lumen into the haemocoel in the aphid vector, *Myzus persicae* Sulz. Arch. Virol. **131:**377-392.

74. **Garret, A., C. Kerlan, and D. Thomas.** 1996. Ultrastructural study of acquisition and retention of potato leafroll luteovirus in the alimentary canal of its aphid vector, *Myzus persicae* Sulz. Arch. Virol. **141:**1279-1292.

75. **Gazo, B. M., P. Murphy, J. R. Gatchel, and K. S. Browning.** 2004. A novel interaction of cap-binding protein complexes eukaryotic initiation factor (eIF) 4F and eIF(iso)4F with a region in the 3'-untranslated region of satellite tobacco necrosis virus. J. Biol. Chem. **279:**13584-13592.

76. **Gildow, F. E.** 1993. Evidence for receptor-mediated endocytosis regulating luteovirus acquisition by aphids. Phytopathology **83:**270-277.

77. **Gildow, F. E., and S. M. Gray.** 1993. The aphid salivary gland basal lamina as a selective barrier associated with vector-specific transmission of barley yellow dwarf luteovirus. Phytopathology **83:**1293-1302.

78. **Guan, H., C. D. Carpenter, and A. E. Simon.** 2000. Analysis of *cis*-acting sequences involved in plus-strand synthesis of a turnip crinkle virus-associated satellite RNA identifies a new carmovirus replication element. Virology **268:**345-354.

79. **Guan, H., C. D. Carpenter, and A. E. Simon.** 2000. Requirement of a 5'-proximal linear sequence on minus strands for plus-strand synthesis of a satellite RNA associated with turnip crinkle virus. Virology **268:**355-363.

80. **Guogas, L. M., D. J. Filman, J. M. Hogle, and L. Gehrke.** 2004. Cofolding organizes alfalfa mosaic virus RNA and coat protein for replication. Science **306:**2108-2111.

81. **Hacker, D. L., I. T. Petty, N. Wei, and T. J. Morris.** 1992. Turnip crinkle virus genes required for RNA replication and virus movement. Virology **186:**1-8.

82. **Haley, A., T. Hunter, P. Kiberstis, and D. Zimmern.** 1995. Multiple serine phosphorylation sites on the 30 kDa TMV cell-to-cell movement protein synthesized in tobacco protoplasts. Plant J. **8:**715-724.

83. **Haseloff, J., and R. H. Symons.** 1982. Comparative sequence and structure of viroid-like RNAs of two plant viruses. Nucleic Acids Res. **10:**3681-3691.

84. **Haupt, S., T. Stroganova, E. Ryabov, S. H. Kim, G. Fraser, G. Duncan, M. A. Mayo, H. Barker, and M. Taliansky.** 2005. Nucleolar localization of potato leafroll virus capsid proteins. J. Gen. Virol. **86:**2891-2896.

85. **Hayes, R. J., and K. W. Buck.** 1990. Complete replication of a eukaryotic virus RNA in vitro by a purified RNA-dependent RNA polymerase. Cell **63:**363-368.

86. **Hearne, P. Q., D. A. Knorr, B. I. Hillman, and T. J. Morris.** 1990. The complete genome structure and synthesis of infectious RNA from clones of tomato bushy stunt virus. Virology **177:**141-151.

87. **Hemmer, O., C. Oncino, and C. Fritsch.** 1993. Efficient replication of the in vitro transcripts from cloned cDNA of tomato black ring virus satellite RNA requires the 48K satellite RNA-encoded protein. Virology **194:**800-806.

88. **Hemsley, A., N. Arnheim, M. D. Toney, G. Cortopassi, and D. J. Galas.** 1989. A simple method for site-directed mutagenesis using the polymerase chain reaction. Nucleic Acids Res. **17:**6545-6551.

89. **Hilf, M. E., and W. O. Dawson.** 1993. The tobamovirus capsid protein functions as a host-specific determinant of long-distance movement. Virology **193:**106-114.

90. **Hillman, B. I., R. Foglia, and W. Yuan.** 2000. Satellite and defective RNAs of Cryphonectria hypovirus 3-grand haven 2, a virus species in the family *Hypoviridae* with a single open reading frame. Virology **276:**181-189.

91. **Hinton, T. M., F. Li, and B. S. Crabb.** 2000. Internal ribosomal entry site-mediated translation initiation in equine rhinitis A virus: similarities to and differences from that of foot-and-mouth disease virus. J. Virol. **74:**11708-11716.

92. **Hiscox, J. A., T. Wurm, L. Wilson, P. Britton, D. Cavanagh, and G. Brooks.** 2001. The coronavirus infectious bronchitis virus nucleoprotein localizes to the nucleolus. J. Virol. **75:**506-512.

93. **Ho, S. N., H. D. Hunt, R. M. Horton, J. K. Pullen, and L. R. Pease.** 1989. Site-directed mutagenesis by overlap extension using the polymerase chain reaction. Gene **77:**51-59.

94. **Hodgman, T. C.** 1988. A new superfamily of replicative proteins. Nature **333:**22-23.

95. **Holcomb, G. E., T. Y. Z. Liu, and K. S. Derrick.** 1989. Comparison of isolates of panicum mosaic virus from St. Augustinegrass and centipedegrass. Plant Dis. **73:**355-358.

96. **Holeva, R. C., and S. A. MacFarlane.** 2006. Yeast two-hybrid study of tobacco rattle virus coat protein and 2b protein interactions. Arch. Virol. **151:**2123-2132.

97. **Houser-Scott, F., P. Ansel-McKinney, J. M. Cai, and L. Gehrke.** 1997. In vitro genetic selection analysis of alfalfa mosaic virus coat protein binding to 3'-terminal AUGC repeats in the viral RNAs. J. Virol. **71:**2310-2319.

98. **Houwing, C. J., and E. M. Jaspars.** 1993. Coat protein stimulates replication complexes of alfalfa mosaic virus to produce virion RNAs .. Biochimie **75:**617-621.

99. **Hsu, Y. H., H. C. Chen, J. Cheng, P. Annamalai, B. Y. Lin, C. T. Wu, W. B. Yeh, and N. S. Lin.** 2006. Crucial role of the 5'- conserved structure of bamboo mosaic virus satellite RNA in downregulation of helper viral RNA replication. J. Virol. **80:**2566-2574.

100. **Ivanov, K. I., P. Puustinen, R. Gabrenaite, H. Vihinen, L. Ronnstrand, L. Valmu, N. Kalkkinen, and K. Makinen.** 2003. Phosphorylation of the potyvirus capsid protein by protein kinase CK2 and its relevance for virus infection. Plant Cell **15:**2124-2139.

101. **Ivanov, K. I., P. Puustinen, A. Merits, M. Saarma, and K. Makinen.** 2001. Phosphorylation down-regulates the RNA binding function of the coat protein of potato virus A. J. Biol. Chem. **276:**13530-13540.

102. **Jaspars, E. M., and C. J. Houwing.** 2002. A genome-activating N-terminal coat protein peptide of alfalfa mosaic virus is able to activate infection by RNAs 1, 2 and 3 but not by RNAs 1 and 2. Further support for the messenger release hypothesis. Arch. Virol. **147:**857-863.

103. **Jones, D. H.** 1994. PCR mutagenesis and recombination in vivo. PCR Methods Appl. **3:**S141-148.

104. **Jones, D. H., and S. C. Winistorfer.** 1992. Recombinant circle PCR and recombination PCR for site-specific mutagenesis without PCR product purification. Biotechniques **12:**528-535.

105. **Kaper, J. M., and M. E. Tousignant.** 1977. Cucumber mosaic virus-associating RNA 5. I. Role of host plant and helper strain in determining amount of associated RNA 5 with virions. Virology **80:**186-195.

106. **Kaper, J. M., M. E. Tousignant, and G. Steger.** 1988. Nucleotide sequence predicts circularity and self-cleavage of 300-ribonucleotide satellite of arabis mosaic virus. Biochem. Biophys. Res. Commun. **154:**318-325.

107. **Kaplan, I. B., L. Zhang, and P. Palukaitis.** 1998. Characterization of cucumber mosaic virus. V. Cell-to-cell movement requires capsid protein but not virions. Virology **246:**221-231.

108. **Kassanis, B.** 1968. Satellitism and related phenomena in plant and animal viruses. Adv. Virus. Res. **13:**147-180.

109. **Kassanis, B., and H. L. Nixon.** 1960. Activation of one plant virus by another. Nature **187:**713-714.

110. **Kassanis, B., and M. P. Phillips.** 1970. Serological relationship of strains of tobacco necrosis virus and their ability to activate strains of satellite virus. J. Gen. Virol. **9:**119-126.

111. **Kasteel, D., J. Wellink, J. Verver, J. van Lent, R. Goldbach, and A. van Kammen.** 1993. The involvement of cowpea mosaic virus mRNA-encoded proteins in tubule formation. J. Gen. Virol. **74:**1721-1724.

112. **Kasteel, D. T., N. N. van der Wel, K. A. Jansen, R. W. Goldbach, and J. W. van Lent.** 1997. Tubule-forming capacity of the movement proteins of alfalfa mosaic virus and brome mosaic virus. J. Gen. Virol. **78:**2089-2093.

113. **Kawakami, S., H. S. Padgett, D. Hosokawa, Y. Okada, R. N. Beachy, and Y. Watanabe.** 1999. Phosphorylation and/or presence of serine 37 in the movement protein of tomato mosaic tobamovirus is essential for intracellular localization and stability in vivo. J. Virol. **73:**6831-6840.

114. **Kim, S. H., E. V. Ryabov, N. O. Kalinina, D. V. Rakitina, T. Gillespie, S. Macfarlane, S. Haupt, J. W. Brown, and M. Taliansky.** 2007. Cajal bodies and the nucleolus are required for a plant virus systemic infection. EMBO J. **26:**2169-2179.

115. **Kiss-Laszlo, Z., Y. Henry, J. P. Bachellerie, M. Caizergues-Ferrer, and T. Kiss.** 1996. Site-specific ribose methylation of preribosomal RNA: a novel function for small nucleolar RNAs. Cell **85:**1077-1088.

116. **Kong, Q., J. Wang, and A. E. Simon.** 1997. Satellite RNA-mediated resistance to turnip crinkle virus in Arabidopsis involves a reduction in virus movement. Plant Cell **9:**2051-2063.

117. **Kozak, M.** 1995. Adherence to the first-AUG rule when a second AUG codon follows closely upon the first. Proc. Natl. Acad. Sci. USA **92:**2662-2666.

118. **Kozak, M.** 1996. Interpreting cDNA sequences: Some insights from studies on translation. Mamm. Genome **7:**563-574.

119. **Kozak, M.** 2002. Pushing the limits of the scanning mechanism for initiation of translation. Gene **299:**1-34.

120. **Krol, M. A., N. H. Olson, J. Tate, J. E. Johnson, T. S. Baker, and P. Ahlquist.** 1999. RNA-controlled polymorphism in the in vivo assembly of 180-subunit and 120-subunit virions from a single capsid protein. Proc. Natl. Acad. Sci. USA **96:**13650-13655.

121. **Kunkel, T. A., J. D. Roberts, and R. A. Zakour.** 1987. Rapid and efficient site-specific mutagenesis without phenotypic selection. Proc. Natl. Acad. Sci. USA **82:**488-492.

122. **Landt, O., H.-P. Grunert, and U. Hahn.** 1990. A general method for rapid site-directed mutagenesis using the polymerase chain reaction. Gene **96:**125-128.

123. **Larson, S. B., and A. McPherson.** 2001. Satellite tobacco mosaic virus RNA: structure and implications for assembly. Curr. Opin. Struct. Biol. **11:**59-65.

124. **Law, L. M., J. C. Everitt, M. D. Beatch, C. F. Holmes, and T. C. Hobman.** 2003. Phosphorylation of rubella virus capsid regulates its RNA binding activity and virus replication. J. Virol. **77:**1764-1771.

125. **Lee, J. Y., and W.J. Lucas.** 2001. Phosphorylation of viral movement proteins-regulation of cell-to-cell trafficking. Trends Microbiol. **9:**5-8.

126. **Lee, Y. S., Y. H. Hsu, and N. S. Lin.** 2000. Generation of subgenomic RNA directed by a satellite RNA associated with bamboo mosaic potexvirus: analyses of potexvirus subgenomic RNA promoter. J. Virol. **74:**10341-10348.

127. **Leung, D. W., K. S. Browning, J. E. Heckman, U. L. RajBhandary, and J. M. Clark, Jr.** 1979. Nucleotide sequence of the 5' terminus of satellite tobacco necrosis virus ribonucleic acid. Biochemistry **18:**1361-1366.

128. **Li, D., S. A. Behjatnia, I. B. Dry, J. W. Randles, O. Eini, and M. A. Rezaian.** 2007. Genomic regions of tomato leaf curl virus DNA satellite required for replication and for satellite-mediated delivery of heterologous DNAs. J. Gen. Virol. **88:**2073-2077.

129. **Li, W. X., and S. W. Ding.** 2001. Viral suppressors of RNA silencing. Curr. Opin. Biotechnol. **12:**150-154.

130. **Li, X. H., and A. E. Simon.** 1990. Symptom intensification on cruciferous hosts by the virulent satellite RNA of turnip crinkle virus. Phytopathology **80:**238-242.

131. **Lin, M. K., C. C. Hu, N. S. Lin, B. Y. Chang, and Y. H. Hsu.** 2006. Movement of potexviruses requires species-specific interactions among the cognate triple gene block proteins, as revealed by a trans-complementation assay based on the bamboo mosaic virus satellite RNA-mediated expression system. J. Gen. Virol. **87:**1357-1367.

132. **Lin, N. S., and Y. H. Hsu.** 1994. A satellite RNA associated with bamboo mosaic potexvirus. Virology **202:**707-714.

133. **Lin, N. S., Y. S. Lee, B. Y. Lin, C. W. Lee, and Y. H. Hsu.** 1996. The open reading frame of bamboo mosaic potexvirus satellite RNA is not essential for its replication and can be replaced with a bacterial gene. Proc. Natl. Acad. Sci. USA **93:**3138-3142.

134. **Lin, N. S., B. Y. Lin, N. W. Lo, C. C. Hu, T. Y. Chow, and Y. H. Hsu.** 1994. Nucleotide sequence of the genomic RNA of bamboo mosaic potexvirus. J. Gen. Virol. **75:**2513-2518.

135. **Liu, J., G. Prolla, A. Rostagno, R. Chiarle, H. Feiner, and G. Inghirami.** 2000. Initiation of translation from a downstream in-frame AUG codon on BRCA1 can generate the novel isoform protein ΔBRCA1(17aa). Oncogene **19:**2767-2773.

136. **Liu, S., X. He, G. Park, C. Josefsson, and K. L. Perry.** 2002. A conserved capsid protein surface domain of Cucumber mosaic virus is essential for efficient aphid vector transmission. J. Virol. **76:**9756-9762.

137. **Loeschfries, L. S., N. P. Jarvis, K. J. Krahn, S. E. Nelson, and T. C. Hall.** 1985. Expression of alfalfa mosaic virus RNA-4 cDNA transcripts in vitro and in vivo. Virology **146:**177-187.

138. **Lough, T. J., N. E. Netzler, S. J. Emerson, P. Sutherland, F. Carr, D. L. Beck, W. J. Lucas, and R. L. Forster.** 2000. Cell-to-cell movement of potexviruses: evidence for a ribonucleoprotein complex involving the coat protein and first triple gene block protein. Mol. Plant-Microbe Interact. **13:**962-974.

139. **Makino, D. L., J. Day, S. B. Larson, and A. McPherson.** 2006. Investigation of RNA structure in satellite panicum mosaic virus. Virology **351:**420-431.

140. **Makino, D. L., S. B. Larson, and A. McPherson.** 2005. Preliminary analysis of crystals of panicum mosaic virus (PMV) by X-ray diffraction and atomic force microscopy. Acta Crystallogr. D Biol. Crystallogr. **61:**173-179.

141. **Masuta, C., and Y. Takanami.** 1989. Determination of sequence and structural requirements for pathogenicity of a cucumber mosaic virus satellite RNA (Y-satRNA). Plant Cell **1:**1165-1173.

142. **Masuta, C., D. Zuidema, B. G. Hunter, L. A. Heaton, D. S. Sopher, and A. O. Jackson.** 1987. Analysis of the genome of satellite panicum mosaic virus. Virology **159:**329-338.

143. **Matera, A. G.** 1999. Nuclear bodies: multifaceted subdomains of the interchromatin space. Trends Cell Biol. **9:**302-309.

144. **Matsushita, Y., K. Yoshioka, T. Shigyo, H. Takahashi, and H. Nyunoy.** 2002. Phosphorylation of the movement protein of cucumber mosaic virus in transgenic tobacco plants. Virus Genes **24:**231-234.

145. **Maule, A. J.** 1994. Plant virus movement: de novo process or redeployed machinery? Trends Microbiol. **2:**305-306.

146. **Mavrakis, M., S. Mehouas, E. Real, F. Iseni, D. Blondel, N. Tordo, and R. W. Ruigrok.** 2006. Rabies virus chaperone: identification of the phosphoprotein peptide that keeps nucleoprotein soluble and free from non-specific RNA. Virology **349:**422-429.

147. **Mayo, M. A., and V. Ziegler-Graff.** 1996. Molecular biology of luteoviruses. Adv. Virus Res. **46:**413-460.

148. **McGarvey, P. B., J. M. Kaper, M. J. Avila-Rincon, L. Pena, and J. R. Diaz-Ruiz.** 1990. Transformed tomato plants express a satellite RNA of cucumber mosaic virus and produce lethal necrosis upon infection with viral RNA. Biochem. Biophys. Res. Commun. **170:**548-555.

149. **Meulewaeter, F., X. Danthinne, M. Van Montagu, and M. Cornelissen.** 1998. 5'- and 3'-sequences of satellite tobacco necrosis virus RNA promoting translation in tobacco. Plant J. **14:**169-176.

150. **Meulewaeter, F., M. Van Montagu, and M. Cornelissen.** 1998. Features of the autonomous function of the translational enhancer domain of satellite tobacco necrosis virus. RNA **4:**1347-1356.

151. **Michel, M. R., M. Elgizoli, Y. Dai, R. Jakob, H. Koblet, and A. P. Arrigo.** 1990. Karyophilic properties of Semliki Forest virus nucleocapsid protein. J. Virol. **64:**5123-31.

152. **Mirkov, T. E., D. M. Mathews, D. H. Du Plessis, and J. A. Dodds.** 1989. Nucleotide sequence and translation of satellite tobacco mosaic virus RNA. Virology **170:**139-146.

153. **Monis, J., D. S. Sopher, and A. O. Jackson.** 1992. Biologically active cDNA clones of panicum mosaic virus satellites. Phytopathology **82:**1175.

154. **Moser, O., M. Fuchs, L. Pinck, and C. Stussi-Garaud.** 1992. Immunodetection of grapevine fanleaf virus satellite RNA-encoded protein in infected *Chenopodium quinoa*. J. Gen. Virol. **73:**3033-3038.

155. **Mullis, K. B., and F. A. Faloona.** 1987. Specific synthesis of DNA in vitro via a polymerase-catalyzed chain reaction. Methods Enzymol. **155:**335-350.

156. **Murant, A. F.** 1990. Dependence of groundnut rosette virus on its satellite RNA as well as on groundnut rosette assistor luteovirus for transmission by *Aphis craccivora*. J. Gen. Virol. **71:**2163-2166.

157. **Murant, A. F., and I. K. Kumar.** 1990. Different variants of the satellite RNA of groundnut rosette virus are responsible for the chlorotic and green forms of groundnut rosette disease. Ann. Appl. Biol. **117:**85-92.

158. **Murant, A. F., and M. A. Mayo.** 1982. Satellites of plant viruses. Annu. Rev. Phytopathol. **20:**49-70.

159. **Murant, A. F., R. Rajeshwari, D. J. Robinson, and J. H. Raschke.** 1988. A satellite RNA of groundnut rosette virus that is largely responsible for symptoms of groundnut rosette disease. J. Gen. Virol. **69:**1479-1486.

160. **Nagano, H., K. Mise, T. Okuno, and I. Furusawa.** 1999. The cognate coat protein is required for cell-to-cell movement of a chimeric brome mosaic virus mediated by the cucumber mosaic virus movement protein. Virology **265:**226-234.

161. **Neeleman, L., E. A. G. Van der Vossen, and J. F. Bol.** 1993. Infection of tobacco with alfalfa mosaic virus cDNA sheds light on the early function of the coat protein. Virology **196:**883-887.

162. **Ngon, A. Yassi M., and J. A. Dodds.** 1998. Specific sequence changes in the 5'-terminal region of the genome of satellite tobacco mosaic virus are required for adaptation to tobacco mosaic virus. J. Gen. Virol. **79:**905-913.

163. **Ni, J., A. L. Tien, and M. J. Fournier.** 1997. Small nucleolar RNAs direct site-specific synthesis of pseudouridine in ribosomal RNA. Cell **89:**565-573.

164. **Nitta, N., Y. Takanami, S. Kuwata, and S. Kubo.** 1988. Inoculation with RNA-1 and RNA-2 of cucumber mosaic virus induces viral RNA replicase activity in tobacco mesophyll protoplasts. J. Gen. Virol. **69:**2695-2700.

165. **Noris, E., A. M. Vaira, P. Caciagli, V. Masenga, B. Gronenborn, and G. P. Accotto.** 1998. Amino acids in the capsid protein of tomato yellow leaf curl virus that are crucial for systemic infection, particle formation, and insect transmission. J. Virol. **72:**10050-10057.

166. **Okinaka, Y., K. Mise, T. Okuno, and I. Furusawa.** 2003. Characterization of a novel barley protein, HCP1, that interacts with the brome mosaic virus coat protein. Mol. Plant-Microbe Interact. **16:**352-359.

167. **Okinaka, Y., K. Mise, E. Suzuki, T. Okuno, and I. Furusawa.** 2001. The C-terminus of brome mosaic virus coat protein controls viral cell-to-cell and long-distance movement. J. Virol. **75:**5385-5390.

168. **Omarov, R. T., D. Qi, and K.-B. G. Scholthof.** 2005. The capsid protein of satellite panicum mosaic virus contributes to systemic invasion and interacts with its helper virus. J. Virol. **79:**9756-9764.

169. **Osman, F., G. L. Grantham, and A. L. Rao.** 1997. Molecular studies on bromovirus capsid protein. IV. Coat protein exchanges between brome mosaic and cowpea chlorotic mottle viruses exhibit neutral effects in heterologous hosts. Virology **238:**452-459.

170. **Owens, R. A., and I. R. Schneider.** 1977. Satellite of tobacco ringspot virus RNA lacks detectable mRNA activity. Virology **80:**222-224.

171. **Peeples, M. E., C. Wang, K. C. Gupta, and N. Coleman.** 1992. Nuclear entry and nucleolar localization of the Newcastle disease virus (NDV) matrix protein occur early in infection and do not require other NDV proteins. J. Virol. **66:**3263-3269.

172. **Qiu, W., and K.-B. G. Scholthof.** 2001. Defective interfering RNAs of a satellite virus. J. Virol. **75:**5429-5432.

173. **Qiu, W., and K.-B. G. Scholthof.** 2001. Genetic identification of multiple biological roles associated with the capsid protein of satellite panicum mosaic virus. Mol. Plant-Microbe Interact. **14:**21-30.

174. **Qiu, W., and K.-B. G. Scholthof.** 2000. In vitro- and in vivo-generated defective RNAs of satellite panicum mosaic virus define *cis*-acting RNA elements required for replication and movement. J. Virol. **74:**2247-2254.

175. **Qiu, W., and K.-B. G. Scholthof.** 2004. Satellite panicum mosaic virus capsid protein elicits symptoms on a nonhost plant and interferes with a suppressor of virus-induced gene silencing. Mol. Plant-Microbe Interact. **17:**263-271.

176. **Qu, F., T. Ren, and T. J. Morris.** 2003. The coat protein of turnip crinkle virus suppresses posttranscriptional gene silencing at an early initiation step. J. Virol. **77:**511-522.

177. **Quadt, R., and E. M. Jaspars.** 1991. Characterization of cucumber mosaic virus RNA-dependent RNA polymerase. FEBS Lett. **279:**273-276.

178. **Quadt, R., H. J. M. Rosdorff, T. W. Hunt, and E. M. J. Jaspars.** 1991. Analysis of the protein composition of alfalfa mosaic virus RNA dependent RNA polymerase. Virology **182:**309-315.

179. **Quillet, L., H. Guilley, G. Jonard, and K. Richards.** 1989. In vitro synthesis of biologically active beet necrotic yellow vein virus RNA. Virology **172:**293-301.

180. **Rao, A. L. N.** 2006. Genome packaging by spherical plant RNA viruses. Annu. Rev. Phytopathol. **44:**61-87.

181. **Rao, A. L. N.** 1997. Molecular studies on bromovirus capsid protein. III. Analysis of cell-to-cell movement competence of coat protein defective variants of cowpea chlorotic mottle virus. Virology **232:**385-395.

182. **Rao, A. L. N., and G. L. Grantham.** 1996. Molecular studies on bromovirus capsid protein. II. Functional analysis of the amino-terminal arginine-rich motif and its role in encapsidation, movement, and pathology. Virology **226:**294-305.

183. **Reichert, V. L., M. Choi, J. E. Petrillo, and L. Gehrke.** 2007. Alfalfa mosaic virus coat protein bridges RNA and RNA-dependent RNA polymerase in vitro. Virology **364:**214-226.

184. **Reinbold, C., F. E. Gildow, E. Herrbach, V. Ziegler-Graff, M. C. Gonçalves, J. F. van den Heuvel, and V. Brault.** 2001. Studies on the role of the minor capsid protein in transport of Beet western yellows virus through *Myzus persicae*. J. Gen. Virol. **82:**1995-2007.

185. **Reusken, C. B., L. Neeleman, F. T. Brederode, and J. F. Bol.** 1997. Mutations in coat protein binding sites of alfalfa mosaic virus RNA 3 affect subgenomic RNA 4 accumulation and encapsidation of viral RNAs. J. Virol. **71:**8385-8391.

186. **Reusken, C. B. E. M., and J. F. Bol.** 1996. Structural elements of 3'-terminal coat protein binding site in alfalfa mosaic virus RNAs. Nucleic Acids Res. **24:**2660-2665.

187. **Rezaian, M. A., R. H. Williams, and R. H. Symons.** 1985. Nucleotide sequence of cucumber mosaic virus RNA. 1. Presence of a sequence complementary to part of the viral satellite RNA and homologies with other viral RNAs. Eur. J. Biochem. **150:**331-339.

188. **Rodriguezalvarado, G., G. Kurath, and J. A. Dodds.** 1994. Symptom modification by satellite tobacco mosaic virus in pepper types and cultivars infected with helper tobamoviruses. Phytopathology **84:**617-621.

189. **Roossinck, M. J., D. Sleat, and P. Palukaitis.** 1992. Satellite RNAs of plant viruses: structures and biological effects. Microbiol. Rev. **56:**265-279.

190. **Routh, G., J. A. Dodds, L. Fitzmaurice, and T. E. Mirkov.** 1995. Characterization of deletion and frameshift mutants of satellite tobacco mosaic virus. Virology **212:**121-127.

191. **Rubino, L., J. Burgyan, F. Grieco, and M. Russo.** 1990. Sequence analysis of cymbidium ringspot virus satellite and defective interfering RNAs. J. Gen. Virol. **71:**1655-1660.

192. **Rubino, L., J. C. Carrington, and M. Russo.** 1992. Biologically active cymbidium ringspot virus satellite RNA in transgenic plants suppresses accumulation of DI RNA. Virology **188:**429-437.

193. **Rubino, L., M. E. Tousignant, G. Steger, and J. M. Kaper.** 1990. Nucleotide sequence and structural analysis of two satellite RNAs associated with chicory yellow mottle virus. J. Gen. Virol. **71:**1897-1903.

194. **Ryabov, E. V., S. H. Kim, and M. Taliansky.** 2004. Identification of a nuclear localization signal and nuclear export signal of the umbraviral long-distance RNA movement protein. J. Gen. Virol. **85:**1329-1333.

195. **Ryabov, E. V., D. J. Robinson, and M. E. Taliansky.** 1999. A plant virus-encoded protein facilitates long-distance movement of heterologous viral RNA. Proc. Natl. Acad. Sci. USA **96:**1212-1217.

196. **Sacher, R., and P. Ahlquist.** 1989. Effects of deletions in the N-terminal basic arm of brome mosaic virus coat protein on RNA packaging and systemic infection. J. Virol. **63:**4545-4552.

197. **Sambrook, J., Fritsch, E. F. and Maniatis, T. .** 1989. Molecular Cloning: A Laboratory Mannual. Cold Spring Harbor Laboratory Press, Cold Spring Harbor, NY.

198. **Satyanarayana, T., S. Gowda, M. Mawassi, M. R. Albiach-Marti, M. A. Aylion, C. Robertson, S. M. Garnsey, and W. O. Dawson.** 2000. Closterovirus encoded HSP70 homolog and p61 in addition to both coat proteins function in efficient virion assembly. Virology **278:**253-265.

199. **Saunders, K., and J. Stanley.** 1999. A nanovirus-like DNA component associated with yellow vein disease of *Ageratum conyzoides:* evidence for interfamilial recombination between plant DNA viruses. Virology **264:**142-152.

200. **Sawai, E. T., and J. S. Butel.** 1992. Epitope mapping and conformational analysis of SV40 T-antigen deletion mutants. Virology **189:**782-785.

201. **Schmitz, I., and A. L. Rao.** 1996. Molecular studies on bromovirus capsid protein. I. Characterization of cell-to-cell movement-defective RNA3 variants of brome mosaic virus. Virology **226:**281-293.

202. **Schmitz, I., and A. L. N. Rao.** 1998. Deletions in the conserved amino-terminal basic arm of cucumber mosaic virus coat protein disrupt virion assembly but do not abolish infectivity and cell-to-cell movement. Virology **248:**323-331.

203. **Schneider, I. R.** 1971. Characteristics of a satellite-like virus of tobacco ringspot virus. Virology **45:**108-122.

204. **Schneider, W. L., A. E. Greene, and R. F. Allison.** 1997. The carboxy-terminal two-thirds of the cowpea chlorotic mottle bromovirus capsid protein is incapable of virion formation yet supports systemic movement. J. Virol. **71:**4862-4865.

205. **Scholthof, H. B.** 2005. Plant virus transport: motions of functional equivalence. Trends Plant. Sci. **10:**376-382.

206. **Scholthof, H. B., T. J. Morris, and A. O. Jackson.** 1993. The capsid protein gene of tomato bushy stunty virus is dispensable for systemic movement and can be replaced for localized expression of foreign genes. Mol. Plant-Microbe Interact. **6:**309-322.

207. **Scholthof, H. B., K.-B. G. Scholthof, and A. O. Jackson.** 1996. Plant virus gene vectors for transient expression of foreign proteins in plants. Annu. Rev. Phytopathol. **34:**299-323.

208. **Scholthof, K.-B. G.** 1999. A synergism induced by satellite panicum mosaic virus. Mol. Plant-Microbe Interact. **12:**163-166.

209. **Scholthof, K.-B. G., B. I. Hillman, B. Modrell, L. A. Heaton, and A. O. Jackson.** 1994. Characterization and detection of sc4: a sixth gene encoded by sonchus yellow net virus. Virology **204:**279-288.

210. **Scholthof, K.-B. G., R. W. Jones, and A. O. Jackson.** 1999. Biology and structure of plant satellite viruses activated by icosahedral helper viruses. Curr. Top. Microbiol. Immunol. **239:**123-143.

211. **Shaw, B. D., and S. Upadhyay.** 2005. *Aspergillus nidulans* swoK encodes an RNA binding protein that is important for cell polarity. Fungal Genet. Biol. **42:**862-872.

212. **Silber, G., and L. G. Burk.** 1965. Infectivity of tobacco mosaic virus stored for fifty years in extracted, 'unpreserved' plant juice. Nature **206:**740-741.

213. **Silhavy, D., and J. Burgyan.** 2004. Effects and side-effects of viral RNA silencing suppressors on short RNAs. Trends Plant Sci. **9:**76-83.

214. **Simon, A., and S. Howell.** 1986. Small pathogenic RNAs associated with turnip crinkle virus. J. Cell. Biochem. 42-42. Suppl. 10C.

215. **Simon, A. E., H. Engel, R. P. Johnson, and S. H. Howell.** 1988. Identification of regions affecting virulence, RNA processing and infectivity in the virulent satellite of turnip crinkle virus. EMBO J. **7:**2645-2651.

216. **Simon, A. E., and S. H. Howell.** 1987. Synthesis in vitro infectious RNA copies of the virulent satellite of turnip crinkle virus. Virology **156:**146-152.

217. **Simon, A. E., and S. H. Howell.** 1986. The virulent satellite RNA of turnip crinkle virus has a major domain homologous to the 3' end of the helper virus genome. EMBO J. **5:**3423-3428.

218. **Simon, A. E., M. J. Roossinck, and Z. Havelda.** 2004. Plant virus satellite and defective interfering RNAs: new paradigms for a new century. Annu. Rev. Phytopathol. **42:**415-437.

219. **Sit, T. L., P. R. Haikal, A. S. Callaway, and S. A. Lommel.** 2001. A single amino acid mutation in the carnation ringspot virus capsid protein allows virion formation but prevents systemic infection. J. Virol. **75:**9538-9542.

220. **Sleat, D. E.** 1990. Nucleotide sequence of a new satellite RNA of cucumber mosaic virus. Nucleic Acids Res. **18:**3416.

221. **Sleat, D. E., and P. Palukaitis.** 1990. Site-directed mutagenesis of a plant viral satellite RNA changes its phenotype from ameliorative to necrogenic. Proc. Natl. Acad. Sci. USA **87:**2946-2950.

222. **Solovyev, A. G., T. A. Stroganova, A. A. Zamyatnin, Jr., O. N. Fedorkin, J. Schiemann, and S. Y. Morozov.** 2000. Subcellular sorting of small membrane-associated triple gene block proteins: TGBp3-assisted targeting of TGBp2. Virology **269:**113-127.

223. **Soto, M. J., L. F. Chen, Y. S. Seo, and R. L. Gilbertson.** 2005. Identification of regions of the *Beet mild curly top virus* (family *Geminiviridae*) capsid protein involved in systemic infection, virion formation and leafhopper transmission. Virology **341:**257-270.

224. **Sun, X., and A. E. Simon.** 2003. Fitness of a turnip crinkle virus satellite RNA correlates with a sequence-nonspecific hairpin and flanking sequences that enhance replication and repress the accumulation of virions. J. Virol. **77:**7880-7889.

225. **Tai, J. H., S. C. Chang, C. F. Ip, and S. J. Ong.** 1995. Identification of a satellite double-stranded RNA in the parasitic protozoan *Trichomonas vaginalis* infected with *T. vaginalis* virus T1. Virology **208:**189-196.

226. **Taliansky, M., I. M. Roberts, N. Kalinina, E. V. Ryabov, S. K. Raj, D. J. Robinson, and K. J. Oparka.** 2003. An umbraviral protein, involved in long-distance RNA movement, binds viral RNA and forms unique, protective ribonucleoprotein complexes. J. Virol. **77:**3031-3040.

227. **Taliansky, M. E., and F. Garcia-Arenal.** 1995. Role of cucumovirus capsid protein in long-distance movement within the infected plant. J. Virol. **69:**916-22.

228. **Taliansky, M. E., and D. J. Robinson.** 1997. Trans-acting untranslated elements of groundnut rosette virus satellite RNA are involved in symptom production. J. Gen. Virol. **78 :**1277-1285.

229. **Taliansky, M. E., E. V. Ryabov, D. J. Robinson, and P. Palukaitis.** 1998. Tomato cell death mediated by complementary plant viral satellite RNA sequences. Mol. Plant-Microbe Interact. **11:**1214-1222.

230. **Trutnyeva, K., R. Bachmaier, and E. Waigmann.** 2005. Mimicking carboxyterminal phosphorylation differentially effects subcellular distribution and cell-to-cell movement of tobacco mosaic virus movement protein. Virology **332:**563-577.

231. **Tsai, M. S., Y. H. Hsu, and N. S. Lin.** 1999. Bamboo mosaic potexvirus satellite RNA (satBaMV RNA)-encoded P20 protein preferentially binds to satBaMV RNA. J. Virol. **73:**3032-3039.

232. **Turina, M., B. Desvoyes, and K.-B. G. Scholthof.** 2000. A gene cluster encoded by panicum mosaic virus is associated with virus movement. Virology **266:**120-128.

233. **Turina, M., M. Maruoka, J. Monis, A. O. Jackson, and K.-B. G. Scholthof.** 1998. Nucleotide sequence and infectivity of a full-length cDNA clone of panicum mosaic virus. Virology **241:**141-155.

234. **Valverde, R. A., and J. A. Dodds.** 1986. Evidence for a satellite RNA associated naturally with the U5-Strain and experimentally with the U1-Strain of tobacco mosaic virus. J. Gen. Virol. **67:**1875-1884.

235. **Valverde, R. A., and J. A. Dodds.** 1987. Some properties of isometric virus-particles which contain the satellite RNA of tobacco mosaic virus. J. Gen. Virol. **68:**965-972.

236. **van Lipzig, R., A. P. Gultyaev, C. W. Pleij, M. van Montagu, M. Cornelissen, and F. Meulewaeter.** 2002. The 5' and 3' extremities of the satellite tobacco necrosis virus translational enhancer domain contribute differentially to stimulation of translation. RNA **8:**229-236.

237. **van Rossum, C. M., F. T. Brederode, L. Neeleman, and J. F. Bol.** 1997. Functional equivalence of common and unique sequences in the 3' untranslated regions of alfalfa mosaic virus RNAs 1, 2, and 3. J. Virol. **71:**3811-3816.

238. **van Emmelo, J., P. Ameloot, and W. Fiers.** 1987. Expression in plants of the cloned satellite tobacco necrosis virus genome and of derived insertion mutants. Virology **157:**480-487.

239. **Veidt, I., H. Lot, M. Leiser, D. Scheidecker, H. Guilley, K. Richards, and G. Jonard.** 1988. Nucleotide sequence of beet western yellows virus RNA. Nucleic Acids Res. **16:**9917-9932.

240. **Vijaya Palani, P., V. Kasiviswanathan, J.-C. Chen, W. Chen, Y.-H. Hsu, and N.-S. Lin.** 2006. The arginine-rich motif of bamboo mosaic virus satellite RNA-encoded P20 mediates self-interaction, intracellular targeting, and cell-to-cell movement. Mol. Plant-Microbe Interact. **19:**758-767.

241. **Voinnet, O., Y. M. Pinto, and D. C. Baulcombe.** 1999. Suppression of gene silencing: a general strategy used by diverse DNA and RNA viruses of plants. Proc. Natl. Acad. Sci. USA **96:**14147-14152.

242. **Wang, S. H., W. J. Syu, K. J. Huang, H. Y. Lei, C. W. Yao, C. C. King, and S. T. Hu.** 2002. Intracellular localization and determination of a nuclear localization signal of the core protein of dengue virus. J. Gen. Virol. **83:**3093-3102.

243. **Wang, W., and B. A. Malcolm.** 1999. Two-stage PCR protocol allowing introduction of multiple mutations, deletions and insertions using QuikChange site-directed mutagenesis. Biotechniques **26:**680-682.

244. **Wellink, J., and A. Van Kammen.** 1989. Cell-to-cell transport of cowpea mosaic virus requires both the 58K/48K proteins and the capsid proteins. J. Gen. Virol. **70:**2279–2286.

245. **White, K. A., J. M. Skuzeski, W. Li, N. Wei, and T. J. Morris.** 1995. Immuno-detection, expression strategy and complementation of turnip crinkle virus p28 and p88 replication components. Virology **211:**525-534.

246. **Widada, J. S., and J. R. Bonami.** 2004. Characteristics of the monocistronic genome of extra small virus, a virus-like particle associated with *Macrobrachium rosenbergii* nodavirus: possible candidate for a new species of satellite virus. J. Gen. Virol. **85:**643-646.

247. **Wilson, W. J.** 1974. A histological and ultrastructural study of the St. Augustinegrass strain of panicum mosaic virus in resistant and susceptible St. Augustinegrass and red siberian millet. Ph.D. dissertation. Texas A&M University.

248. **Winkler, F. K., C. E. Schutt, S. C. Harrison, and G. Bricogne.** 1977. Tomato bushy stunt virus at 5.5-Å resolution. Nature **265:**509-513.

249. **Wu, G., and J. M. Kaper.** 1995. Competition of viral and satellite RNAs of cucumber mosaic virus for replication in vitro by viral RNA-dependent RNA polymerase. Res. Virol. **146:**61-67.

250. **Xiang, Y., K. Kakani, R. Reade, E. Hui, and D. Rochon.** 2006. A 38-amino-acid sequence encompassing the arm domain of the cucumber necrosis virus coat protein functions as a chloroplast transit peptide in infected plants. J. Virol. **80:**7952-7964.

251. **Xu, P., E. B. Blancaflor, and M. J. Roossinck.** 2003. In spite of induced multiple defense responses, tomato plants infected with cucumber mosaic virus and D satellite RNA succumb to systemic necrosis. Mol. Plant-Microbe Interact. **16:**467-476.

252. **Xu, P., and M. J. Roossinck.** 2000. Cucumber mosaic virus D satellite RNA-induced programmed cell death in tomato. Plant Cell **12:**1079-1092.

253. **Yang, C. C., J. S. Liu, C. P. Lin, and N. S. Lin.** 1997. Nucleotide sequence and phylogenetic analysis of a bamboo mosaic potexvirus isolate from common bamboo (*Bambusa vulgaris* McClure). Bot. Bull. Acad. Sinica **38:**77-84.

254. **Yeh, W.-B., Y.-H. Hsu, H.-C. Chen, and N.-S. Lin.** 2004. A conserved secondary structure in the hypervariable region at the 5' end of bamboo mosaic virus satellite RNA is functionally interchangeable. Virology **330:**105-115.

255. **Ysebaert, M., J. van Emmelo, and W. Fiers.** 1980. Total nucleotide sequence of a nearly full-size DNA copy of satellite tobacco necrosis virus RNA. J. Mol. Biol. **143:**273-287.

256. **Zhang, C. X., P. J. Cascone, and A. E. Simon.** 1991. Recombination between satellite and genomic RNAs of turnip crinkle virus. Virology **184:**791-794.

257. **Zhang, F., and A. E. Simon.** 2003. Enhanced viral pathogenesis associated with a virulent mutant virus or a virulent satellite RNA correlates with reduced virion accumulation and abundance of free coat protein. Virology **312:**8-13.

258. **Zhang, G., and A. E. Simon.** 2003. A multifunctional turnip crinkle virus replication enhancer revealed by in vivo functional SELEX. J. Mol. Biol. **326:**35-48.

259. **Zhang, L., C. H. Kim, and P. Palukaitis.** 1994. The chlorosis-induction domain of the satellite RNA of cucumber mosaic virus: identifying sequences that affect

accumulation and the degree of chlorosis. Mol. Plant-Microbe Interact. **7:**208-213.

260. **Zhang, L., T. A. Zitter, and P. Palukaitis.** 1991. Helper virus-dependent replication, nucleotide sequence and genome organization of the satellite virus of maize white line mosaic virus. Virology **180:**467-473.

261. **Zheng, L., U. Baumann, and J. L. Reymond.** 2004. An efficient one-step site-directed and site-saturation mutagenesis protocol. Nucleic Acids Res. **32:**e115.

262. **Zhou, F., G. Wu, W. Deng, Y. Pu, C. Wei, and Y. Li.** 2006. Interaction of rice dwarf virus outer capsid P8 protein with rice glycolate oxidase mediates relocalization of P8. FEBS Lett. **581:**34-40.

263. **Zlotnick, A., R. Aldrich, J. M. Johnson, P. Ceres, and M. J. Young.** 2000. Mechanism of capsid assembly for an icosahedral plant virus. Virology **277:**450-456.

VITA

Name:	Dong Qi
Address:	2132 TAMU, Dept Plant Pathology and Microbiology, Texas A&M University, College Station, TX 77843-2132
Email Address:	qidong1978@hotmail.com

Education:	Ph.D. in Plant Pathology; Texas A&M University, College Station (December 2007) B.A. in Plant Protection; Shandong Agricultural University, P. R. China (August 2001)
Selected Awards:	Outstanding Graduate Student, Dept. Plant Pathology and Microbiology, Texas A&MUniversity, 2007 Student Travel Award for ASV annual meeting, 2007 Graduate Assistantship (Non-teaching), 2003-2004 University Scholarship for Undergraduate Students (First Prize), Shandong Agricultural University, 1997-2001
Selected Publications:	Qi, D. and Scholthof, K.-B. G. 20007. A one-step PCR based method for efficient site-directed fragment deletion, insertion and substitution mutagenesis. Submitted Qi, D., Omarov, R., and Scholthof, K.-B. G. 2007. The complex subcellular distribution of satellite panicum mosaic virus capsid protein reflects its multifunctional role during infection. Submitted Omarov, R., Qi, D., and Scholthof, K.-B. G. 2005. The capsid protein of satellite panicum mosaic virus contributes to systemic invasion and interacts with its helper virus. J. Virol., **79**:9756-9764
Professional Activities:	Member of the American Society for Virology, 2007 Member of the American Phytopathological Society, 2005-present Treasurer of Graduate Student Club, Plant Pathology and Microbiology